A SCREENING STUDY OF A NEW WATER GAS SHIFT CATALYST

by

Andrew D. Overstreet

Thesis submitted to the Graduate Faculty of the
Virginia Polytechnic Institute and State University
in partial fulfillment of the requirements for the degree of

MASTER OF SCIENCE

in

Chemical Engineering

APPROVED:

P. R. Rony, Chairman

G. B. Wills

J. P. Wightman

July, 1974

Blacksburg, Virginia

ACKNOWLEDGEMENTS

I wish to thank , my graduate committee chairman and friend, for the support and advice which made my graduate career possible. A special thanks also goes to , co-principal investigator of the "Supported Molten Electrolyte Catalysts" grant. I would also like to express my appreciation to for his translation of German patent literature which appears in this work and to and for their experimental aid.

TABLE OF CONTENTS

TABLE OF CONTENTS - continued

TABLE OF CONTENTS - continued

TABLE OF CONTENTS - continued

TABLE OF CONTENTS - continued

LIST OF FIGURES

LIST OF FIGURES - continued

LIST OF FIGURES - continued

LIST OF TABLES

LIST OF TABLES - continued

I. INTRODUCTION

The water gas shift reaction,

$$CO + H_2O \rightleftarrows CO_2 + H_2$$

is currently an important commercial reaction, one that will become even more important in the future with the advent of new coal gassification and other fuel-to-fuel conversion processes. The shift reaction is used in five of the eight major processes for making synthetic natural gas (SNG) from coal[1]: the molten carbonate, Bigas, Synthane, Hygas-Oxygen, and BuMines Hydrogassification processes. Steadily increasing requirements for hydrogen in coal liquefaction processes[1] indicate that an important source of hydrogen will be from water via the water gas shift reaction of a fossil fuel.

A sulfur-tolerant water gas shift catalyst has recently appeared in the literature, but it seems to have escaped the attention of most catalytic scientists. It is included among a series of German patents[2] issued to Esso Research and Engineering over the last several years, and consists of cobalt oxide/molybdenum oxide/cesium acetate supported on porous alumina. This catalyst will henceforth be called the "Aldridge" catalyst, in tribute to its principal discoverer, Clyde L. Aldridge at Esso. Aldridge believes that this

catalyst contains a molten electrolyte under reaction conditions, presumably a consequence of some type of low-melting-point cesium salt.

A sulfur tolerant water gas shift catalyst has many possibilities in view of the fact that coal may contain as much as five to ten weight percent sulfur compounds. The currently used low temperature water gas shift catalyst, a copper oxide-zinc oxide catalyst, is completely intolerant to sulfur compounds.[3] The chromium promoted iron oxide water gas shift catalyst, commercially employed at high temperatures, tolerates 500-1000 ppm of H_2S and 20 ppm of organic sulfur.[3] The "Aldridge" water gas shift catalyst potentially offers considerable advantage over the two currently employed industrial water gas shift catalysts, insofar as sulfur tolerance is concerned.

There exists a strong possibility that the "Aldridge" catalyst could catalyze reactions other than the water gas shift reaction. After all, a cobalt oxide/molybdenum oxide catalyst supported on alumina is the standard industrial hydrodesulfurization catalyst.[4] Very few exploratory studies have been performed anywhere in industry, in our opinion, on the "Aldridge" catalyst's ability to activate hydrogen for a variety of hydrocarbon conversion reactions including the hydrocracking of polynuclear aromatics and the desulfurization of aromatic sulfur compounds.

One of the most interesting features of the "Aldridge" catalyst is the possibility that it is a catalytic melt. Research involving such a catalyst might lead to new principles which would aid the discovery of new and commercially important molten electrolyte catalysts.

One should not be deterred by the fact that the "Aldridge" catalyst may be a molten salt. Two coal conversion processes involve molten salt catalysts[1]: In the Consol synthetic fuel process, an ash-free extract of coal is hydrogenated with molten zinc chloride in an ebullating bed operating at 4200 psia; in the M.W. Kellogg Company process, coal is gassified with steam in a gassifier containing molten sodium carbonate. In addition to such processes, several industrially important catalysts contain molten salts dispersed within porous solids. These include:

1. The vanadium SO_2 oxidation catalyst--consisting of a supported potassium vanadate/potassium pyrosulfate melt--is used to produce much of the 60 billion pounds of sulfuric acid produced in the U. S. every year.[5]
2. A vanadium molten electrolyte catalyst is employed for the partial oxydation of o-xylene or naptha-lene to pthalic anhydride.[6]
3. A $KCl/CuCl/LaCl_3$ melt supported within silica gel is used for the oxidation of HCl to Cl_2, the so-called Deacon process.[7]

Finally, there is some hope that reasonably good science can be performed upon molten electrolyte catalysts. Rony, in his pioneering works, has developed a simple model of supported liquid phase catalysts.[8,9]

In the "Aldridge" catalyst and the other supported molten electrolyte catalysts mentioned above, the corrosive catalytic melt is dispersed within the pores of the porous support. By doing this, the following advantages are realized;

1. Reactor corrosion is avoided, such as that which plagues the Kellogg molten carbonate process.[1]
2. High interfacial areas for gas contacting with the melt are available.

The porous support particles essentially act as non-corroding micro-containers for the melt (Figure 1).

We can summarize here by stating that the "Aldridge" catalyst is worth studying for a number of important reasons:

1. Potentially, it is an important commercial catalyst for the water gas shift reaction since it is sulfur tolerant.
2. The fact that it may be a molten salt dispersed within a porous solid presents few, if any, obstacles to commercialization.
3. There is little published data on the catalyst, even for the water gas shift reaction.

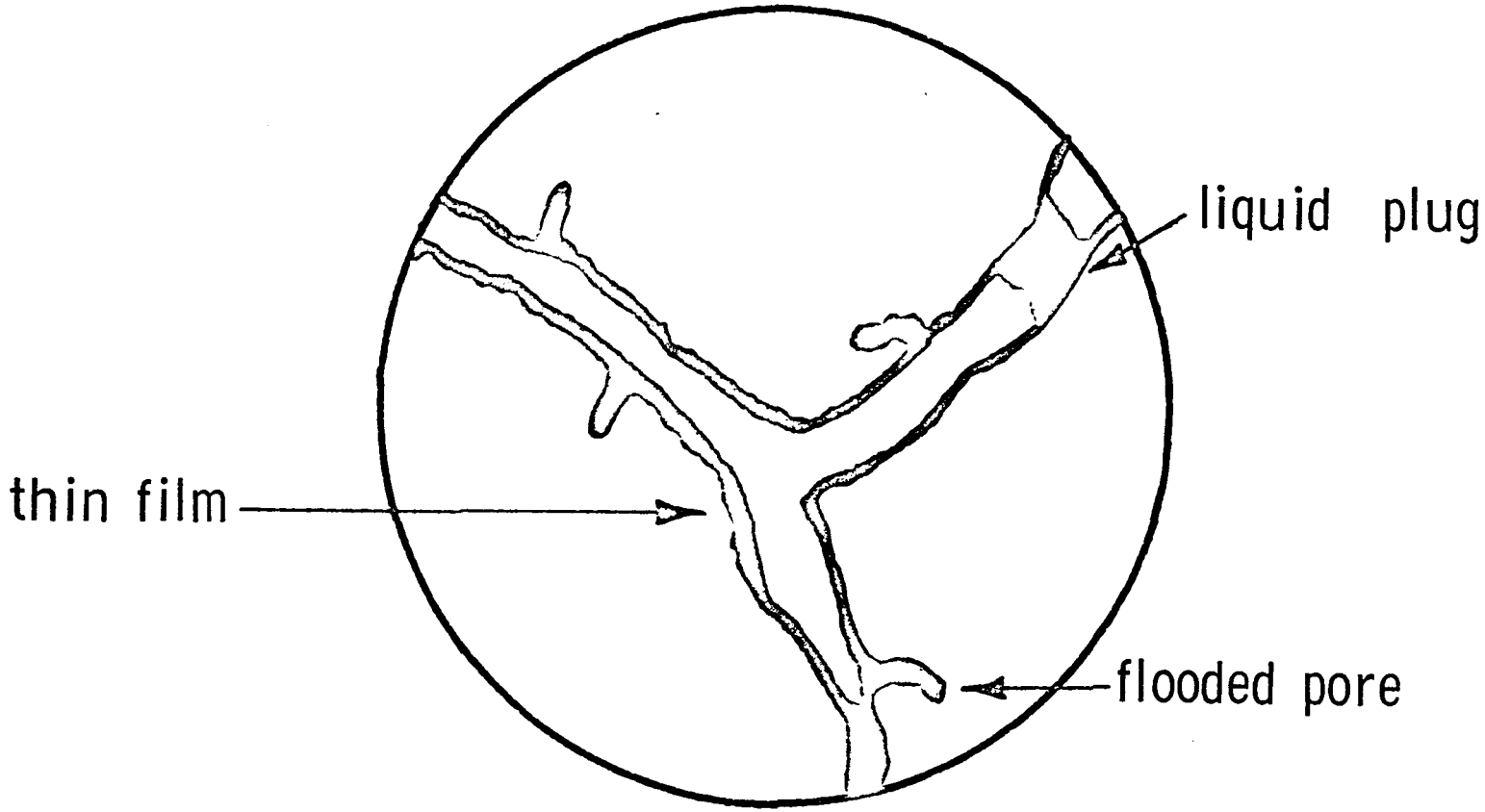

Figure 1. Supported Liquid Phase Catalyst Particle.

4. Potentially, the catalyst may be highly active for other types of fuel-to-fuel conversion reactions as well.
5. The existence of a molten salt within the pores has not been unequivocally demonstrated. Currently, it is only a hypothesis.
6. If the "Aldridge" catalyst does contain a melt under reaction conditions, we may be able to discover one or more principles of catalysis in liquid media that we could possibly apply towards the discovery of other potentially important commercial catalysts.

Clearly the "Aldridge" catalyst is worth studying from many different points of view. The arguments are compelling.

Objectives. The reasons given above for studying the "Aldridge" catalyst are wide encompassing in their range of potential areas of study. The particular objectives of this study are restricted to four topics:

1. Develop techniques for measuring and interpreting catalytic reactor data for the "Aldridge" water gas shift catalyst. Determine intrinsic rate constants and activation energies wherever possible.
2. Vary the relative amount of the molten component of the "Aldridge" catalyst (cesium acetate) and observe the influence of such a change upon rate

constants, activation energies, and presumed melting points.

3. Determine the feasibility of using a resistance drop technique for measuring the melting point of a molten electrolyte.
4. As a first step towards the eventual automation of the catalytic screening microreactor, interface an Autolab digital integrator to a PDP 8/E mini-computer.

Before outlining a specific strategy for this study, it is worthwhile to comment on the RANN (Research Applied to National Needs) division of the National Science Foundation and its influence upon the project goals and strategy. All research performed in this study was supported under a substantial RANN Grant, GI-37991, entitled "Supported Molten Electrolyte Catalysts."

The RANN program is directed toward the discovery of new technology that can be transferred within a short time to industrial research laboratories for further research and development. RANN research projects, therefore, are industrially targeted. With such considerations in mind, our RANN catalysis project is directed at the screening of catalysts for specified applications that might be of "immediate" benefit to industry. The focus of our research work is the development of techniques that would (a) permit us to screen

new catalyst compositions for new types of vapor-phase reactions, and (b) yield data that is both believable and publishable in the technical literature. This specific study is concerned with a study of the "gross" characteristics of the new "Aldridge" water gas shift catalyst. Our first efforts were directed at the following points:

1. Development of a catalytic screening microreactor that would give reproducable data for the "Aldridge" catalyst.
2. Determination of rate constants and "activation energies" at a fixed gas composition. Such data would hopefully allow us or anyone else to develop general guidelines concerning how to conduct detailed kinetic studies of the catalyst.
3. Exploration of techniques that would prove whether or not a molten electrolyte existed at reaction conditions.
4. Development of computer techniques that could work up the gas chromatographic and flow rate data.

This is the first thesis that has resulted from the RANN grant.

II. WATER GAS SHIFT CATALYSTS

Presently, the water gas shift reaction is used for two primary functions:

1. Production of hydrogen from synthesis gas.
2. Conversion of carbon monoxide to carbon dioxide in ammonia synthesis gas.

Current energy trends dictate that the first of the above uses will become increasingly important.[10-12]

The water gas shift reaction is exothermic with a heat of reaction of 9.84 Kcal/gm mole at 25°C. As described by Thomas,[3] the water gas shift reaction is generally performed adiabatically in commercial processes. Thus, there is a temperature increase as the reaction proceeds. Chemical equilibrium favors carbon monoxide production at higher temperatures. It is for this reason that the shift reaction is generally performed in two stages commercially, with intermediate cooling.

Iron Oxide Catalyst

The first stage in commercial water gas shift reactors involves a high temperature water gas shift catalyst. This catalyst is generally a chromium promoted iron oxide catalyst.[13-18] Most processes utilize the following conditions:[3]

Temperature: 315-385°C

Space Velocity: 300-4000 volumes of gas per volume of catalyst per hour at standard conditions on a dry basis (GHSV)

Water to Carbon Monoxide Ratio: 2 to 4

Pressure: Any pressure desired

Sulfur Tolerance: 500-1000 ppm of hydrogen sulfide, 20 ppm of organic sulfur

Support: No support employed

The sulfided form of the catalyst is approximately half as active as the oxidized form.

Copper Oxide-Zinc Oxide Catalyst

The second stage in commercial shift reactors generally utilizes a low temperature catalyst. Usually, this catalyst is a copper oxide-zinc oxide catalyst supported on alumina.[19-21] According to Thomas[3], the following conditions are most often used with the low temperature catalyst:

Temperature: 175-350°C

Space Velocity: 300-4000 volumes of gas per volume of catalyst per hour at standard conditions on a dry basis (GHSV)

Water to Carbon Monoxide Ratio: 1 to 2

Pressure: Any pressure desired

Sulfur Tolerance: Permanently poisoned by sulfur compounds

Note the complete intolerance of the low temperature shift catalyst to sulfur bearing feedstock.

The "Aldridge" Water Gas Shift Catalyst

A third catalyst for the water gas shift reaction has recently been patented in Germany by Esso Research and Engineering Company. The patents actually describe a family of catalysts. The specific combination of cobalt oxide/molybdenum oxide/cesium acetate figured prominantly in the patent examples and was chosen for this study. It is called the "Aldridge" catalyst in this work, after its principal discoverer, Clyde L. Aldridge.

Since no published information exists for the "Aldridge" water gas shift catalyst, we believe that it is useful to summarize the information contained in the German patents.

Aldridge[2] found that the water gas shift reaction occurred at temperatures as low as 149°C when performed with a catalyst having the following two types of components:

1. An alkali metal salt of an acid with a dissociation constant less than 1×10^{-3}.
2. A hydrogenation/dehydrogenation component, which may be impregnated with the alkali salt.

Suitable alkali salts include carbonates, bicarbonates, phosphates, sulfides, bisulfides, silicates, bisulfites, aluminates, hydroxides, acetates, tungstenates, etc. of sodium, potassium, rhubidium, and cesium. In fact the alkali salts of any acid can be used as long as the dissociation constant is less than 1×10^{-3}. Suitable hydrogenation/dehydrogenation components include elements of Group V-B, VI-B, or Group VIII, either alone or in combination. Vanadium, chromium, molybdenum, tungsten, iron, nickel, or cobalt may be used alone although mixtures of iron, nickel, or cobalt together with vanadium, chromium, molybdenum are suitable. Catalysts which meet the two specified criteria are particularly active in the sulfided form. Thus, they are particularly useful for sulfur bearing feeds. The ratio of the hydrogenation/dehydrogenation component to the alkali metal compound may range between 0.001 to 10 on a weight basis.

According to Aldridge,[2] the particular combinations of cesium carbonate, cesium acetate, potassium carbonate, or potassium acetate together with cobalt-molybdenum are especially attractive.

Aldridge[2] believes that the alkali salt exists as *a liquid phase in contact with the hydrogenation/dehydrogenation catalyst surface.* This type of system is said to be beneficial to the catalytic process.

A number of tests were made by Aldridge[2] on catalysts which met the previously specified criteria for water gas shift catalysts. The actual results are given in Appendix II. With respect to the cobalt oxide/molybdenum oxide/ cesium acetate catalyst, which was sulfided during a pre-treatment operation, the following information may be deduced:

1. $CoO-MoO_3$ is more effective as the hydrogenation/ dehydrogenation component that either component alone.
2. Potassium acetate and cesium carbonate are nearly as effective as cesium acetate for the alkali metal component.
3. Fe-Mo and Ni-Mo combinations are not as effective as the Co-Mo combination for the hydrogenation/ dehydrogenation component.
4. Co-V and Co-Cr are not as effective as Co-Mo for the hydrogenation/dehydrogenation component.

5a. A catalyst pretreated with H_2S and run with a reactant stream containing no H_2S is much more active than a catalyst which was not pretreated and run with reactants containing no H_2S.

b. A catalyst not pretreated, but used with a reactant gas stream containing H_2S is also much more active than a catalyst which was not

pretreated and run with no H_2S in the feed stream.

6. The support used makes very little difference.
7. Na_2CO_3 is as effective as cesium acetate for the alkali metal component.

Comparison of Water Gas Shift Catalysts

Thermodynamic equilibrium of the water gas shift reaction is favored by low temperature. However, the currently used low temperature shift catalyst, Cu-Zn, is completely intolerant to sulfur compounds. Coal and coke used in hydrogen manufacture contain between five and ten weight percent sulfur compounds--hence, the Cu-Zn catalyst is often unattractive. The iron based shift catalyst is somewhat sulfur tolerant, but it is a high temperature catalyst, making it thermodynamically unappealing.

Since the "Aldridge" water gas shift catalyst is sulfur activated, it is desirable to know where its activity lies with respect to the iron based catalyst and the Cu-Zn based catalyst. It is quite difficult to make such comparisons from literature data for a number of reasons: differences in pressure, temperature, feed gas composition, surface area of support, reactor size, pellet size and many other variables. Such differences generally make strict comparisons invalid.

However, to obtain a simple order of magnitude comparison between the "Aldridge" catalyst and the two commercial

catalysts, two sets of data from the literature were examined.

Iron Oxide-Chromium Oxide Catalyst. Atwood[18] studied an unspecified industrial iron oxide-chromium oxide catalyst. One of the runs he made was at the following conditions:

Reactor pressure = one atmosphere
Reactor temperature = 760°F
Catalyst mesh range = 16/20 mesh
Inlet dry reactor gas = synthesis gas containing 23.1% carbon monoxide
Inlet steam to dry gas ratio = 0.9

From his conversion-space velocity data, a pseudo-first order rate constant can be computed. Details of this calculation are given in Appendix IV. The rate constant found was 81.2 min^{-1}. The rate was most likely pore diffusion limited, since other data of Atwood showed an increase in rate with a decrease in particle size.

Zinc Oxide-Copper Oxide Catalyst. Shchibrya[21] studied a zinc oxide/chromium oxide/copper oxide catalyst. He employed the following conditions in one of his runs:

Grain size of catalyst = between 0.1/1.0 mm
Reactor pressure = one atmosphere
Reactor temperature = 300°C

Inlet reactor gas = 9.7% CO/82.8% H_2O/4.2% H_2/
4.2% CO_2

From the conversion-space time data, a pseudo first order rate constant was found to be 80 min^{-1}. This calculation is also in Appendix IV.

The "Aldridge" Catalyst. For a dry gas feed of 49% CO/49% H_2/2% COS and a steam-to-dry-gas ratio of 1.0 to 3.35, rate constants were determined as a function of temperature for one atmosphere total pressure. The data are presented and explained fully later in this study. They are used here solely for comparative purposes.

For a temperature of 760°F, the most active "Aldridge" catalyst had a pseudo-first order rate constant of 6481 min^{-1}, as opposed to 81.2 min^{-1} for the commercial iron based catalyst. At 300°C, the "Aldridge" catalyst had a pseudo-first order rate constant of 418.9 min^{-1}, as compared to 80 min^{-1} using the copper based catalyst.

Although the above comparison of catalysts may not be strictly valid in the absolute sense, it certainly points out that the "Aldridge" catalyst is competitive with the best industrial water gas shift catalysts.

III. EXPERIMENTAL

The following section contains detailed experimental descriptions of the following:

Catalytic reactor system
Experimental procedures for measuring
rate constants and activation energies
for water gas shift catalysts
A melting point determination apparatus
for molten electrolytes

A brief description of an interface between an Autolab digital integrator and a PDP 8/E minicomputer is also given; additional details of this interface are presented in Appendix V.

Overall Reactor System

The overall reactor system was constructed by the principal investigator, Dr. P. R. Rony, for the "Supported Molten Electrolyte Catalysts" grant. The apparatus itself can be subdivided into three parts, shown schematically in Figures 2 through 4:

1. The Gas Handling System
2. The Catalytic Microreactor and Water Saturator
3. The Gas Sampling and Analysis System

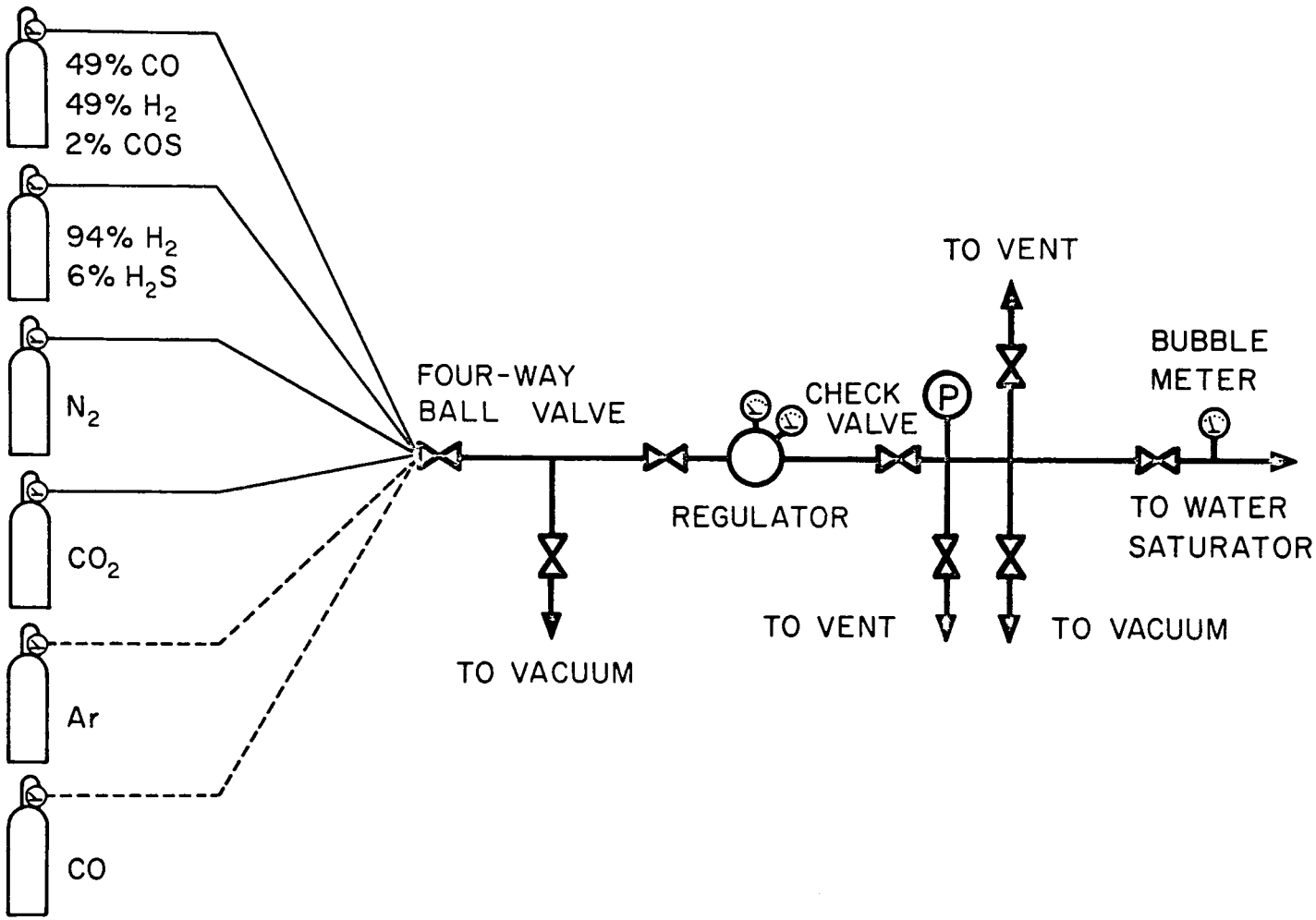

Figure 2. Gas Handling System.

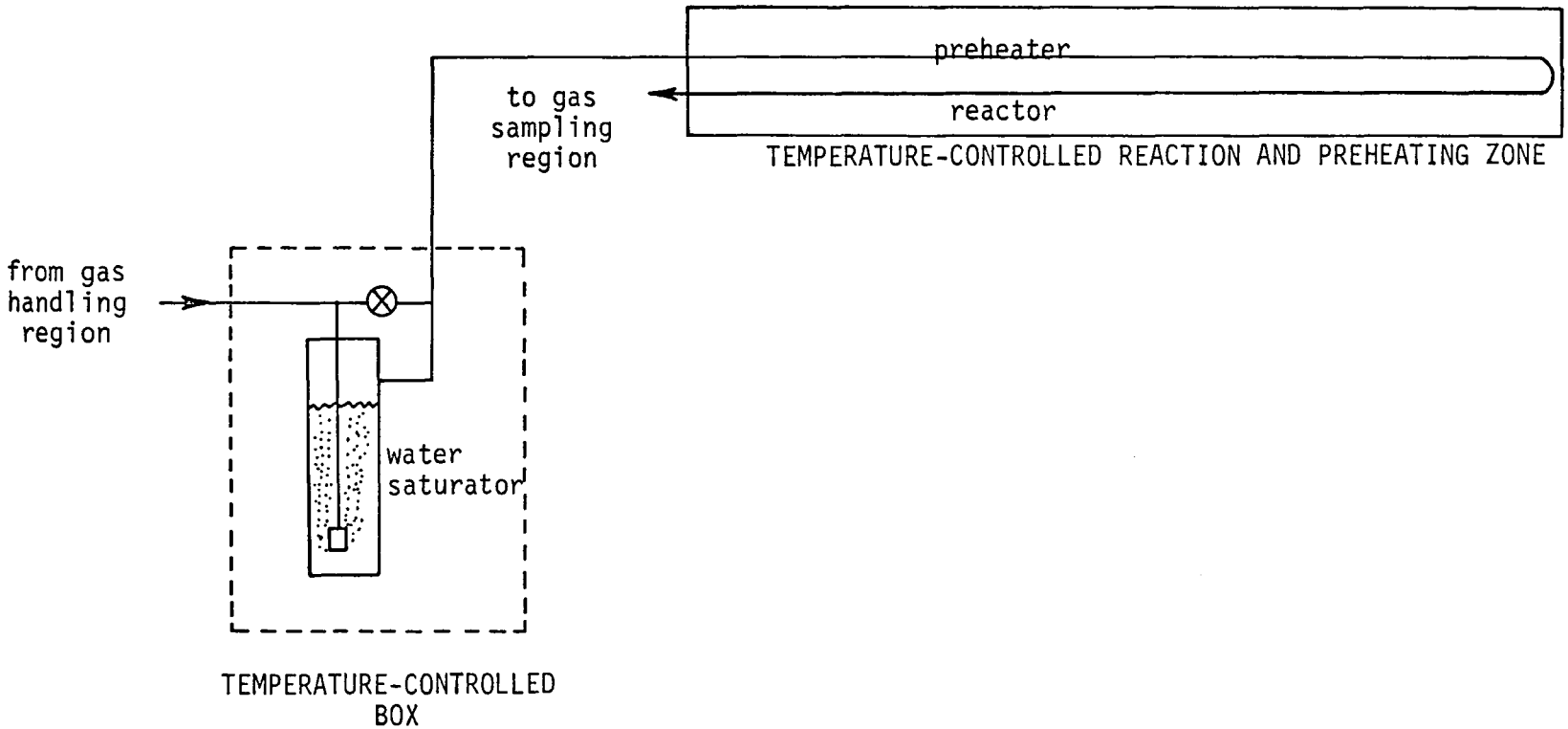

Figure 3. Catalytic Reactor and Water Saturator.

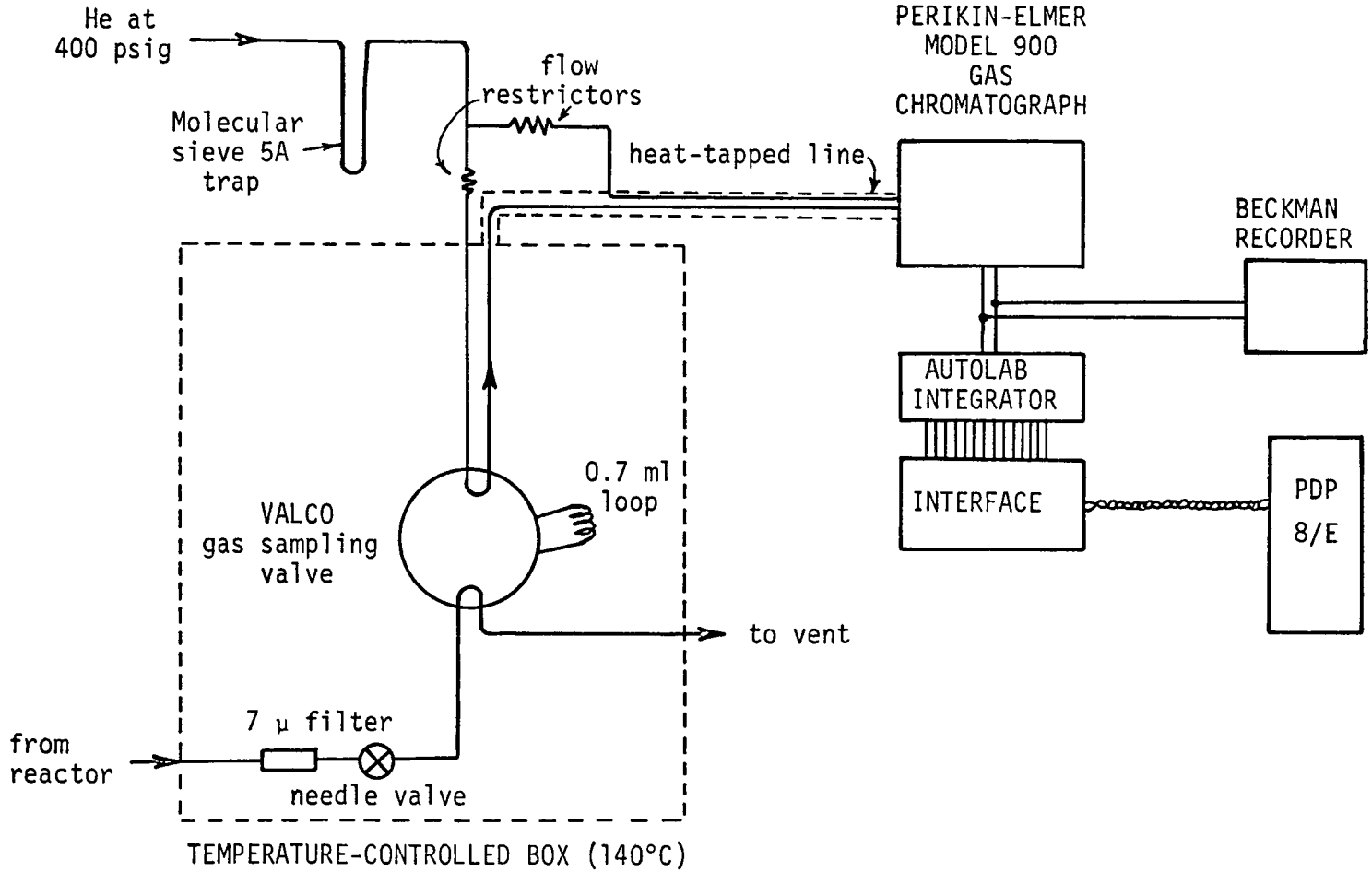

Figure 4. Gas Sampling and Analysis System.

The reactor is contained in a spacious aluminum and Lucite hood, of dimensions eight feet by four feet by five feet. Photographs of the reactor system are given in Figures 5 through 7.

Gas Handling System

A single feed gas passes through a four-way ball valve, an on/off valve, a two-stage gas regulator, a check valve, a relief valve set at 500 psig, a pressure gauge, a vent line, a vacuum line, a precision fine-metering valve, and a bubble meter in the order given. With the aid of the four-way ball valve, different feed gases may be readily selected: nitrogen for preliminary studies and leak checks; CO and CO_2 for calibration of the gas chromatograph; 6% H_2S/ 94% H_2 for pretreating the "Aldridge" catalyst; and 2% COS/ 49% CO/49% H_2 for studying the water gas shift reaction. A bubble meter is used to measure dry gas flow rates.

Reactor and Water Saturator

After the precision metering valve, the feed gas passes through a high pressure water saturator [equipped with a 1/8-inch stainless steel bypass valve] maintained at approximately 60°C, a heat-tapped stainless-steel line, a seven-foot reactor-gas preheater tube, and a five foot fixed-bed catalytic reactor maintained between 150°C and 650°C

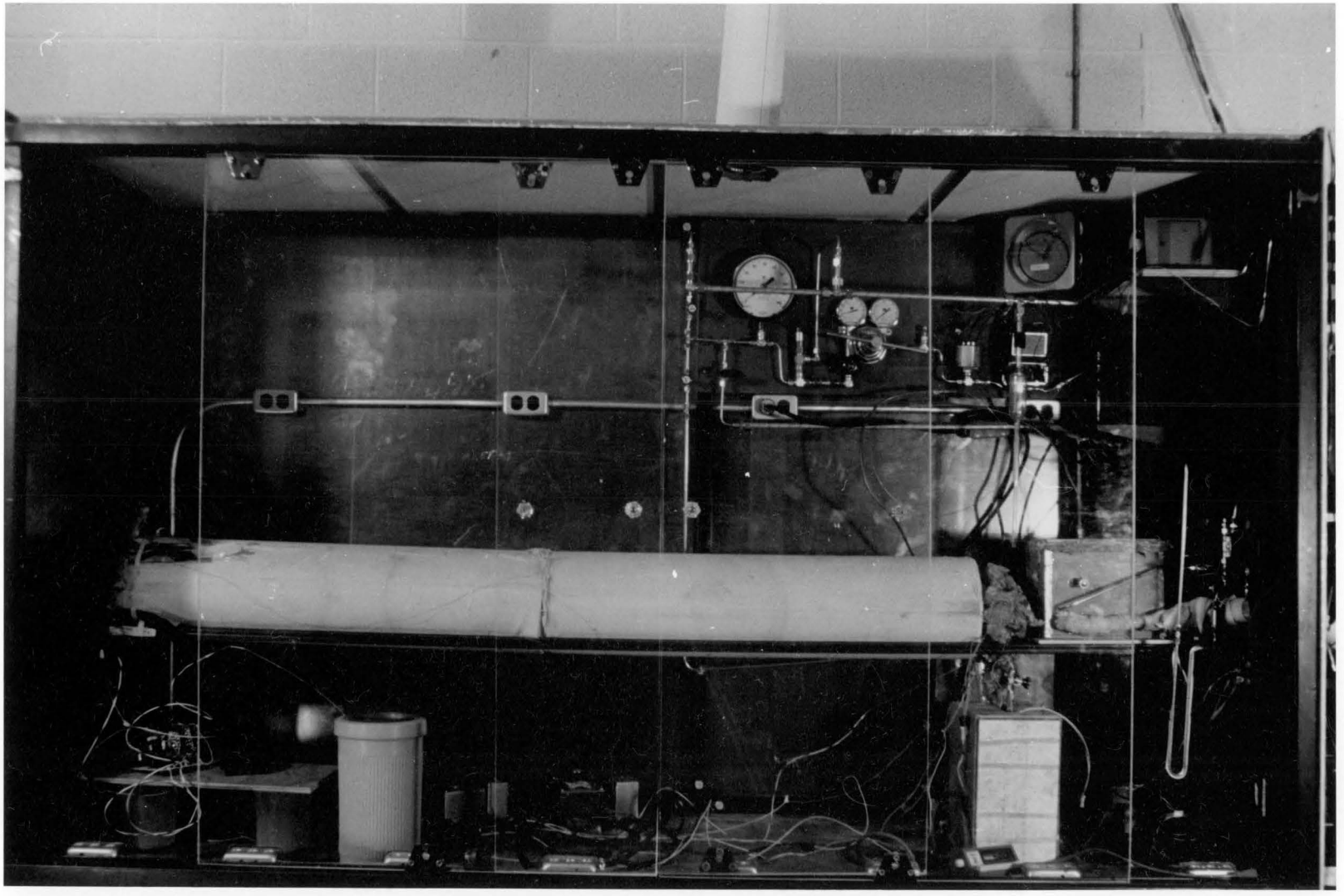

Figure 5. Catalytic Reactor in Aluminum Hood.

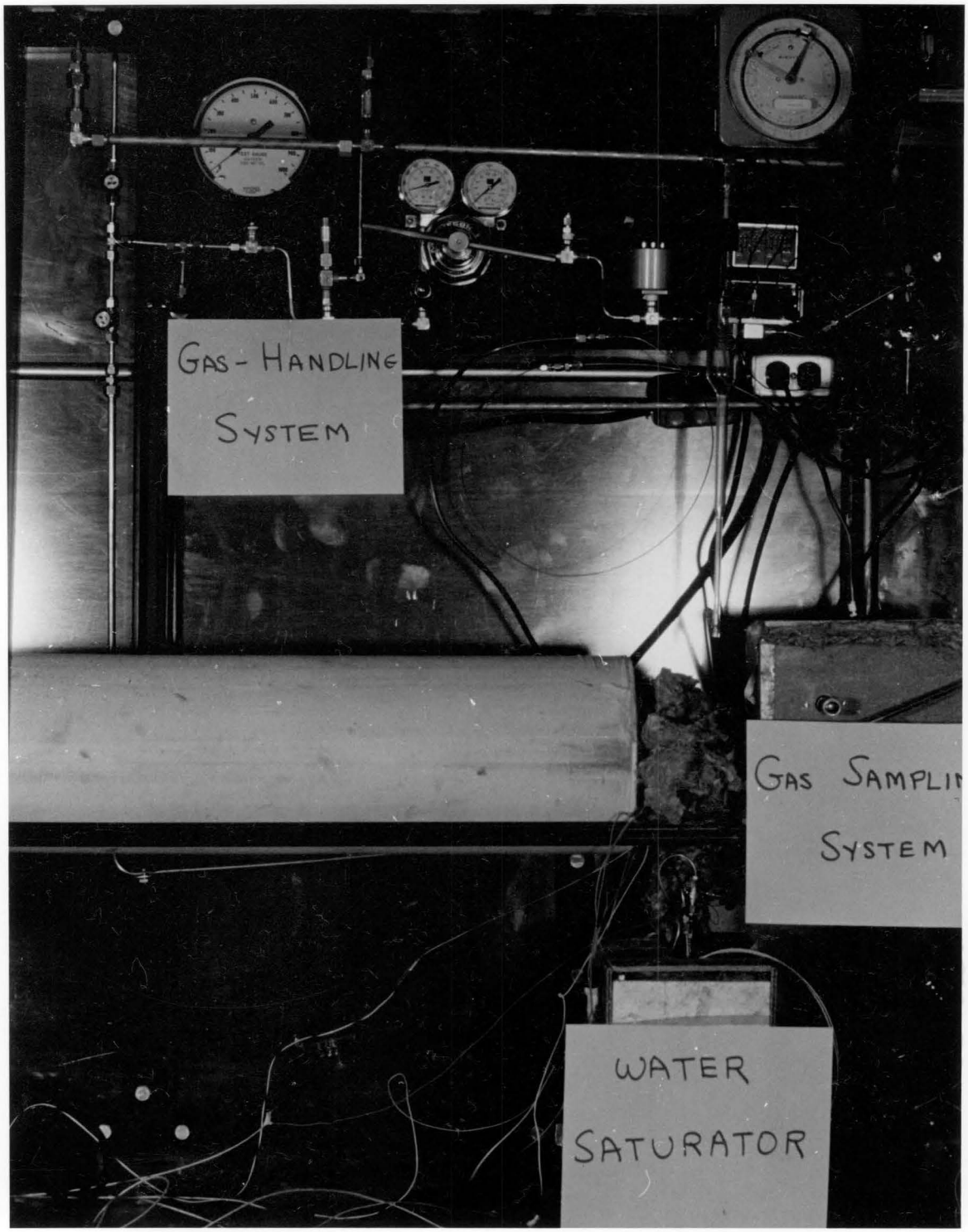

Figure 6. Sampling Valve Region of Reactor.

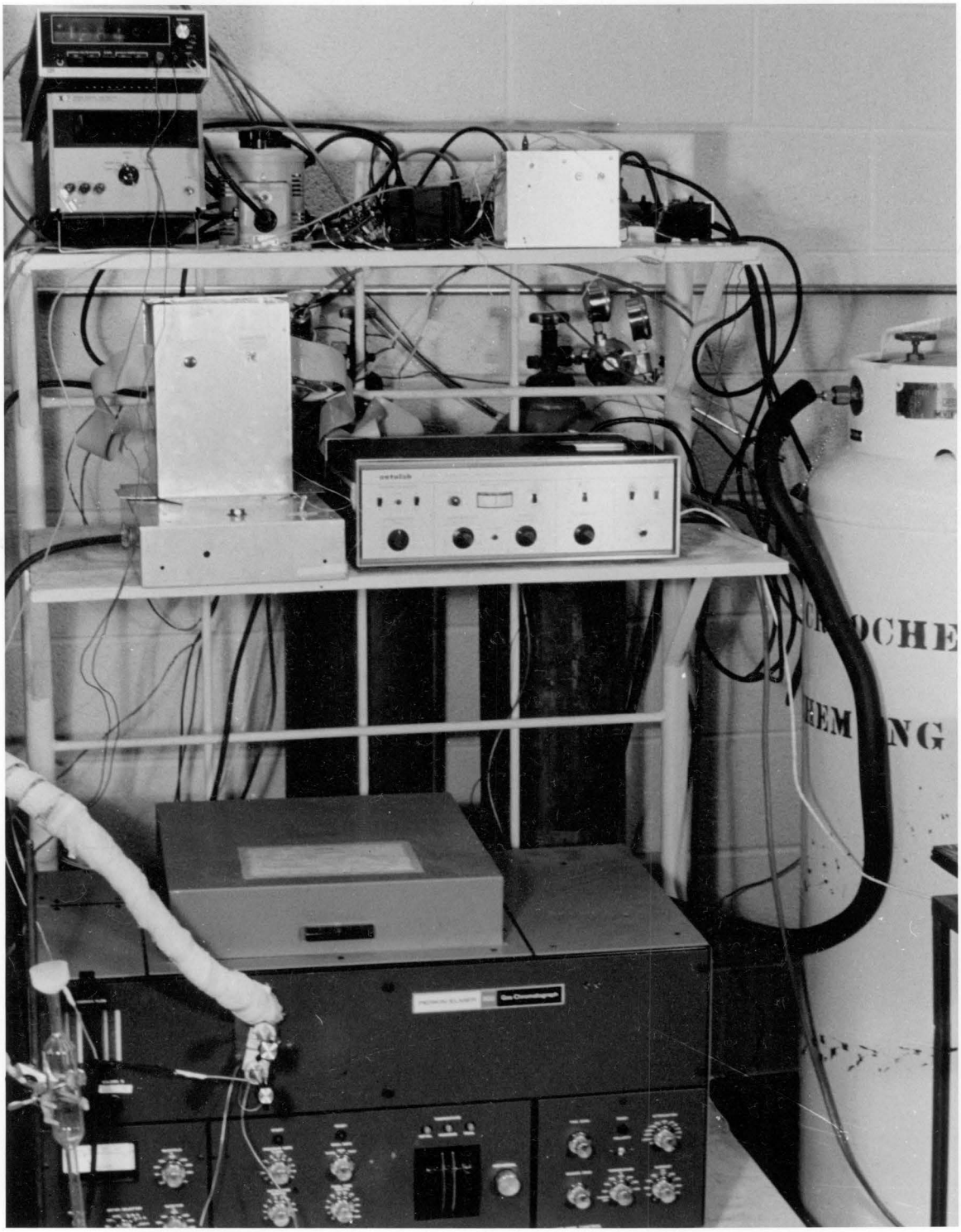

Figure 7. Analytical System of Reactor.

and packed with 20/60 mesh catalyst. Four inches of insulation surround a 3/4-inch I.D. steel tube which contains the 1/8-inch I.D. preheater tube and 3/16 inch I.D. reactor tube.

Heating of the reactor is accomplished by a one-inch-by-six-foot length of heating tape stretched adjacent to the 3/4-inch I.D. steel tube. Additional short lengths of heating tape are wound at each end of the steel tube to reflect heat back into the center of the furnace and to minimize axial temperature profiles.

Figures 8 and 9 demonstrate the temperature profiles actually established over the length of the reactor. It is clear that 120 cm is usable at 250°C with $\pm$ 2°C precision or at 500°C with $\pm$ 4°C precision.

A water saturator is employed as the method for metering water into the flowing reactant gas stream of COS, CO, and H_2. Gases enter at the top of a stainless steel bomb and pass through a fritted glass tube through approximately 200 ml of water. The saturated gas passes out through a heat-tapped side arm and into the catalytic reactor via an additional segment of heat tapped line.

Alternative approaches to the metering of water into the feed gas, such as a liquid metering pump or steam generator/needle valve, were rejected. The important advantage of a water saturator is that the fixed gas feed

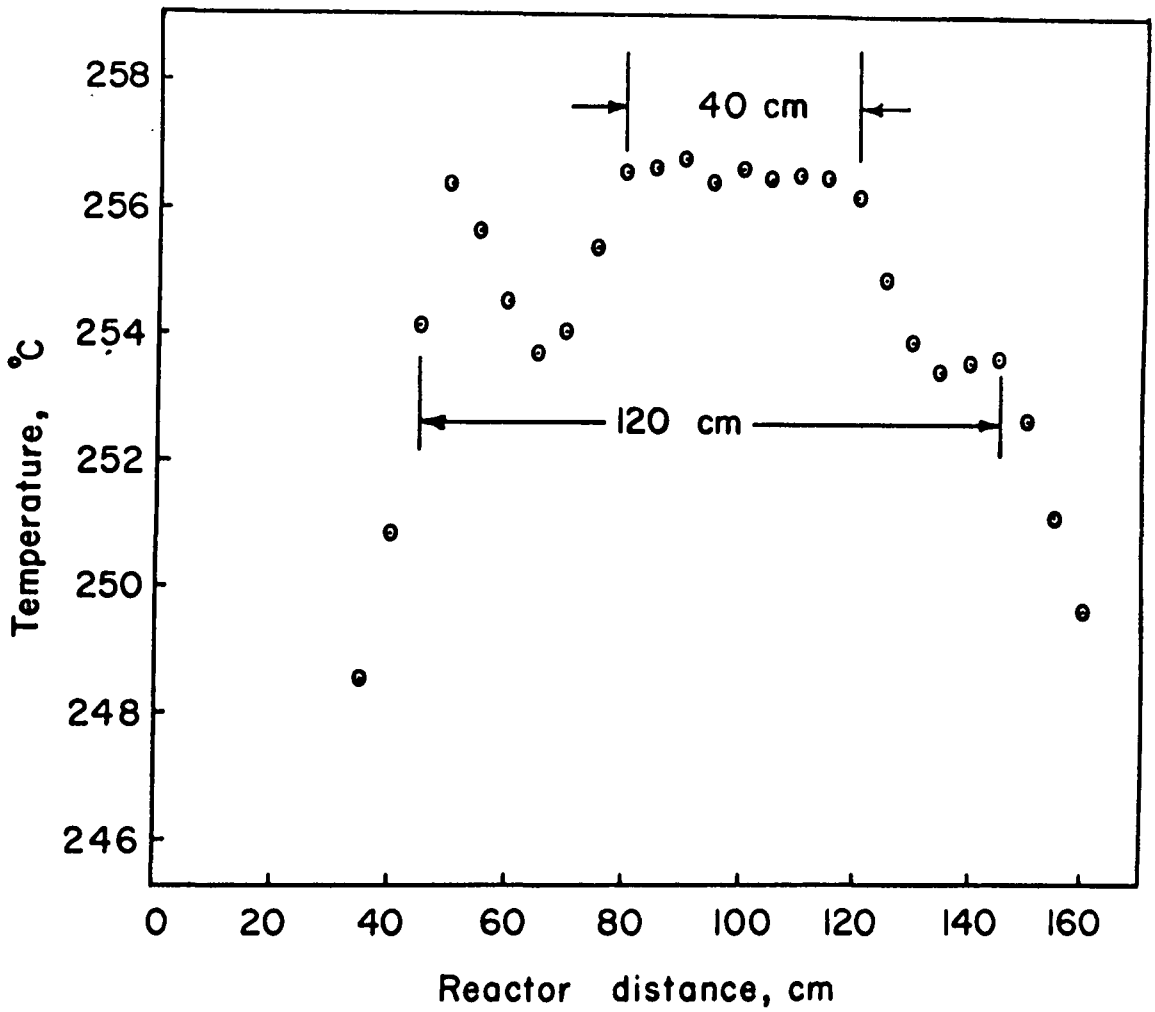

Figure 8. Temperature Profile of Reactor at 250°C.

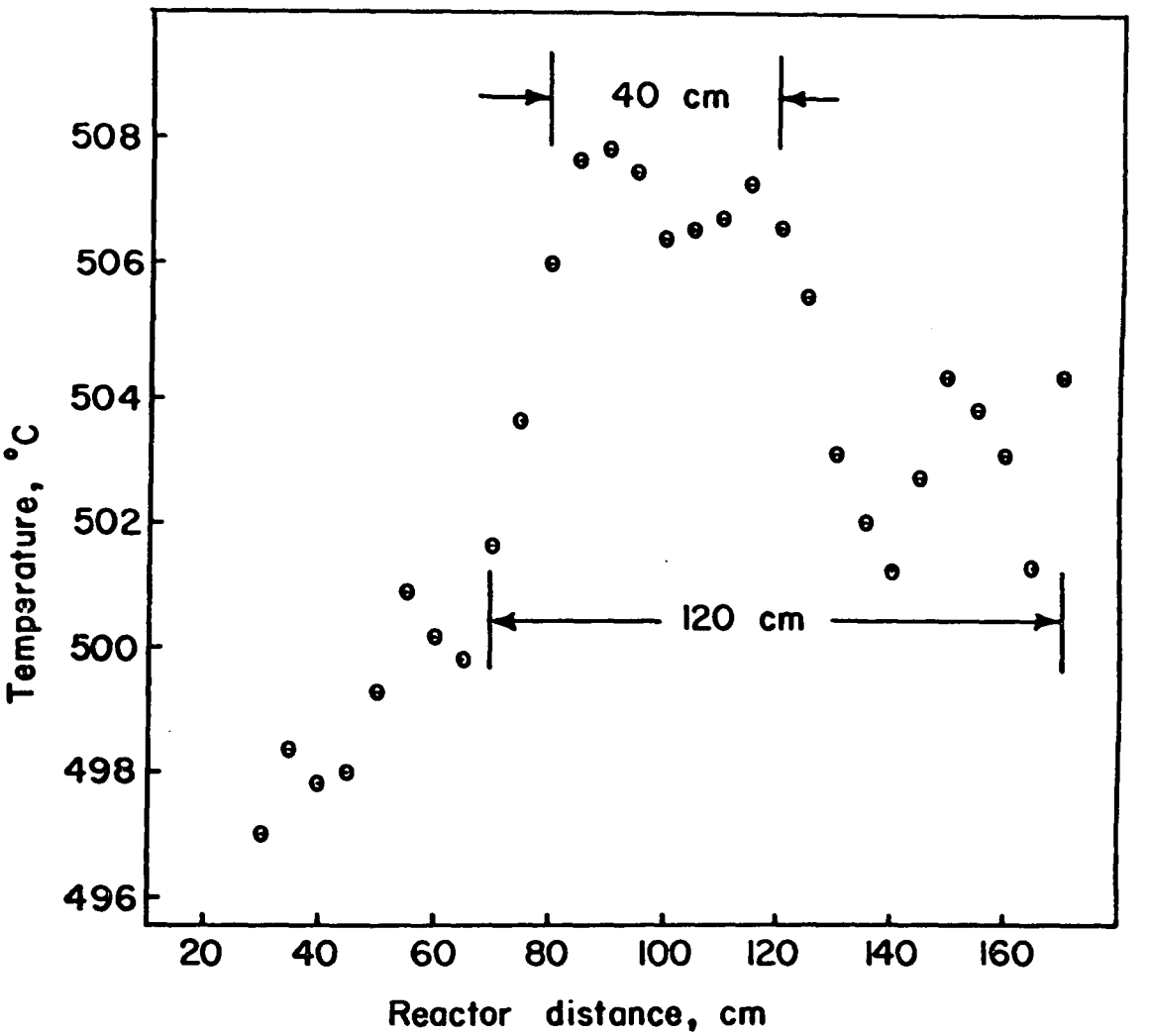

Figure 9. Temperature Profile of Reactor at 500°C.

rate can be varied without significantly changing the percent water in the feed stream entering the catalytic reactor. With the saturator, only *one* flow rate adjustment needs to be made to adjust the flow rate at constant composition. With the metering pump and steam generator, two flow rate adjustments need to be made in order to change the gas flow rate while maintaining constant gas composition.

Gas Sampling and Analysis System

After the fixed bed catalytic reactor, the effluent gases pass through a heat-tapped line, a gas sampling valve equipped with a 0.7 ml sampling loop, a trap for water vapor, and finally, a vent. The sampled gas passes through a heat-tapped line to a nearby gas chromatograph, where it is analyzed for low molecular weight organic and inorganic gases. The peripheral equipment associated with the gas chromatograph include a digital integrator, a homemade digital interface to a minicomputer located five laboratories away, and a recorder.

Procedures Used

The procedures used in this experiment may be divided into three parts:

1. Catalyst Preparation
2. Catalyst Pretreatment
3. Reactor Operation

Catalyst Preparation

Nalcomo 474 Hydrotreating Catalyst was chosen as the hydrogenation/dehydrogenation component for the "Aldridge" catalysts prepared. This catalyst is a general-purpose hydrotreating catalyst that has the following specifications:

% MoO_3	12.5
% CoO	3.5
Support	Al_2O_3
Surface area, m^2/gm	270
Pore volume, cm^3/gm	0.51
Form	1/8-inch extrudate

The Nalcomo catalyst was ground up via mortar and pestle and then sifted to a 20/60 standard sieve range (250 to 841 micron diameter particles). The sieved catalyst was then dried for two hours at 150°C.

Cesium acetate was chosen as the alkali salt component for the "Aldridge" catalysts that were prepared. Fifty grams of cesium acetate were dissolved in sufficient deionized water to form fifty milliliters of solution.

Impregnation Procedure. The following procedure for impregnating the CoO-MoO_3 hydrotreating catalyst with cesium acetate was used:

1. Weigh out 5.59 grams of the $CoO-MoO_3$ hydrotreating catalyst into a 50-ml bottle with plastic cap.
2. Temporarily remove the hydrotreating catalyst from the 50 ml bottle and store it in a 100 ml beaker.
3. Pipet between 0.0 and 3.0 ml of the cesium acetate solution into the 50 ml bottle. This solution had a concentration of one gram of cesium acetate per ml of solution.
4. Pipet enough deionized water into the 50 ml bottle so that the total volume of deionized water plus cesium acetate solution is equal to 3.0 ml.
5. Mix the deionized water and cesium acetate solution. Transfer the 5.59 grams of hydrotreating catalyst back into the 50 ml bottle.
6. Shake the 50 ml bottle so that the cesium acetate solution is dispersed throughout the hydrotreating catalyst.
7. Dry the final "Aldridge" catalyst inside the bottle for two hours at 150°C.

Composition of Catalysts Prepared. Ten catalysts were prepared; their compositions are given in Table I. The 3.0 ml combined volume of water and cesium acetate solution is

Table I

COMPOSITION OF CATALYSTS PREPARED

	Catalyst No.									
	1	2	3	4	5	5A	5B	5C	5D	6
grams of Nalcomo 474 Hydrotreating catalyst	5.613	5.630	5.592	5.602	5.596	5.574	5.571	5.607	5.539	5.616
ml of CsOAc solution added[a]	3.0	2.0	1.5	1.2	1.0	0.7	0.4	0.2	0.1	0.0
ml of water added	0.0	1.0	1.5	1.8	2.0	2.3	2.6	2.8	2.9	3.0
grams of CsOAc per cm^3 of pore volume	1.048	0.697	0.526	0.420	0.350	0.246	0.141	0.070	0.035	0.0

[a] The solution contains 50.0 grams of cesium acetate per 50.0 ml of solution.

5% greater than the pore volume of 5.59 grams of Nalcomo 474 hydrotreating catalyst. Consequently the entire internal pore volume is initially filled prior to drying of the catalyst.

Catalyst Pretreatment

For the "Aldridge" catalysts studied, the following pretreatment procedure was generally followed:

1. Weigh out a catalyst bed of 1.5 grams containing between 0.1 grams and 1.5 grams of "Aldridge" catalyst, with the remainder of the bed being inert alumina (Air Products and Chemicals 200S alumina, 20/60 sieve range).
2. Pour the catalyst powder midway into the reactor tube and provide a plug of quartz wool at one end to prevent catalyst loss into the flowing reactant gas stream.
3. Establish slow gas flow rate of approximately 1 ml/10 sec at ambient conditions of 6% H_2S/94% H_2.
4. Set the controller for the central portion of the reactor at 550°C and the controller for the two ends of the reactor tube at 400°C.
5. After the desired temperatures are established, continue the pretreatment for one and one-half

hours. The water saturator is bypassed at all times during pretreatment.

The basic function of pretreatment is to sulfide the "Aldridge" catalyst. The H_2S in the pretreatment gas serves as the sulfur source.

Reactor Operation

A dry gas feed of 49% H_2/49% CO/2% COS was used in this study. An equimolar ratio of hydrogen and carbon monoxide is called "synthesis gas"; such a gas composition is frequently found as an intermediate stage in hydrogen production. A substantial amount of carbonyl sulfide was added both to demonstrate the sulfur tolerance of the "Aldridge" catalysts studied and to maintain the sulfide level within the catalysts.

By choosing a water saturator temperature of 60°C, a steam-to-dry-gas ratio of one to 3.35 was established. Higher temperatures led to problems of varying water composition with changing feed gas flow rates.

Startup. The startup of the reactor system proceeds as follows:

1. Ready the chromatograph by setting the column heater to 60°C, the hot wire detector to a temperature of 250°C, and the hot wire current to 125 milliamps. Crimped flow restrictors

permanently establish the helium carrier gas flow to the chromatograph at 24 milliliters per minute.

2. Turn on the digital integrator and recorder.
3. Adjust the regulator on the reactant gas tank to achieve maximum delivery pressure and open the regulator valve to establish flow.
4. Adjust the regulator inside the hood to achieve maximum delivery pressure and then open the regulator valve.
5. Adjust the precision metering valve to establish flow to the reactor itself. By setting high delivery pressures using the regulators, very steady flows can be observed past the precision metering valve. The water saturator is initially bypassed.
6. After flow through the reactor has been observed, turn on the two reactor temperature controllers to the lowest experimental temperature of interest.
7. Set the temperature controllers for the water saturator, the sampling valve region, and the region between the reactor exit and sampling valve at 60°C, 150°C, and 150°C, respectively.
8. Switch on autotransformers controlling the heat-tapped exit lines and carrier lines between the sampling valve and chromatograph.

9. After a period of ten minutes, close the water saturator bypass valve, thus causing the dry reactant gas stream to become saturated with water vapor.

Run Procedure. Data were taken after the initial steady state temperature profile was established in the reactor, a warm-up time that took approximately 45 minutes. The initial temperature used was generally 200°C which was then increased to 400°C in 25°C increments. Data for a single "Aldridge" catalyst could be obtained in one 8-hour day.

For any given "Aldridge" catalyst, the following procedure was used for obtaining data:

1. Establish a dry-gas flow rate using the precision metering valve. Determine the actual dry gas flow rate using a bubble meter. Flow rates generally range from 15 ml/min to 75 ml/min at ambient temperature and pressure. Allow two or three minutes for equilibration of the reactor system.
2. Switch the sampling valve to the fill position. Allow 30 seconds for the sample loop to fill.
3. Switch the sample valve to the sample position while simultaneously pressing the injection reset/totalize button on the digital integrator.

4. Observe the output for the five detected components in the order: CO, CO_2, H_2S, H_2O, and COS. The gas chromatograph output for each component is given in analog fashion by the recorder and in digital form by the digital integrator.
5. Repeat steps (1) through (4) between three and five times.
6. Disconnect the thermocouple attached to the central reactor temperature controller. Connect it to a digital voltmeter and record the actual temperature at the center of the reactor.
7. After all desired flows at a given temperature are run, raise the reactor temperature 25°C by adjusting the two reactor temperature controllers.
8. Allow thirty minutes for the reactor to come to equilibrium at the new temperature.
9. Repeat steps (1) through (6).
10. Repeat steps (7) through (9) as often as desired or until an upper temperature limit is reached.

The flow rates chosen for a given catalyst depend upon (a) the reactor temperature, (b) the type of catalyst, and (c) the amount of catalyst in the microreactor. For example, flows were maintained in the faster flow regime for a "hot"

catalyst at higher temperatures. For such a catalyst, slower flow rates led to equilibrium conversions.

Shutdown. Shutdown procedures are similar to startup procedures:

1. Shut down the gas chromatograph by turning off the column heater, the hot wire detector heater, and the hot wire current.
2. Turn off the recorder and digital integrator detector.
3. Disconnect the power to the temperature controller for the two reactor zones, the water saturator, the sampling valve region, and the region between the reactor exit and sampling valve.
4. Switch off autotransformers controlling the heat-tapped exit lines and carrier lines between the sampling valve and chromatograph.
5. Open the water saturator bypass.
6. Allow fifteen minutes for cooling before shutting off dry reactant gas flow; then close the flow valves for the two regulators. Finally, close the precision metering valve.

Summary. A summary of the overall operating conditions for the catalytic microreactor apparatus is shown in Table II.

Table II

SUMMARY: OVERALL OPERATING CONDITIONS USED FOR THE STUDY OF "ALDRIDGE" WATER GAS SHIFT CATALYSTS

Operating Pressure Range:	approximately 1 atm.
Operating Temperature Range:	150°C to 450°C
Flow Rate Range:	100 ml/min to 10 ml/min. dry gas basis at room temperature and pressure
Length of Catalyst Bed:	less than 10 cm
Size of Reactor Tube:	Nominally 3/16-I.D. stainless steel tubing
Water Saturator Temperature:	60°C
Temperature of Gas Sampling Region:	150°C
Temperature of gas chromatographic column:	60°C
Quantity of catalyst:	from 0.1 gm to 1.5 gm
Space Velocity:	GHSV greater than 1000 at STP
Reactants:	H_2, CO, COS, H_2O
Products:	H_2, CO, COS, H_2O, CO_2, H_2S
Time for reactor to equilibrate for 25°C temperature change;	30 minutes
Chromatographic Analysis Time:	Approximately 5 minutes per sample

Melting Point Determination Apparatus

The following section describes an apparatus for determining in situ melting points of inorganic electrolytes.

Apparatus. The simple apparatus employed in melting point experiments is shown in Figure 10. It consists of:

1. A section of 4-hole 1/8-inch O.D. alumina rod that has a small trough at one end to contain the melt.
2. Two No. 24 gauge platinum wires threaded through the 6-inch length of alumina tubing and protruding into the small trough.
3. An iron-constantan thermocouple threaded through the remaining two holes of the alumina tubing and extending into the trough.

To heat the alumina tubing, an aluminum block with holes drilled for the tubing, a cartridge heater, and nitrogen sweep gas was built.

Procedure. The following procedure was followed for testing the suitability of the resistance drop technique for melting point determinations:

1. Place a several hundred milligram sample of 42.5 mole % $LiNO_3$/57.5 mole % KNO_3 eutectic mixture in the trough. This particular eutectic is useful for testing purposes because of its low

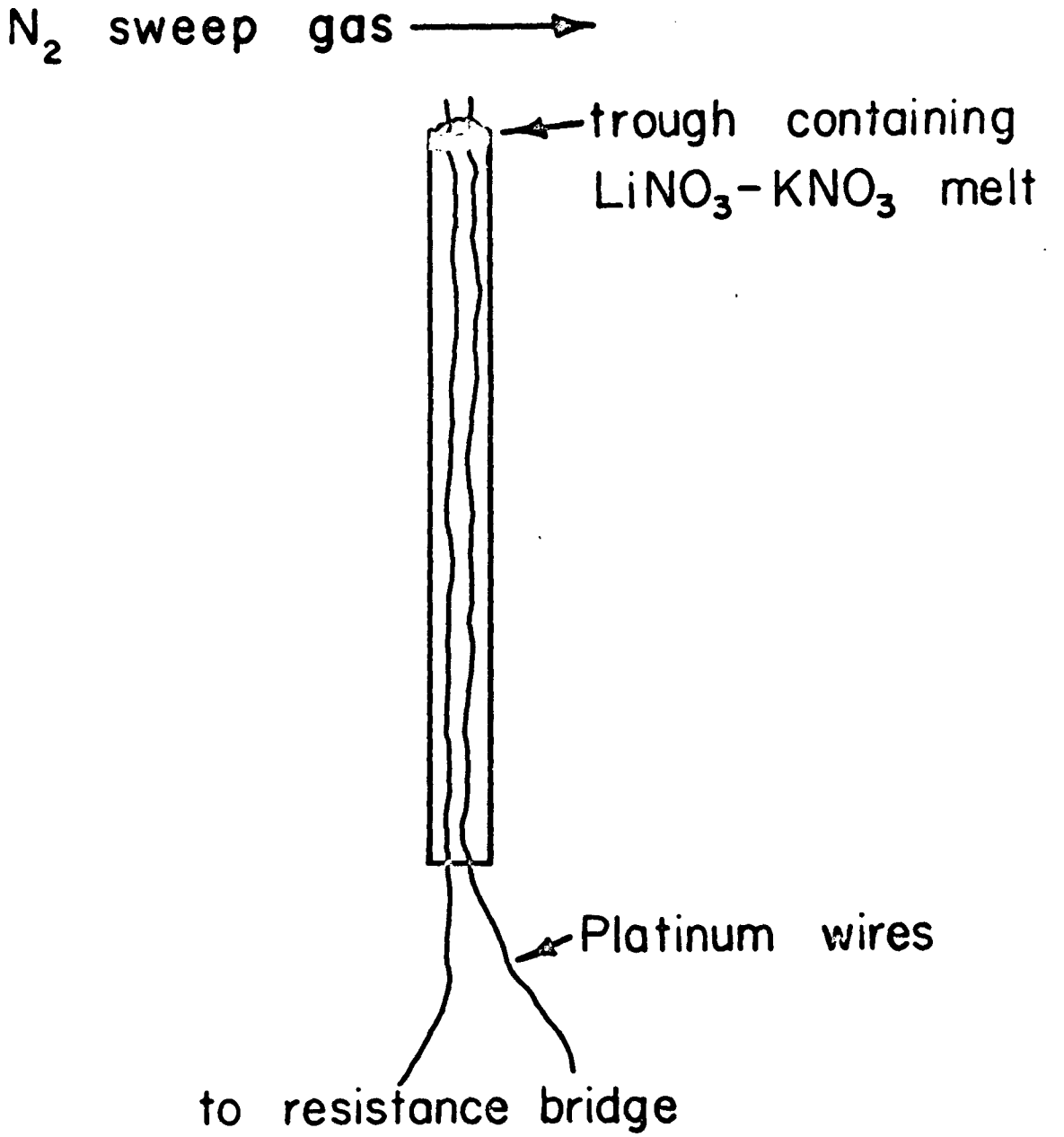

Figure 10. Schematic Diagram of Apparatus to Measure in situ Melting Points.

melting point of 124°C.

2. Insert the alumina rod into the aluminum block and bathe the trough with a flowing stream of nitrogen in order to maintain anhydrous conditions. [NOTE: This precaution is absolutely necessary].
3. Incorporate the platinum wire into a wheatstone bridge driven at 1 KHz via an audio oscillator. Use a digital multimeter set on the AC volts scale as a null indicator. Make no attempt to null the stray capacitance in the bridge.
4. Heat the aluminum block slowly by controlling the cartridge heater with an autotransformer.
5. Record temperature as a function of time.
6. Record resistance as a function of time, using a decade resistance box to null the bridge.

A typical plot shown in Figure 11, demonstrates that a melting point at about 130°C, could be readily identified by a ten-fold change in resistance. The two data points at the highest resistance were questionable due to the large intervals in the decade resistance box at high resistances. A ten-fold drop in resistance, though significant, was not as high as expected.[22]

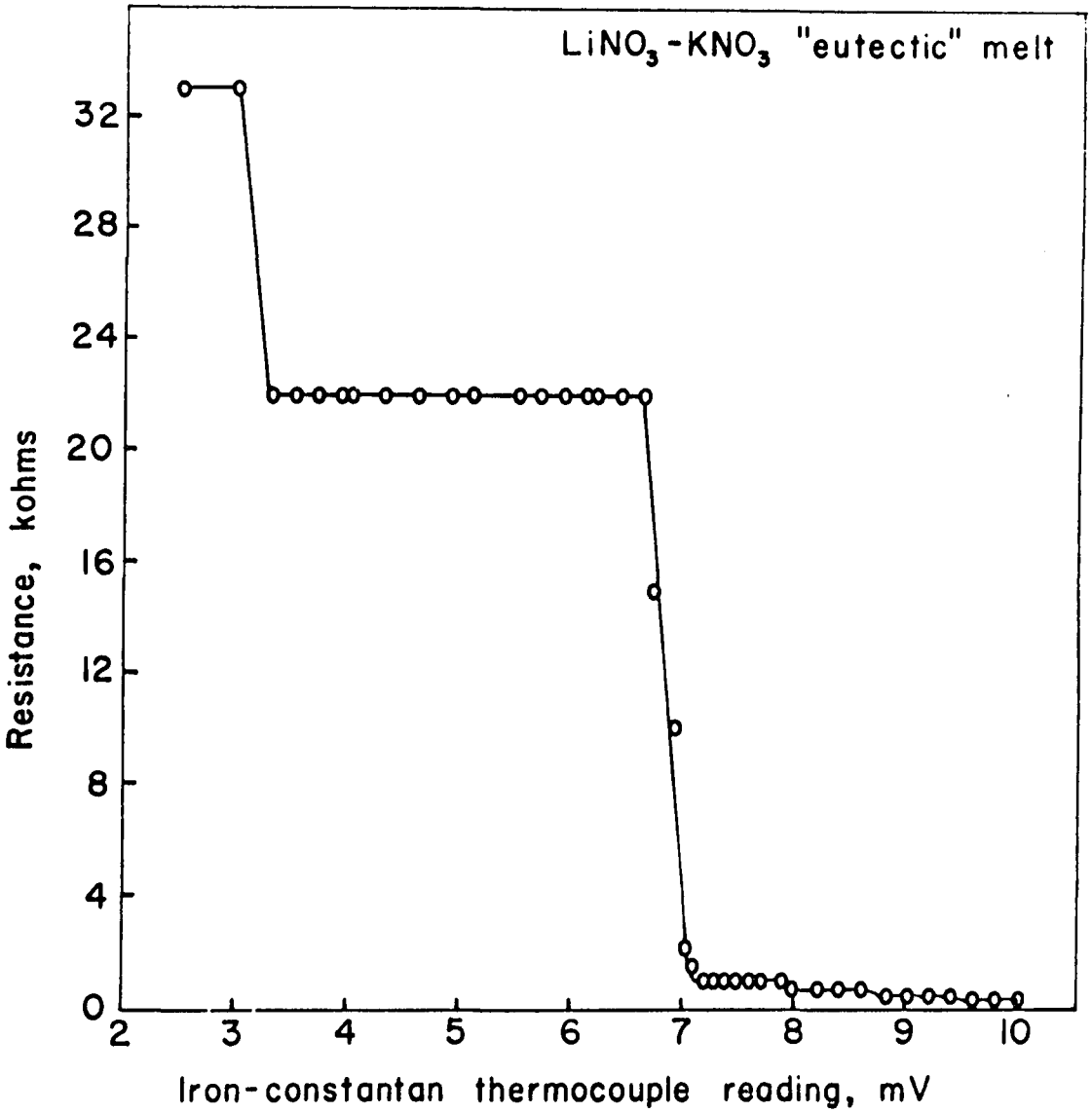

Figure 11. Determination of the Melting Point of a $LiNO_3$-KNO_3 "eutectic" Melt Using the Apparatus of Figure 10.

Digital Integrator-Minicomputer Interface. As a first step towards the construction of a completely automated reactor system, an interface was designed and built to transmit data from the Autolab digital integrator to a PDP 8/E minicomputer. Since this interface will be expanded by subsequent researchers, a complete description of it is included in Appendix V.

The interface, in its present state of development, can perform several functions:

1. Transmit peak areas and retention times for the components detected by the gas chromatograph to the PDP 8/E minicomputer located five laboratories away.
2. Assuming that a mass balance exists, calculate initial and final mole fractions for all detected components.
3. Print out this information on a teletypewriter located at the minicomputer.

Since no provision exists for transmitting reactor temperature and flow rates, a full analysis of reactor data, especially for systems which are close to equilibrium, is not possible.

The interface was fully tested during one full day of reactor operation and was found to perform quite well. However, it was not used in the studies of the "Aldridge"

catalyst due to its limitations for data analysis. The main function of the interface is as a first step towards eventual reactor automation.

IV. THEORETICAL

Seven "Aldridge" catalysts, differing only in the amount of cesium acetate added to the Nalcomo 474 Co-Mo/Al_2O_3 catalyst, were investigated in the fixed-bed microrector. Product gas composition was analyzed as a function of flow rate and temperature. For each catalyst, a dry gas feed stream of 49% H_2/49% CO/2% COS saturated with water vapor at a temperature of 60°C was employed.

The techniques whereby data for this study were manipulated and analyzed is presented in this section.

Steady State Plug Flow Reactor Model

A steady state plug flow reactor model is a material balance for an idealized tubular reactor. When discussing the plug flow reactor model, a convenient term that one uses is the space time, defined as the time to process one reactor volume of feed at reactor conditions, or,

$$\text{space time} = \tau = \frac{V}{F} \quad \frac{\text{reactor volume}}{\text{volumetric feed rate at reactor conditions}}$$

Levenspiel[23] gives the relationship between space time, reactor conversion, and the rate of reaction for a steady-state plug flow reactor:

$$\tau = C_{A0} \int_{X_A^o}^{X_A} \frac{dx_A}{-r_A} \qquad (1)$$

where, C_{A0} = inlet concentration of A, gm moles/liter

X_{A0} = initial conversion of A

X_A = final conversion of A

$-r_A$ = rate of loss of A, moles of A lost/ unit volume of reactor-time

Equation (1), known as the design equation for a steady state plug flow reactor is used as the design equation for the catalytic microreactor.

Overall Rate of Reaction

Before equation (1), the plug flow reactor design equation, can be integrated, an expression is needed for the rate of reaction, $-r_A$. Since phase boundaries are present in heterogeneous systems, a variety of forms for the rate of reaction are possible. Smith[24] outlines seven steps that must occur in series for the conversion of reactants to products in porous, heterogeneous catalyts:

1. Transport of reactants from the bulk fluid to the fluid-solid interface (exterior mass transfer).
2. Intraparticle transport of reactants into the catalyst particle (pore diffusion).

3. Adsorption of reactants at interior sites of the catalyst particle.
4. Chemical reaction of adsorbed reactants to form adsorbed products (surface reaction).
5. Desorption of adsorbed products.
6. Transport of products from the interior sites to the outer sites of the catalyst particle (pore diffusion).
7. Transport of products from the fluid-solid interface into the bulk-fluid stream (exterior mass transfer).

The potential existence of a molten salt existing within the pores will change some of the above seven steps. Thus, steps (3) through (5) in Smith's list most likely must be replaced by the following:

3. Dissolution of reactants in the melt or adsorption of the reactants on the surface of the melt.
4. Homogeneous reaction within the melt or surface reaction on the surface of the melt to form products.
5. Dissolution of products from the bulk melt or desorption of products from the surface of the melt.

A determination of the actual reaction sequence for a molten salt catalyst is beyond the scope of this study.

Physical Processes

It is desirable in catalytic studies to make step (4) in the above lists the rate-controlling step in the reaction sequence. In order to do this, the resistances caused by intraparticle and interparticle diffusion must be made small.

Exterior Mass Transfer. The rate of exterior mass transfer may be represented by:

$$\text{rate of mass transfer} = k_g\, a_p\, \Delta c \text{ (moles/sec)}$$

in which a_p = catalyst particle area, cm^2

Δc = concentration difference, gm moles/cm^3

k_g = mass transfer coefficient, cm/sec

The film coefficient, k_g, is proportional to the catalyst particle diameter and the gas velocity relative to the surface of the particle. For packed catalyst beds and flow past spheres, the proportionality is[25]:

$$k_g \propto (u/d_p)^{1/2}$$

in which u = bulk gas velocity, cm/sec

d_p = catalyst particle diameter, cm

A large mass transfer coefficient is desirable for negligible mass transfer resistance, which implies that catalyst particles should be small and gas velocities relative to the surface should be high.

Pore Diffusion. A second type of transport effect is diffusion control within the catalyst particle, where the majority of surface area is found. Mass diffusion into pores produces an intraparticle concentration gradient, the effect of which on the rate of reaction is accounted for by the effectiveness factor introduced by Thiele[26]:

$$\varepsilon = \frac{\text{average reaction rate within a pore}}{\text{maximum reaction rate if pore diffusion was absent}}$$

Aris[27] and others have related the effectiveness factor to Φ, the Thiele modulus, for an average catalyst pore:

$$\varepsilon = \frac{\tanh \Phi}{\Phi} \qquad (2)$$

The Thiele modulus is defined by:

$$\Phi = L \sqrt{k/D} \qquad (3)$$

where, L = length of catalyst pore, cm

k = pseudo first order rate constant on a volumetric basis, per time

D = effective volumetric diffusion coefficient in catalyst, area/time

For the effectiveness factor to be close to unity, small pore lengths, slow rates of reaction, and large diffusion coefficients are required. More detailed treatments of the Thiele modulus are given by Peterson[28] and by Satterfield[29].

Integration of the Plug Flow Reactor Design Expression

Once we have convinced ourselves that our experimental design will serve to eliminate the effect of physical processes on the rate of reaction, we may integrate equation (1), the plug flow reactor design expression.

First, equation (1) is cast in terms of carbon monoxide concentration:

$$\tau = \frac{V}{F} = - \int_{C_{co}^{o}}^{C_{co}} \frac{dC_{co}}{-r_{co}} \qquad (4)$$

in which, V = volume of effective catalyst bed volume (inerts excluded), cm^3

F = flow rate of reactant gases at reactor conditions, cm^3/min

C_{co}^{o}, C_{co} = initial and final carbon monoxide concentrations, gm moles/cm^3

$-r_{co}$ = rate of loss of carbon monoxide, $\frac{\text{gm moles}}{cm^3 \text{ of effective catalyst bed volume-min}}$

Equation (4) is now written in a more appropriate form for a reversible reaction which involves C_{co}^{eq}, the concentration of carbon monoxide at equilibrium conversion:

$$\frac{V}{F} = - \int_{C_{co}^{o}}^{C_{co}} \frac{d[C_{co} - C_{co}^{eq}]}{-r_{co}} \tag{5}$$

If we take advantage of the fact that d ln x = 1/x dx, equation (5) may be written as:

$$V/F = - \int_{C_{co}^{o}}^{C_{co}} \left\{ \frac{C_{co} - C_{co}^{eq}}{-r_{co}} \right\} d \ln (C_{co} - C_{co}^{eq}) \tag{6}$$

We now assume, *for sufficiently low conversions,* that the quantity $\left\{ \frac{C_{co} - C_{co}^{eq}}{-r_{co}} \right\}$ is approximately constant.

Note that this assumption differs from Levenspiel's definition of a differential reactor; he assumes only the inverse rate to be constant.[30] Integrating equation (6) with the above assumption yields:

$$\frac{V}{F} = - \left\{ \frac{C_{co} - C_{co}^{eq}}{-r_{co}} \right\} \ln \left\{ \frac{C_{co} - C_{co}^{eq}}{C_{co}^{o} - C_{co}^{eq}} \right\} \tag{7}$$

Equation (7) represents the final, integrated form of the plug flow reactor design equation.

From equation (7) we note that a plot of $-\ln\left\{\frac{C_{co}-C_{co}^{eq}}{C_{co}^{o}-C_{co}^{eq}}\right\}$ versus 1/F has a slope of $V \times \frac{-r_{co}}{C_{co} - C_{co}^{eq}}$. We now note that a rate expression which is first order and reversible in carbon monoxide concentration has the form:

$$-r_{co} = k\ (C_{co} - C_{co}^{eq}) \qquad (8)$$

in which k is the first order rate constant, min^{-1}. In such a case, our slope equals kV. However, no rate expression was assumed in deriving equation (7); only that the quantity $(\frac{C_{co}-C_{co}^{eq}}{-r_{co}})$ is constant. The quality of our assumption over the entire range of conversions studied can be experimentally tested by the linearity of the plot of

$$-\ln\left\{\frac{C_{co}-C_{co}^{eq}}{C_{co}^{o}-C_{co}^{eq}}\right\} \text{ versus } 1/F.$$ Thus we may use conversion versus flow rate data to determine either absolute rates or pseudo-first order rate constants.

Arrhenius Plot

A series of conversion versus flow rate data for various temperatures gives kV versus temperature data for a catalyst.

The kV values are first normalized by the weight of catalyst used, W, to give kV/W vs temperature data. The actual weights used for normalization purposes consist of only the unimpregnated $CoO\text{-}MoO_3$ catalyst. The cesium acetate contribution to the catalyst weight is not included because cesium acetate is not known to have any catalytic properties. By using the unimpregnated weight, the true value of the molten cesium component may be more easily seen. The weight of the inert alumina filler is also not included in the computation of W. Because of this choice for W, the value of V referred to above is actually the volume of unimpregnated hydrotreating catalyst and does not include the inert alumina filler.

Values of ln(kV/W) are plotted versus reciprocal temperature. The standard Arrhenius form is assumed for k:

$$k = k_o \, e^{-E_a/RT}$$

where, k_o = frequency factor, $time^{-1}$

E_a = activation energy, cal/gm mole

R = gas low constant

T = temperature, °K

Clearly, a plot of $\ln (\frac{kV}{W})$ versus 1/T will have a slope of $-E_a/R$ and an intercept of $\ln (k_o V/W)$.

The intercept of $\ln \frac{k_o V}{W}$ allows the value of $k_o V/W$ to be determined, where k_o is a frequency factor, V is the catalyst bed volume, and W is the weight of catalyst. A value of W/V for unimpregnated $CoO\text{-}MoO_3$ catalyst of 20/60 seize size particles was found to be 0.65 gms/cm^3. The frequency factor can thus be obtained by multiplying $k_o V/W$ by the W/V value.

The Arrhenius plots are used to give the temperature dependance of the pseudo-first order rate constants. Where an obvious change of slope occurs in the plots of ln (kV/W) versus reciprocal temperature, two straight lines are used to fit the data.

Sample Calculations

To demonstrate the application of the preceeding theoretical development, sample calculations of all steps involved in the conversion of data are now presented. The example involves catalyst No. 4.

Conversion of Raw Chromatographic Data

A typical chromatogram for catalyst No. 4 is shown in Figure 12. The data shown were obtained for a single flow rate at a single temperature. Similar data were obtained for each flow rate at each temperature for all catalysts studied. A total of approximately 250 data

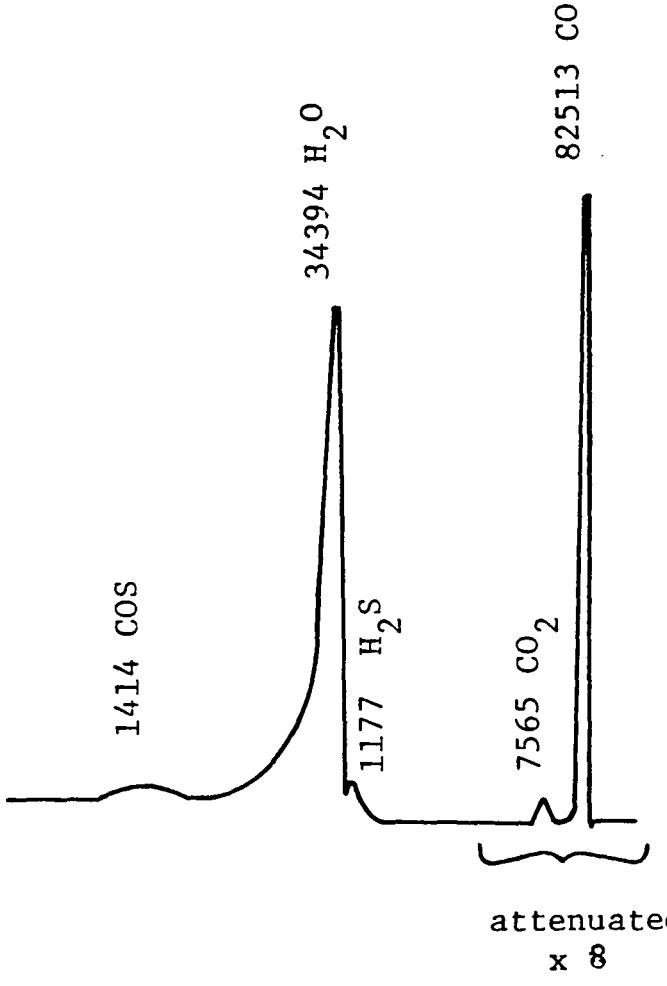

Catalyst No. 4

Flow = 10 ml/27.7 sec at room temperature = 25°C

Reactor Temperature = 229°C

Figure 12. Typical Chromatogram and Peak Areas.

points were thus obtained.

Two reactions occurred in the catalytic screening microreactor. The first of these was the water gas shift reaction:

$$CO + H_2O \rightleftharpoons H_2 + CO_2 \qquad (9)$$

The second reaction was of minor consequence due to the small amount of carbonyl sulfide present in the reactant gas feed:

$$H_2S + CO \rightleftharpoons COS + H_2 \qquad (10)$$

With a reactant gas feed of H_2, CO, COS, and H_2O the effluent gas should contain H_2S and CO_2 in addition to the four reactants. As seen in Figure 12, no peak is eluted for hydrogen, owing to the fact that the thermal conductivity of hydrogen is lower than that for the helium carrier. It was necessary to assume a mass balance in order to calculate initial and final mole fractions for all components.

Sensitivity Factors. Sensitivity factors obtained by McNair[31] (shown in Table III) are used in the first step in analyzing the data of Figure 12, which is to multiply the peak areas by the respective molar sensitivity factors. Assume a basis of moles of each component equalling the corrected area. Let N_{CO}, N_{CO_2}, N_{H_2S}, N_{H_2O},

and N_{cos} equal the corrected molar peak counts for each component. Then,

$$N_{co} = \begin{matrix}\text{peak area} \\ \text{of co}\end{matrix} \times \begin{matrix}\text{sensitivity factor} \\ \text{of co}\end{matrix} = 82513 \times 1.1506$$

$$= 94939$$

$$N_{co_2} = \begin{matrix}\text{peak area} \\ \text{of } co_2\end{matrix} \times \begin{matrix}\text{sensitivity factor} \\ \text{of } co_2\end{matrix} = 7565 \times 1.0$$

$$= 7565$$

$$N_{H_2S} = \begin{matrix}\text{peak area} \\ \text{of } H_2S\end{matrix} \times \begin{matrix}\text{sensitivity factor} \\ \text{of } H_2S\end{matrix} = 1177 \times 1.2587$$

$$= 1481$$

$$N_{H_20} = \begin{matrix}\text{peak area} \\ \text{of } H_20\end{matrix} \times \begin{matrix}\text{sensitivity factor} \\ \text{of } H_20\end{matrix} = 34394 \times 1.4693$$

$$= 50535$$

$$N_{cos} = \begin{matrix}\text{peak area} \\ \text{of COS}\end{matrix} \times \begin{matrix}\text{sensitivity factor} \\ \text{of COS}\end{matrix} = 1414 \times 1.0$$

$$= 1414$$

Backcalculated Mass Balance. Using the corrected molar peak counts of CO, CO_2, H_2S, H_20, and COS, a backcalculated mass balance can be made. Let N^o_{co}, $N^o_{co_2}$, $N^o_{H_2S}$, $N^o_{H_20}$, N^o_{COS}, and $N^o_{H_2}$ be the initial number of moles for each component. The fact that hydrogen and carbon monoxide were initially present in equal amounts in the feed, and that no hydrogen sulfide or carbon dioxide were present

Table III

SENSITIVITY FACTORS FOR ELUTED COMPONENTS

	Component				
	CO	CO_2	H_2S	H_2O	COS
Sensitivity factor on a weight basis	0.67	0.915	0.89	0.55	
Sensitivity factor on a molar basis	0.02393	0.0208	0.0262	0.03055	
Normalized molar sensitivity factor	1.15066	1.0	1.2587	1.4693	(1.0)[a]

Values obtained from McNair, "Basic Gas Chromatography," Varian Aerograph, (1967).

[a]Value for COS was assumed.

initially, was used in making such a mass balance. The mass balance is made as follows, utilizing the stoichiometry of equations (9) and (10):

1. The initial number of moles of CO must equal the final number of moles of CO plus the final number of moles of CO_2 less the moles of CO produced by the conversion of COS, or:

$$N^{o}_{co} = N_{co} + N_{co_2} - N_{H_2S}$$

$$N^{o}_{co} = 94939 + 7565 - 1481 = 101023$$

2. From equation (9), the initial moles of water must equal the final number of moles of water plus the number of moles converted to CO_2, or:

$$N^{o}_{H_2O} = N_{H_2O} + N_{co_2}$$

$$N^{o}_{co_2} = 50535 + 7565 = 58100$$

3. From equation (10), the initial number of moles of COS must equal the final number of moles of COS plus the amount of COS converted to H_2S, or:

$$N^{o}_{cos} = N_{cos} + N_{H_2S}$$

$$N^{o}_{cos} = 1414 + 1481 = 2895$$

4. From the initial conditions, the number of moles of H_2 equals the number of moles of CO; also, the initial number of moles of CO_2 and H_2S equal zero, or:

$$N^o_{H_2} = N^o_{CO} = 101023$$

$$N^o_{H_2S} = 0$$

$$N^o_{CO_2} = 0$$

5. The final number of moles of H_2 equals the initial moles of H_2 plus the amount created in equation (9) less the amount used via equation (10), or,

$$N_{H_2} = N^o_{H_2} + N_{CO_2} - N_{H_2S}$$

$$N_{H_2} = 101023 + 7565 - 1481 = 107107$$

Once the initial and final number of moles are known for all components, they are normalized to yield mole fractions:

Component	Initial Mole Fraction	Final Mole Fraction
CO	0.384	0.301
H_2O	0.221	0.192
H_2	0.384	0.407
CO_2	0.0	0.029
COS	0.011	0.005
H_2S	0.0	0.006

Integral Data Analysis

As shown by equation (7), written in terms of mole fractions, a plot of $- \ln \left\{ \frac{X_{co} - X_{co}^{eq}}{X_{co}^{o} - X_{co}^{eq}} \right\}$ versus the reciprocal flow rate should be linear and have a slope of kV. The initial and final mole fractions of carbon monoxide are obtained by the material balance. The equilibrium concentration of carbon monoxide must be obtained from equilibrium data. The reciprocal flow rate must be calculated on a wet basis at reactor conditions.

Equilibrium Calculations. For the temperature of 229°C shown in Figure 12, the equilibrium constants are, for equations (9) and (10), respectively[32]:

$$K1 = 126.65 \quad \text{(dimensionless)}$$

$$K2 = 0.1428 \quad \text{(dimensionless)}$$

where K1 is the equilibrium constant for equation (9) and K2 is the equilibrium constant for equation (10). The equilibrium constants were found by a logarithmic interpolation procedure from tables of equilibrium constants.

If we let X equal the number of moles of carbon monoxide consumed in equation (9), Y equal the number of moles of carbon monoxide consumed in equation (10), and take a basis of one mole of reactant gas, then the following calculation can be made:

Component	Initial No. of Moles	Final No. of Moles at equilibrium
CO	0.384	0.384 - X - Y
H_2O	0.221	0.221 - X
H_2	0.384	0.384 + X + Y
CO_2	0.0	0.0 + X
COS	0.011	0.011 + Y
H_2S	0.0	0.0 - Y

Also, from the definition of the equilibrium constants,

$$K1 = 126.65 = \frac{(0.384 + X + Y)\ (0.0 + X)}{(0.384 - X - Y)\ (0.221 - X)}$$

$$\text{and } K2 = 0.1428 = \frac{(0.0384 + X + Y)\ (0.011 + Y)}{(0.384 - X - Y)\ (0.0 - Y)}$$

Solving these two equations by a simultaneous Newton-Rapheson procedure gives the solution for X and Y:

$$X = 0.21525$$

$$Y = -\ 0.01055$$

Knowing X and Y enables us to compute final mole fractions for all components:

Component	Final Mole Fraction at equilibrium
CO	0.179
H_2O	0.006
H_2	0.589
CO_2	0.215
COS	0.005
H_2S	0.011

If we know the initial, final, and equilibrium mole fractions for carbon monoxide, we can compute the quantity,

$$- \ln \left\{ \frac{X_{co} - X_{co}^{eq}}{X_{co}^{o} - X_{co}^{eq}} \right\} :$$

$$- \ln \left\{ \frac{X_{co} - X_{co}^{eq}}{X_{co}^{o} - X_{co}^{eq}} \right\} = - \ln \left(\frac{0.361 - 0.179}{0.384 - 0.179} \right) = 0.120$$

Wet Flow Rate. As shown by Figure 12, the dry gas flow rate was 10 ml/27.7 seconds. The bubble meter was at the reactor pressure but at room temperature. To correct this flow rate to a wet basis at reactor conditions, we must multiply by a temperature correction factor and divide by the initial mole fraction of all non-water components:

$$\text{Wet flow rate at reactor conditions} = \frac{\frac{10 \text{ ml}}{27.7 \text{ sec.}} \times \frac{60 \text{ sec.}}{\text{min}} \times \frac{273°K+229°C}{273°K+25°C}}{(1. - 0.384)}$$

$$= 46.9 \text{ cm}^3/\text{min}$$

The flow rate in the reactor is independent of conversion since the stoichiometry of equations (9) and (10) are such that one mole of product is formed for each mole of reactant consumed.

Computer Analysis

A summary of the data analysis technique for a typical catalyst is given below:

1. Set the reactor temperature.
2. Set a reactant gas flow rate and analyze product gas composition.
3. Calculate initial and final mole fractions for all components with the aid of an assumed mass balance.
4. Use the initial mole fractions of all components to calculate the final equilibrium composition of all components assuming the reactions given by equations (9) and (10) both reach equilibrium.
5. Evaluate the quantity $- \ln \left\{ \frac{X_{co} - X_{co}^{eq}}{X_{co}^{o} - X_{co}^{eq}} \right\}$ and reciprocal flow rate on a wet basis.
6. Repeat steps (2) through (5) until all desired flows for a given temperature have been studied.
7. Determine a least square fit of $a - \ln \left\{ \frac{X_{co} - X^{eq}}{X_{co}^{o} - X_{co}^{eq}} \right\}$ versus reciprocal flow rate plot. Obtain correlation coefficients, slopes, and intercepts both with and without (0,0) considered as a data point.

8. Repeat steps (1) through (7) for all reactor temperatures.

A computer program was developed to perform steps (3) through (7) of the above procedure. For each flow rate, the inputs required are: (1) final peak areas for CO, CO_2, H_2S, H_2O, and COS; (2) flow rate on a dry basis at reactor conditions; and (3) reactor temperature.

Figure 13 is an example of computer output for the chromatogram shown in Figure 12. The conversion parameteer referred to is the quantity $- \ln \left\{ \frac{X_{co} - X_{co}^{eq}}{X_{co}^{o} - X_{co}^{eq}} \right\}$.

A listing and explanation of the data analysis program appears in Appendix III.

Reciprocal Flow Plots

The value of 0.120 obtained for the quantity $- \ln \left\{ \frac{X_{co} - X_{co}^{eq}}{X_{co}^{o} - X_{co}^{eq}} \right\}$ and the reciprocal of the wet flow rate of 46.9 cm^3/min, form one point on the curve of $- \ln \left\{ \frac{X_{co} - X_{co}^{eq}}{X_{co}^{o} - X_{co}^{eq}} \right\}$ versus 1/F suggested by equation (7). Between three and five such points are obtained for each temperature, culminating in a plot such as Figure 15 for catalyst No. 4.

Temperature = 229.00 DEG C X = 0.21527 Y = -0.01055 K1 = 126.65740

K2 = 0.1427793 Dry Flow = 36.57500 Flow = 46.94205 1/Flow = 0.0213029

	Carbon Monoxide	Water	Hydrogen	Carbon Dioxide	COS	H. Sulfide
Initial Concentration:	0.38407	0.22085	0.38407	0.00000	0.01101	0.00000
Final Equil. Conc.:	0.17935	0.00558	0.58879	0.21527	0.00046	0.01055
Final Concentration:	0.36094	0.19209	0.40720	0.02876	0.00538	0.00563

Conversion Parameter = 0.11988

Figure 13. Output of Data Analysis Program for One Flow Rate.

The slope of the line for 229°C from Figure 15 equals kV and has a value of 4.84 cm^3/min. The amount of unimpregnated catalyst No. 4 used is 0.129 grams. If kV is normalized by the weight of unimpregnated catalyst, we have a value of kV/W equal to 37.5 cm^3/gm catalyst-min.

Arrhenius Plot

For catalyst No. 4, the logarithms of the normalized kV values are plotted versus reciprocal temperature in the classical Arrhenius fashion, as shown by Figure 24. The plot is broken into two sections, which is a consequence of probable diffusion control at the higher temperatures. The slopes of the Arrhenius plot equal $- E_a/R$, where E_a is the activation energy, cal/gm mole, and R is the gas constant. If we multiply the slopes of the Arrhenius plot by (-R), we obtain values for the activation energies shown on Figure 24. For the low temperature range, E_a equals 17.6 Kcal/gm mole.

The intercepts of the Arrhenius plot equal $\ln \frac{k_o V}{W}$,

where k_o = frequency factor, min^{-1}

V/W = volume to weight ratio of non-impregnated hydrotreating catalyst, cm^3/gm.

The W/V ratio was experimentally determined and found to equal 0.65 gms/cm^3. The k_o value is found by multiplying the exponential of the Arrhenius plot intercept by 0.65 gms/cm^3. For the low temperature range of Figure 24:

$$k_o = 0.65 \exp \text{(intercept)}$$

$$\text{or, } k_o = 0.65 \exp (21.39) = 1.27 \times 10^9 \text{ min}^{-1}.$$

Thus, for the low temperature range of Catalyst No. 4, the temperature dependance of the psuedo-first order rate constant is:

$$k = k_o \, e^{-E_a/RT}$$

$$k = 1.27 \times 10^9 \text{ min}^{-1} \exp (-\ 17600 \text{ cal/gm mole-RT}).$$

A similar analysis holds true for the determination of the activation energy and frequency factor for the high temperature range of Catalyst No. 4.

V. RESULTS

In this section we present results obtained from a study of seven different "Aldridge" water gas shift catalysts.

Preliminary Studies

We conducted a number of preliminary studies in order to determine reaction conditions and the amounts of catalyst that would be required in our final high-precision detailed "kinetic" runs.

Reactor Conditions

The dry gas feed we used in this study consisted of 49% CO/49% H_2/2% COS. Once we had chosen this feed, the two major questions were: (1) At what pressure should the reaction be performed? (2) At what temperature should the water saturation be controlled, i.e., what should be the steam-to-dry-gas ratio?

Reactor Pressure. We initially studied the water gas shift reaction at 100 psig, a pressure at which we encountered problems owing to the presence of a competing methanation reaction,

$$CO + 3H_2 \rightleftarrows CH_4 + H_2O$$

Such a reaction is favored by higher pressure.

After lowering the reactor pressure to one atmosphere, we observed no methane at this pressure. All subsequent water gas shift studies were performed at one atmosphere pressure.

Water Saturator Temperature. The water saturator temperature sets the steam-to-dry-gas ratio in the reactant feed. For any given saturator temperature, the initial steam-to-dry-gas ratio should be constant and determined by the vapor pressure of water at that temperature.

When the water gas shift reaction was initially studied at one atmosphere we observed that the initial percentages of water would vary as a function of the feed gas flow rate. When the flow rate increased, initial water percentage decreased owing to the slightly greater pressure drop at higher flow rates. At higher reactor pressures, this effect was completely masked.

We found that a water saturator temperature of 60°C led to a stable steam-to-dry-gas ratio of 1.0 to 3.35; this saturation temperature was used for all subsequent water gas shift studies. High saturator temperatures, such as 90°C, led to considerable variations in the steam-to-dry gas ratio with changing dry flow rates.

Catalyst Composition

We actually studied seven "Aldridge" catalysts with varying amounts of cesium acetate. We determined, largely by trial and error, that a total bed size of 1.5 grams containing between 0.1 and 1.0 grams of catalyst and inert alumina for the remainder of the bed, gave good results. The inert alumina served to eliminate "hot spots" in the bed.

The catalysts we studied are listed in Table IV. Two different amounts of catalyst No. 5 were used for purposes of studying a high temperature region and a low temperature region.

Catalyst No. 1 was the first "Aldridge" catalyst studied. The catalyst bed was not diluted and therefore we do not compare catalyst No. 1 with the other catalysts studied.

Plug Flow Reactor Rate

As explained in the theoretical section, the integrated design expression for a plug flow reactor is:

$$-\ln \left\{ \frac{x_{co} - x_{co}^{eq}}{x_{co}^{o} - x_{co}^{eq}} \right\} = \left\{ \frac{-r_{co}}{C_{co} - C_{co}^{eq}} \right\} \frac{V}{F} = k \frac{V}{F}$$

Table IV

AMOUNTS OF CATALYST AND INERTS USED FOR WATER GAS SHIFT STUDY

	Catalyst No.							
	1	4	5[1]	5[2]	5A	5B	5C	6
Total catalyst weight, grams	0.112	0.157	1.001	0.283	0.295	0.298	0.349	0.502
Weight of Unimpregnated Hydrotreating catalyst, grams	0.076	0.129	0.861	0.244	0.26	0.276	0.33	0.502
Weight of Inert Alumina Filler, grams	0.0	1.343	0.5	1.217	1.2	1.2	1.15	1.0
Total bed weight, grams	0.112	1.5	1.5	1.5	1.5	1.5	1.5	1.5
Grams of CsOAc per cm^3 pore volume	1.048	0.42	0.35	0.35	0.246	0.141	0.070	0.0

[1] Low temperature range for catalyst 5, 132°C-228°C.

[2] High temperature range for catalyst 5, 202°C-402°C.

where, x_{co}^{o}, x_{co}, x_{co}^{eq} = initial, final, and equilibrium carbon monoxide mole fractions, respectively.

$-r_{co}$ = rate of disappearance of carbon monoxide, $\frac{\text{gm moles}}{\text{cm}^3 \text{ of effective catalyst bed volume-min}}$

C_{co}, C_{co}^{eq} = final and equilibrium carbon monoxide concentrations, respectively, gm moles/cm^3

V = volume of effective catalyst bed volume (inerts excluded), cm^3

F = flow rate of reactant gases at reactor conditions, cm^3/min

k = pseudo-first order rate constant, min^{-1}

If we plot $-\ln \left\{ \frac{x_{co}-x_{co}^{eq}}{x_{co}^{o}-x_{co}^{eq}} \right\}$ versus 1/F, the slope of the resulting line equals $\left(\frac{-r_{co}}{C_{co}-C_{co}^{eq}}\right)$ V or k V.

We obtained plug flow reactor data at several temperatures for the seven catalysts mentioned in Table IV and plotted the data in the manner mentioned above. We also obtained data for a bed of 1.5 grams of inert alumina. The plots are given in Figures 14 through 22.

The inert bed had some activity; however, it was less than five percent of the most inactive "Aldridge" catalyst studied. We made no correction for the effect of the inert

bed on the "Aldridge" catalysts studied.

The lines drawn in the integral data figures were determined via a least squares analysis section of the computer analysis program. Correlation coefficients were greater than 0.95 for all lines drawn. The large volume of data made it impractical for us to include the computer analysis output for all points shown on the plots. The data are adequately represented by the figures given. As stated previously, all data were obtained at one atmosphere with a dry gas feed of 49% H_2/49% CO/2% COS and a steam-to-dry-gas ratio of 1 to 3.35. The slopes of all lines given in Figures 14 through 21 are listed in Tables V through XII as kV in units of cm^3/min.

The data that we presented in Figures 14 through 22 are obviously well correlated by the integrated plug flow reactor design expression. This does not mean, however, that the assumptions made in integrating the design expression would lead to such good results at pressures or reactant gas compositions different from those we employed in this study. This fact is important to note for future work done with the "Aldridge" catalyst. We used a fixed-feed gas composition for our entire study and collected all data at one atmosphere pressure.

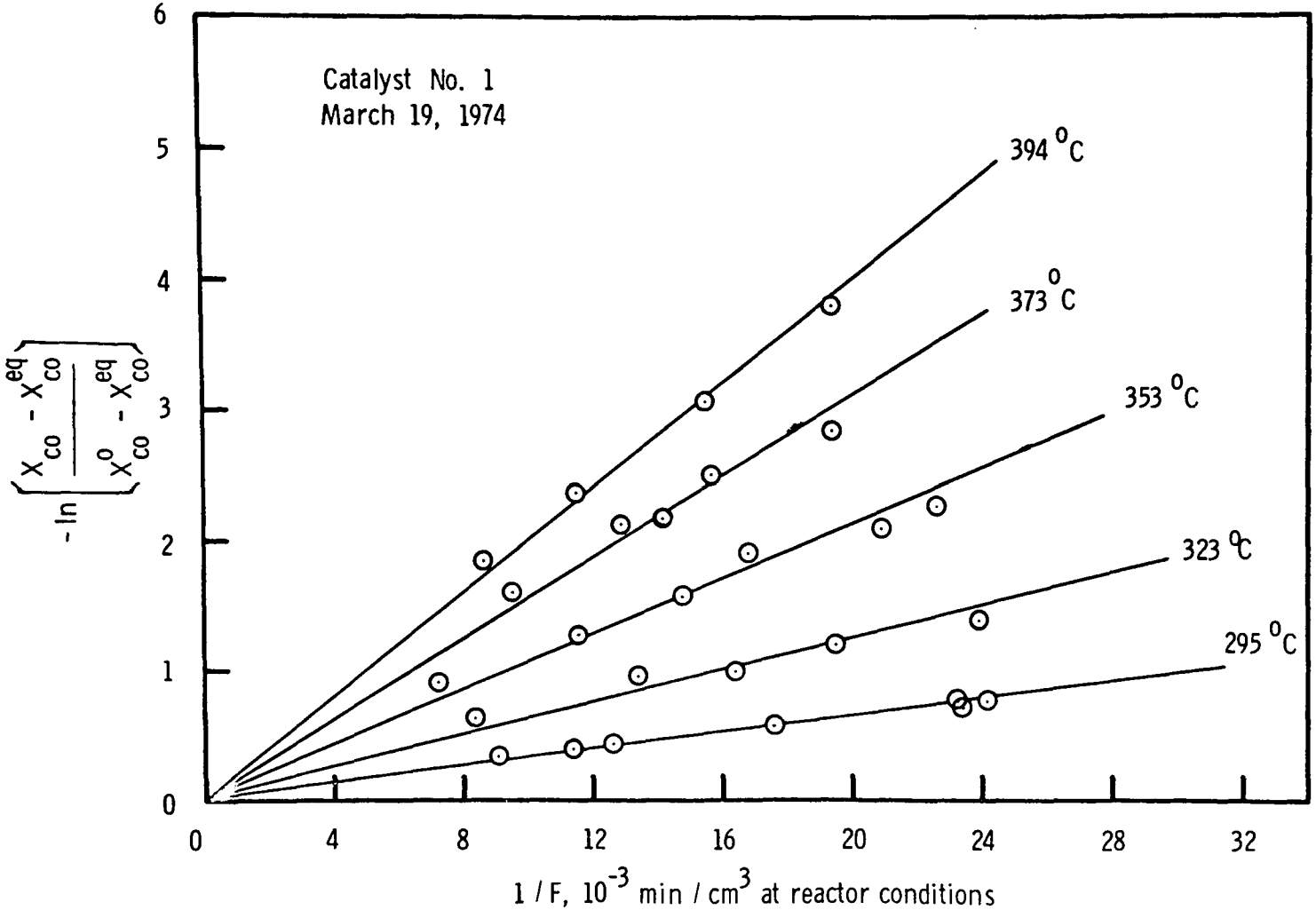

Figure 14. Integral Plug Flow Reactor Data for Catalyst No. 1.

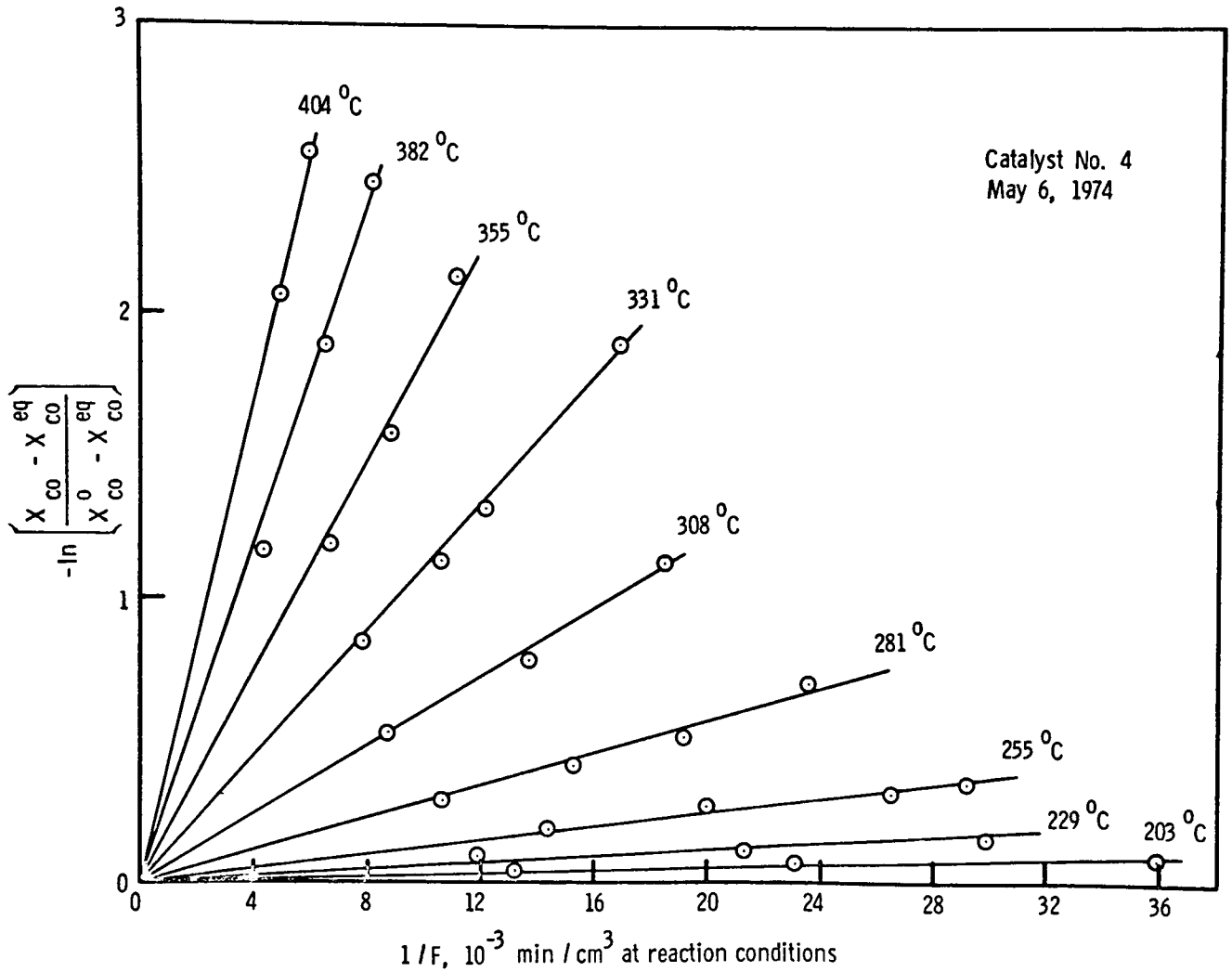

Figure 15. Integral Plug Flow Reactor Data for Catalyst No. 4.

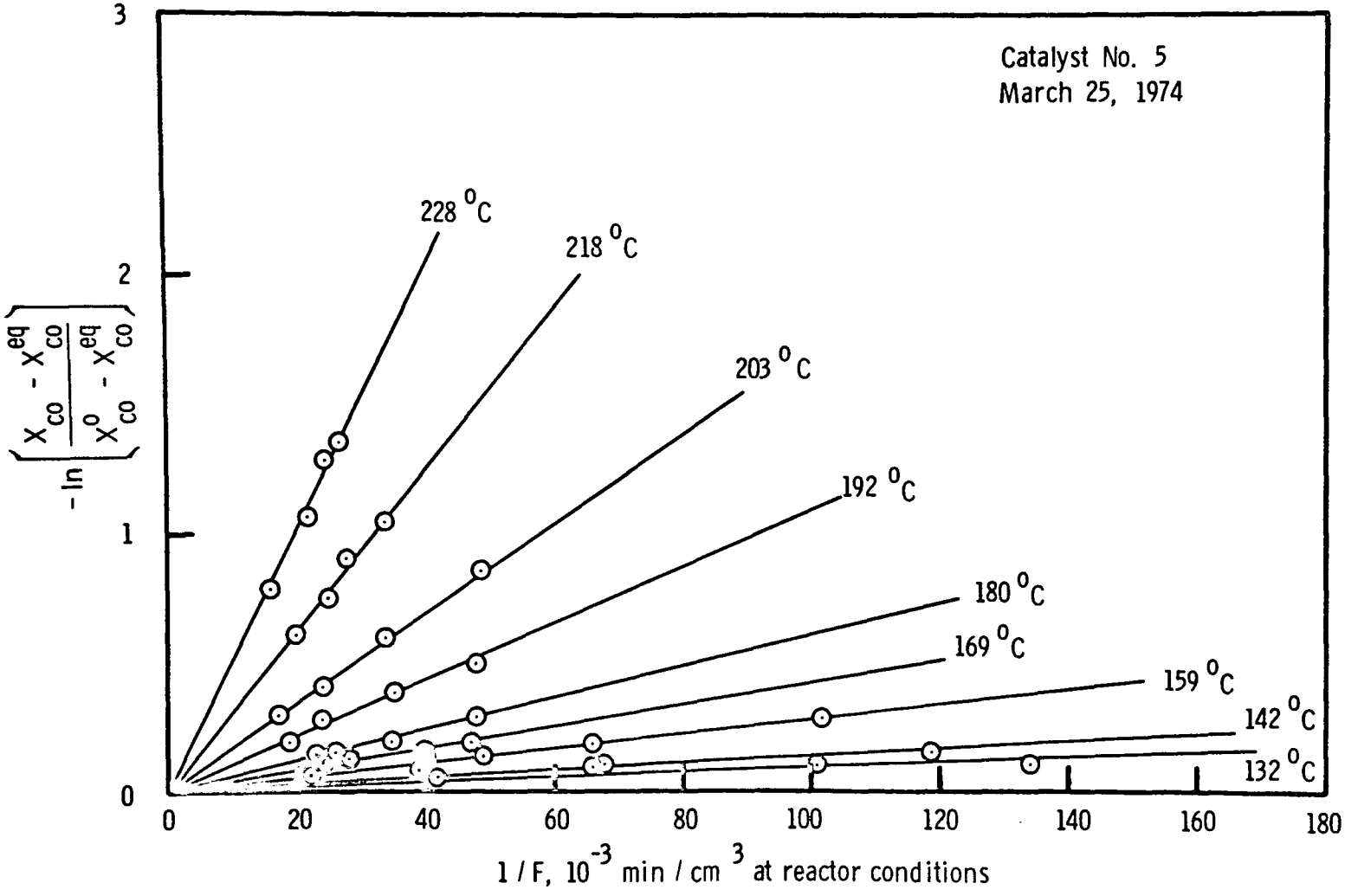

Figure 16. Integral Plug Flow Reactor Data for Catalyst No. 5 between 132°C and 228°C.

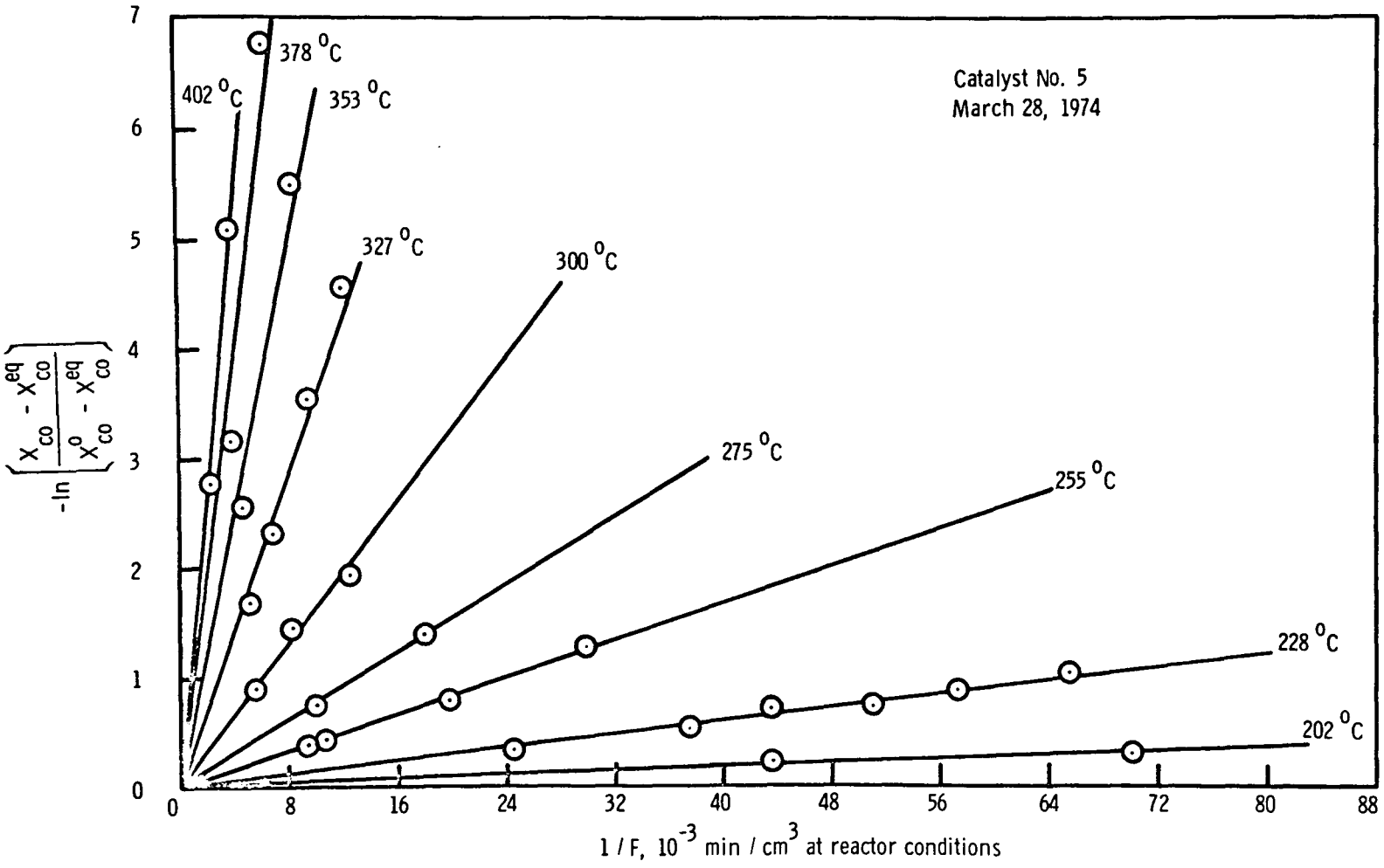

Figure 17. Integral Plug Flow Reactor Data for Catalyst No. 5 between 202°C and 402°C.

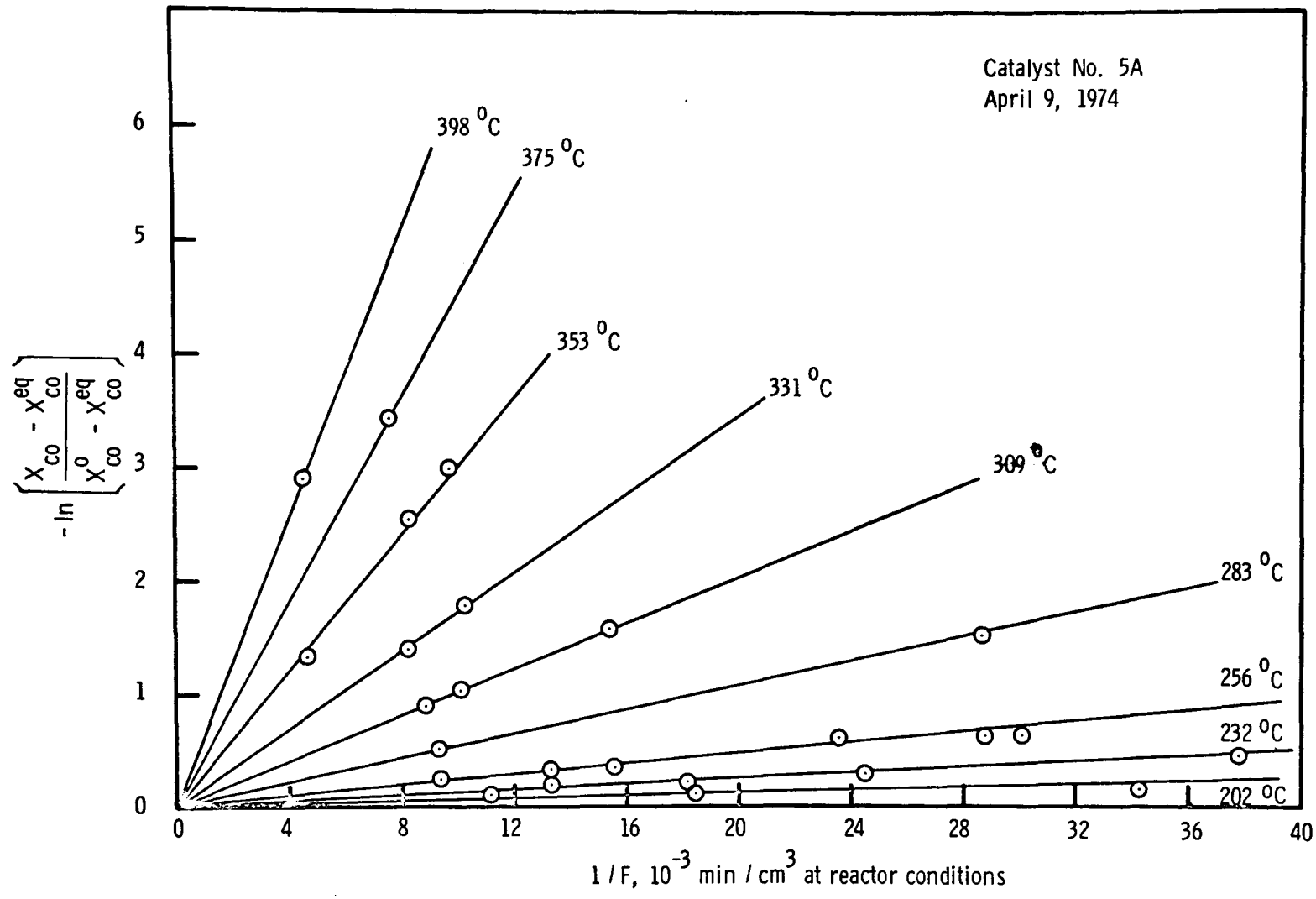

Figure 18. Integral Plug Flow Reactor Data for Catalyst No. 5A.

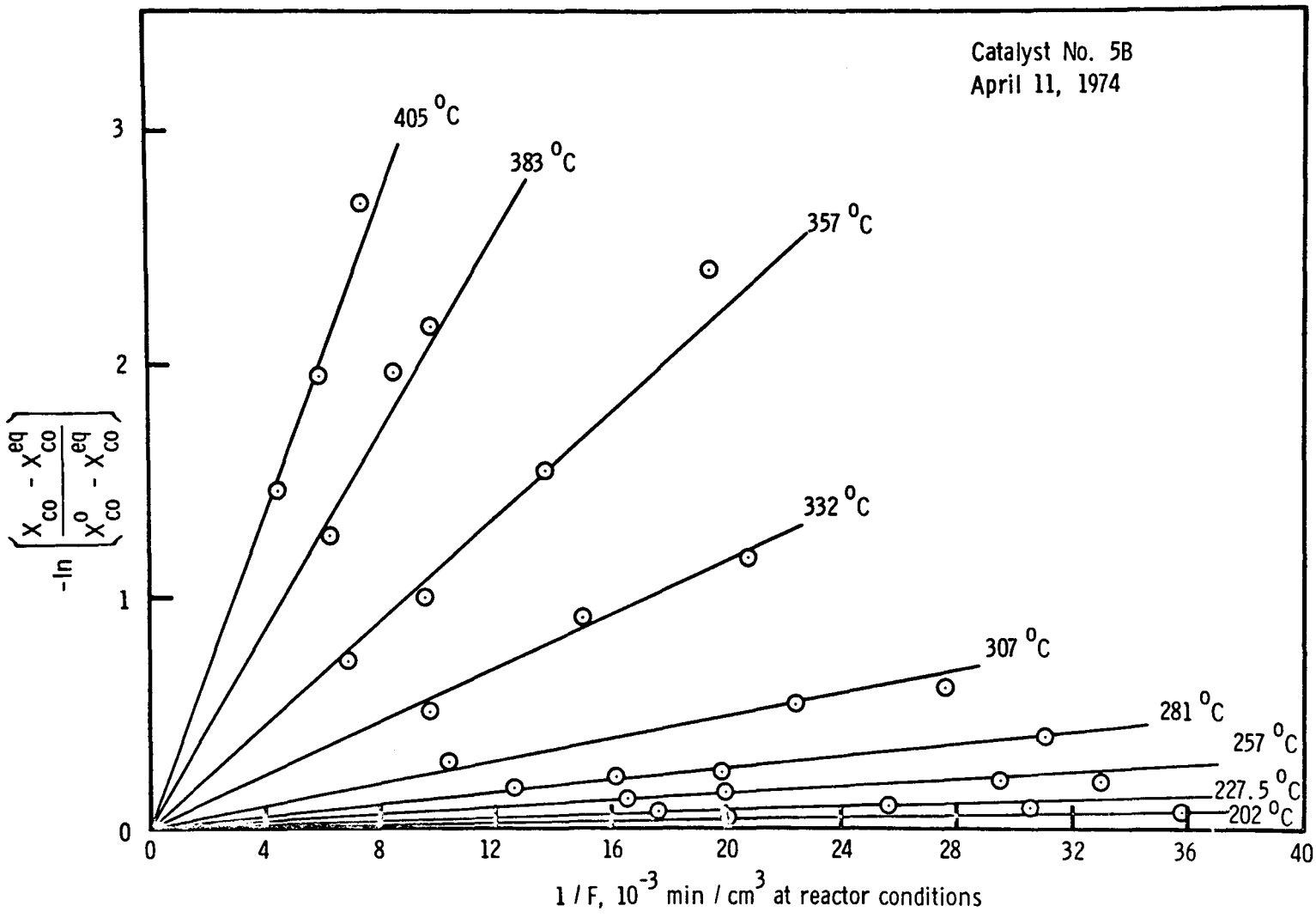

Figure 19. Integral Plug Flow Reactor Data for Catalyst No. 5B.

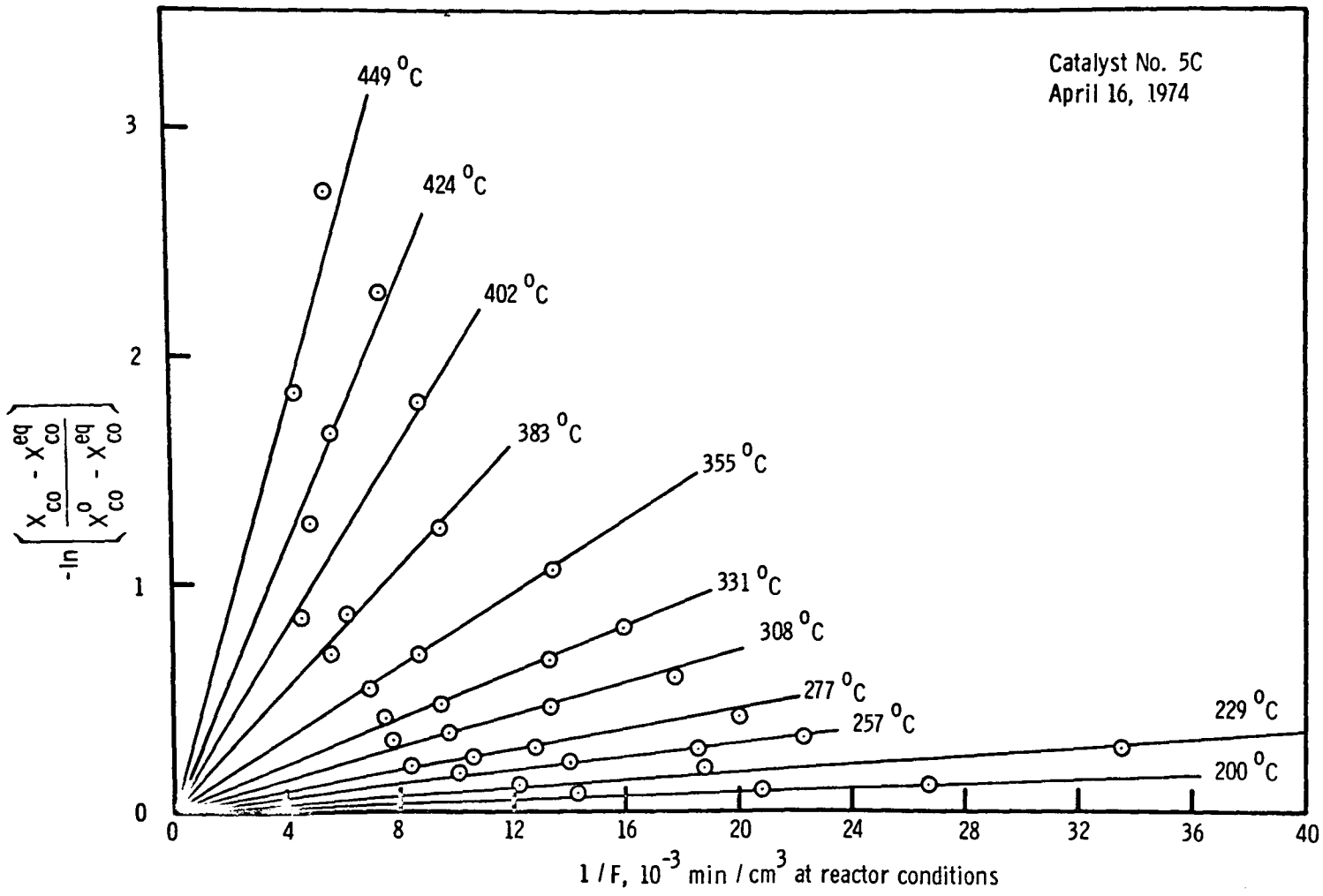

Figure 20. Integral Plug Flow Reactor Data for Catalyst No. 5C.

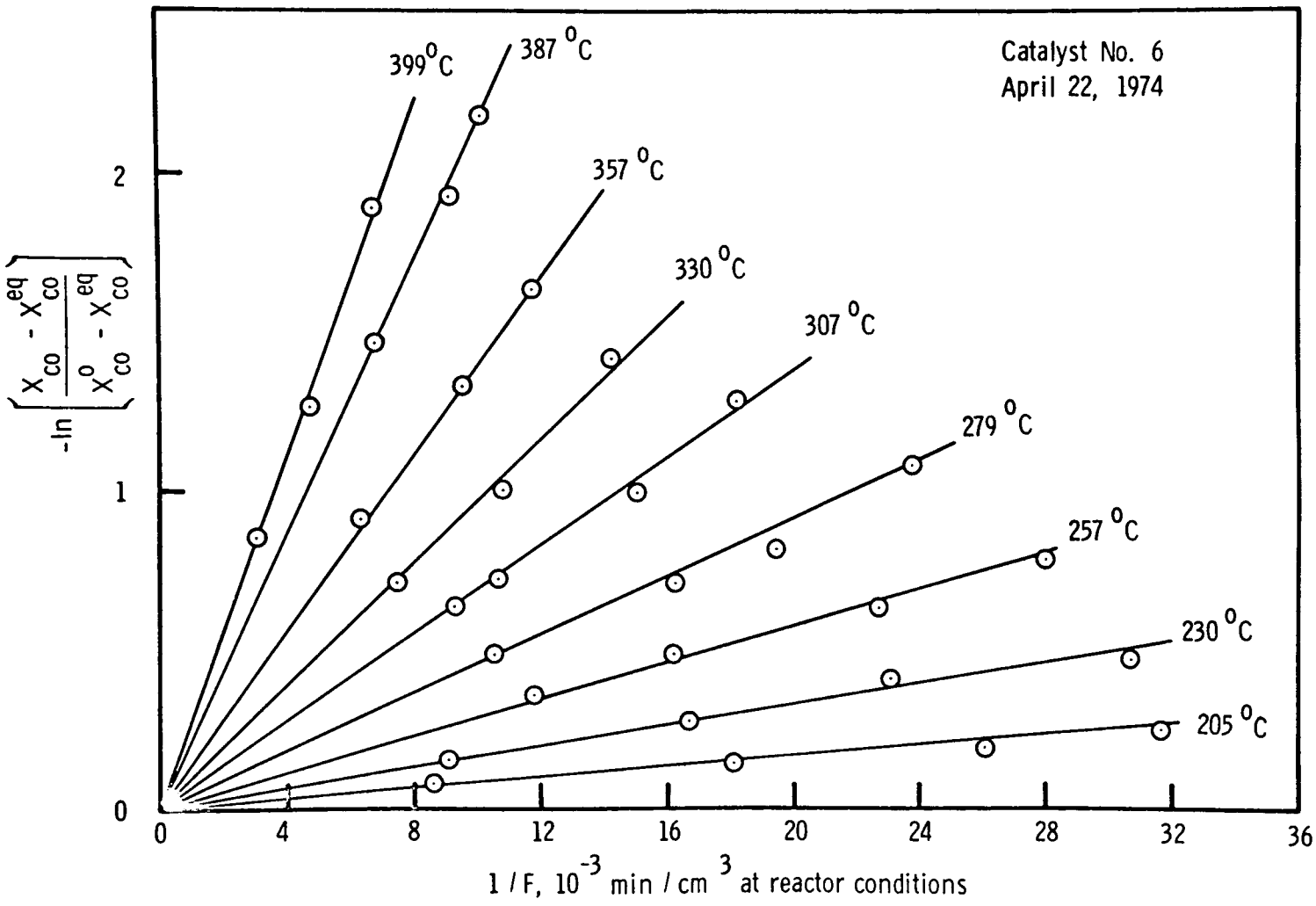

Figure 21. Integral Plug Flow Reactor Data for Catalyst No. 6.

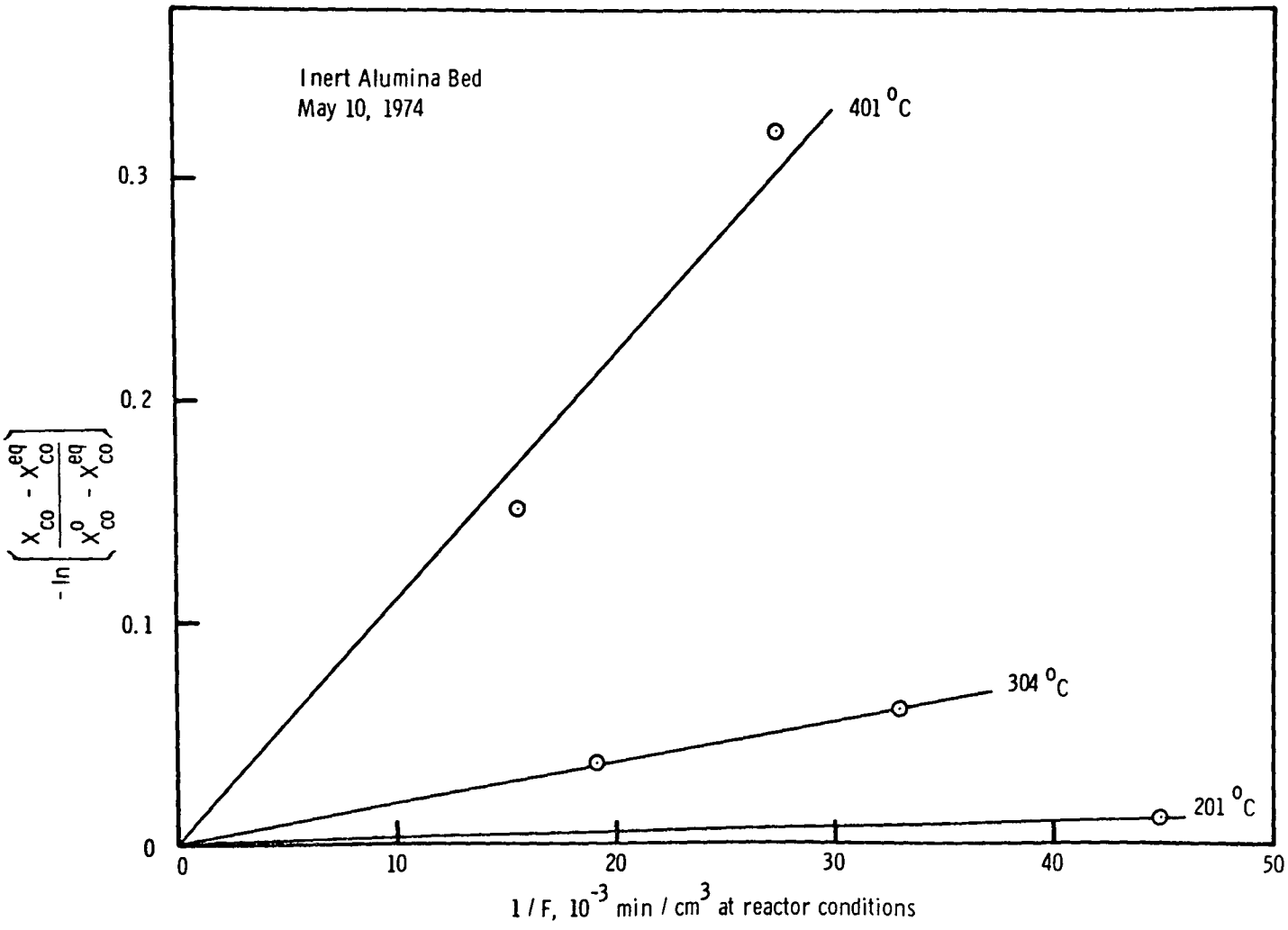

Figure 22. Integral Plug Flow Reactor Data for Inert Bed.

Arrhenius Data

Each line drawn in the integral plug flow reactor plots has a slope equal to kV, the product of the pseudo-first order rate constant at that temperature and the bed volume of the "Aldridge" catalyst used. If we normalize these slopes by W, the weight of the non-impregnated Co-Mo hydrotreating catalyst, and then plot the logarithm of the normalized slopes versus reciprocal temperature, a linear relationship should ensue. The absolute values of the slopes of these lines should equal the activation energy divided by the gas law constant and the intercepts should equal $\ln(k_o\ V/W)$, where k_o is the frequency factor.

Plots of ln(kV/W) versus reciprocal temperature for the catalysts studied are given in Figures 23 through 30. The values that we used to make these plots are given in Tables V through XII. A summary plot of ln(kV/W) versus 1/T for catalysts 4, 5, 5A, 5B, 5C and 6 is given in Figure 32.

Kinetic Determination of Melting Point

We expected to observe a low melting point eutectic melt for all of the "Aldridge" catalysts studied. A change in slope of the Arrhenius plot, indicating a change in activity, was anticipated at the melting point.

We observed a definite decrease in the activation energy at the high temperature range of the Arrhenius plots for catalysts 4 and 5. We assumed that these regions were under diffusion control and fitted them separately by a linear regression analysis.

As explained by Levenspiel,[30] when strong diffusion control prevails, the effectiveness factor becomes closely approximated by the reciprocal Thiele modulus. Thus, as he points out for a first order reaction, rate becomes proportional to the square root of the rate constant and the activation energy approaches half the non-diffusion controlled activation energy.

Actually, the transition to strong diffusion control is not sharp, as we have shown in Figures 24 and 26. A curved transition region exists between the regions of non-diffusion control and strong diffusion control. Our data, in the regions of strong diffusion control for catalysts 4 and 5, are too limited to allow well defined straight lines. Thus, the diffusion controlled slopes indicative of the activation energies deviate slightly from one half of the activation energies for the rate-controlled reactions shown in Figures 24 and 26.

Activation Energies and Frequency Factors

We obtained activation energies and frequency factors for the various assumed linear segments of the Arrhenius

plots, either solid, molten, or diffusion controlled. The results of this analysis are summarized in Table XIV. The activation energies were obtained by multiplying the Arrhenius plot slopes by the negative value of the gas law constant. The frequency factors were determined by multiplying the exponentials of the Arrhenius plot intercepts by 0.65 grams/cm^3, the weight-to-volume ratio of unimpregnated Nalcomo 474 hydrotreating catalyst.

Reproducibility

We studied catalyst No. 5 on two separate occasions: (1) 1.0 grams of catalyst No. 5 was studied between 132°C and 228°C (Figure 25); (2) 0.283 grams of catalyst No. 5 was studied between 202°C and 402°C (Figure 26). Thus, we would expect overlap in the common temperature region between 202°C and 228°C.

In Table XIII, the linear regression data for the supposed molten phase of catalyst No. 5 were actually that obtained from the 1.0 gram sample. The slope and intercept are given as -10.2 and 24.3, respectively. The slope and intercept of the assumed molten phase of the 0.283 gram sample are -10.4 and 24.8, respectively. This excellent agreement can better be seen in Figure 32, in which both runs performed with catalyst No. 5 are superimposed in the common temperature zone.

The close agreement of the two Arrhenius plots for catalyst No. 5 in the common temperature region indicates another fact besides reproducibility: the lack of external, or interparticle, mass transfer control. Levenspiel[30] explains that if a catalyst is studied with two different bed sizes at the same space time, higher conversions would be expected from the larger bed if external mass transfer is significant. This obviously is not the case for catalyst No. 5.

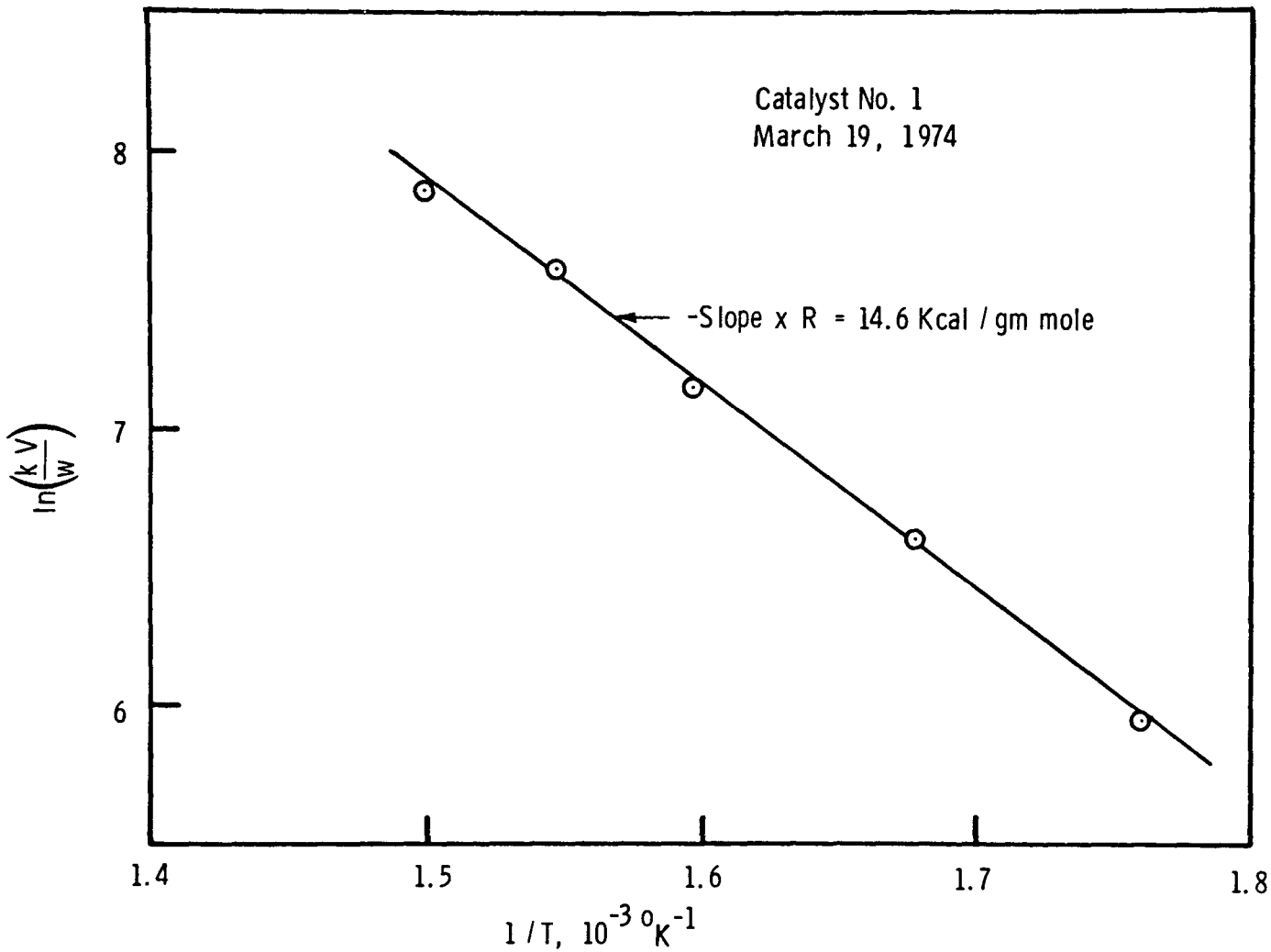

Figure 23. Arrhenius Plot for Catalyst No. 1.

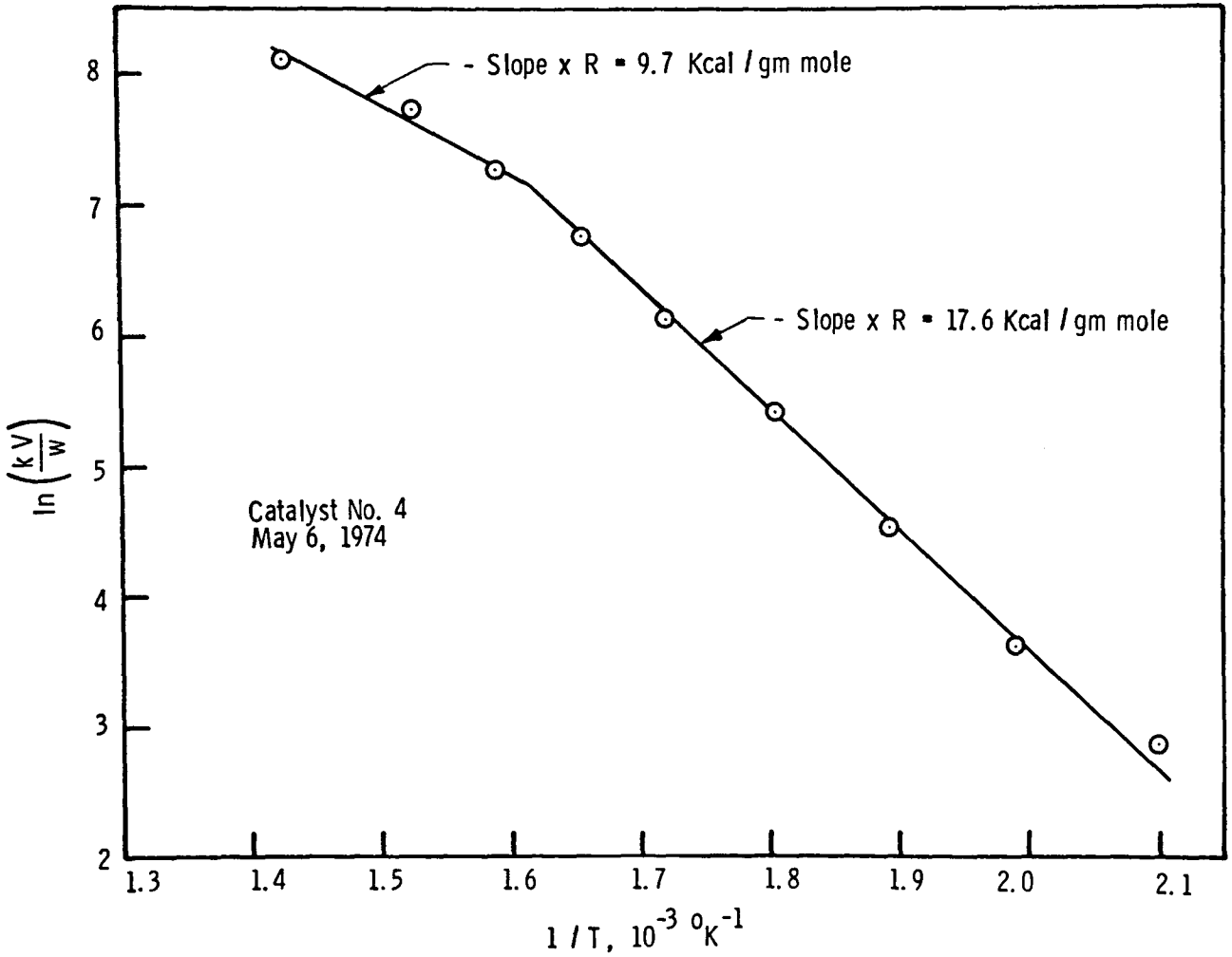

Figure 24. Arrhenius Plot for Catalyst No. 4.

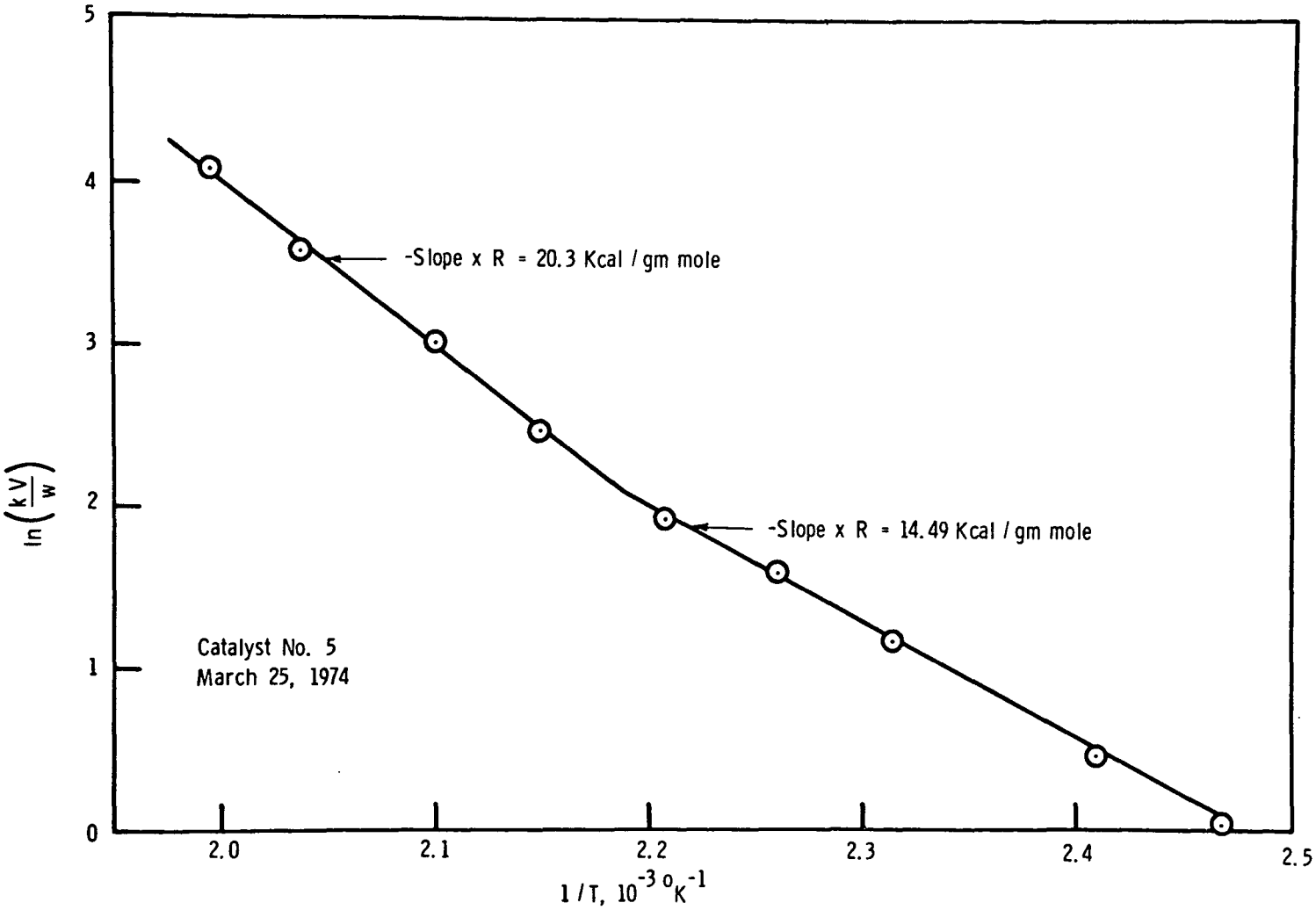

Figure 25. Arrhenius Plot for Catalyst No. 5 between 132°C and 228°C.

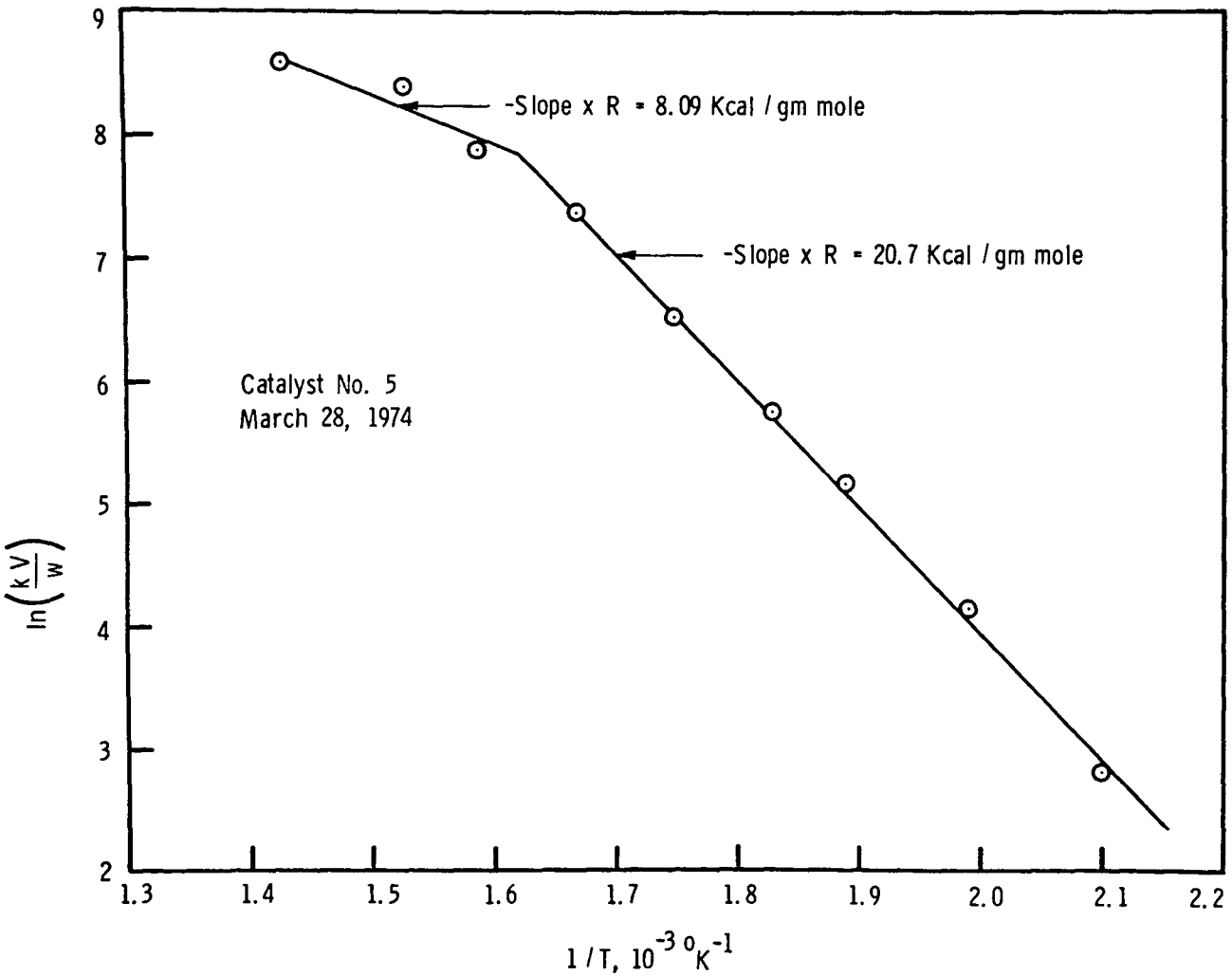

Figure 26. Arrhenius Plot for Catalyst No. 5 between 202°C and 402°C.

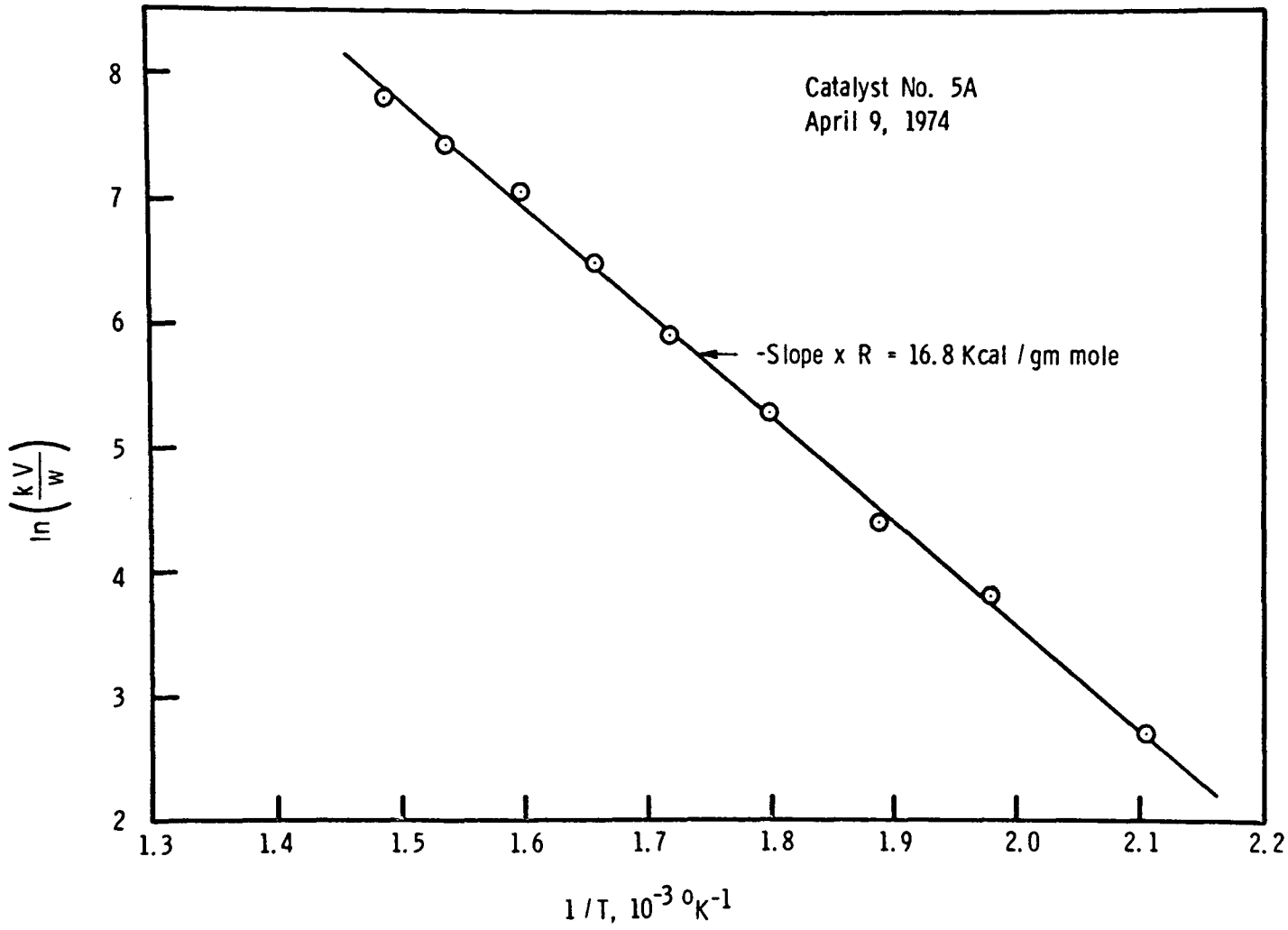

Figure 27. Arrhenius Plot for Catalyst No. 5A.

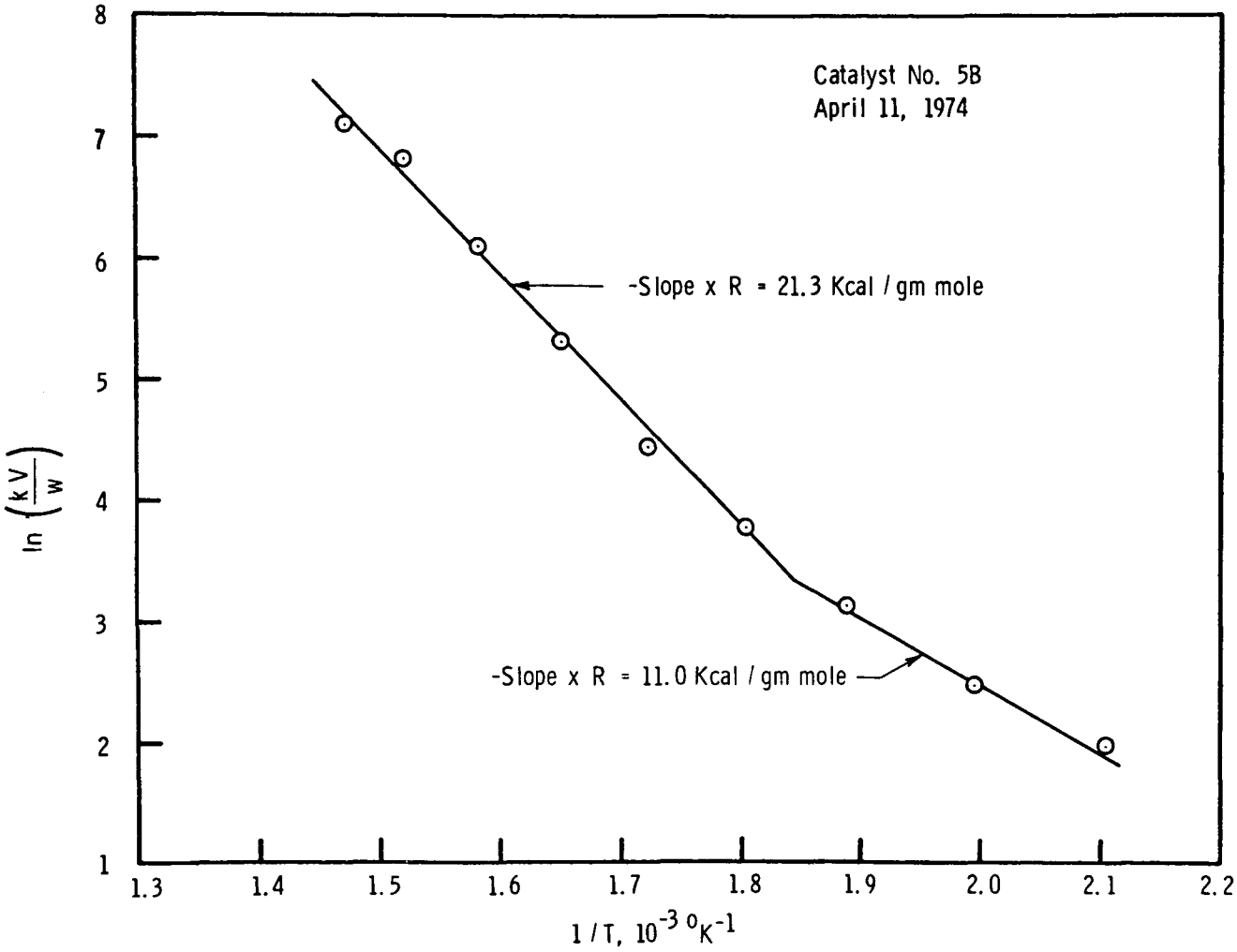

Figure 28. Arrhenius Plot for Catalyst No. 5B.

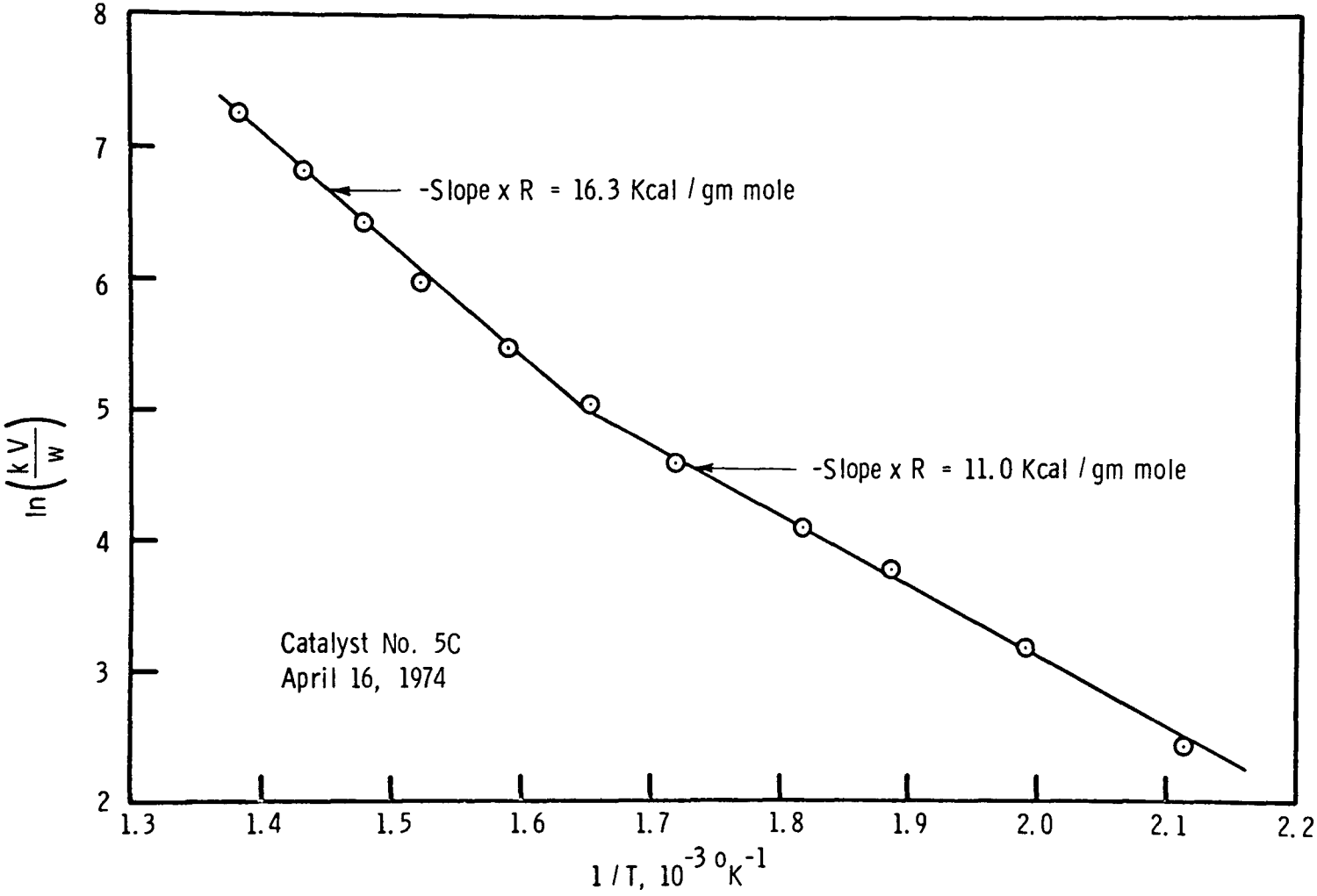

Figure 29. Arrhenius Plot for Catalyst No. 5C.

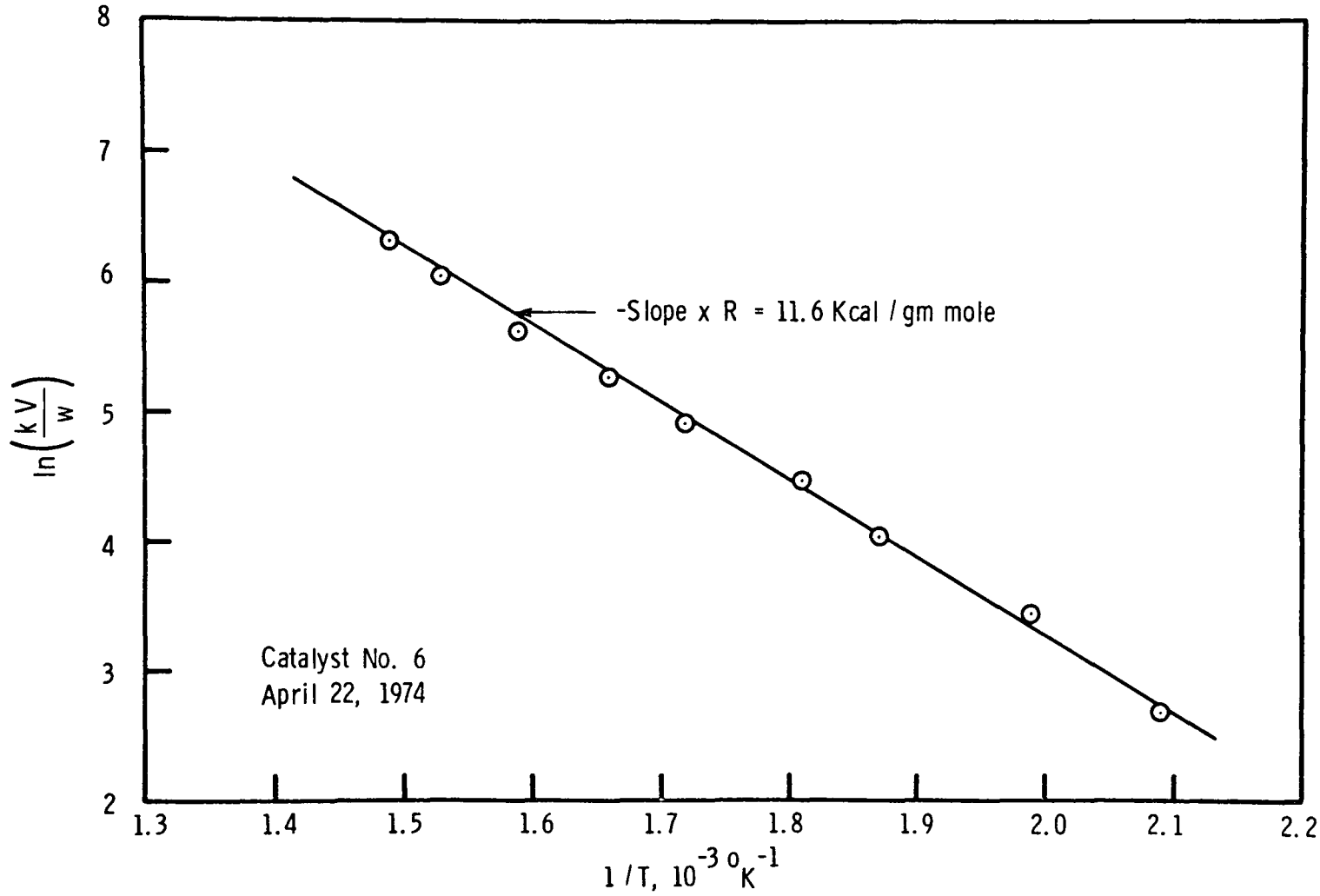

Figure 30. Arrhenius Plot for Catalyst No. 6.

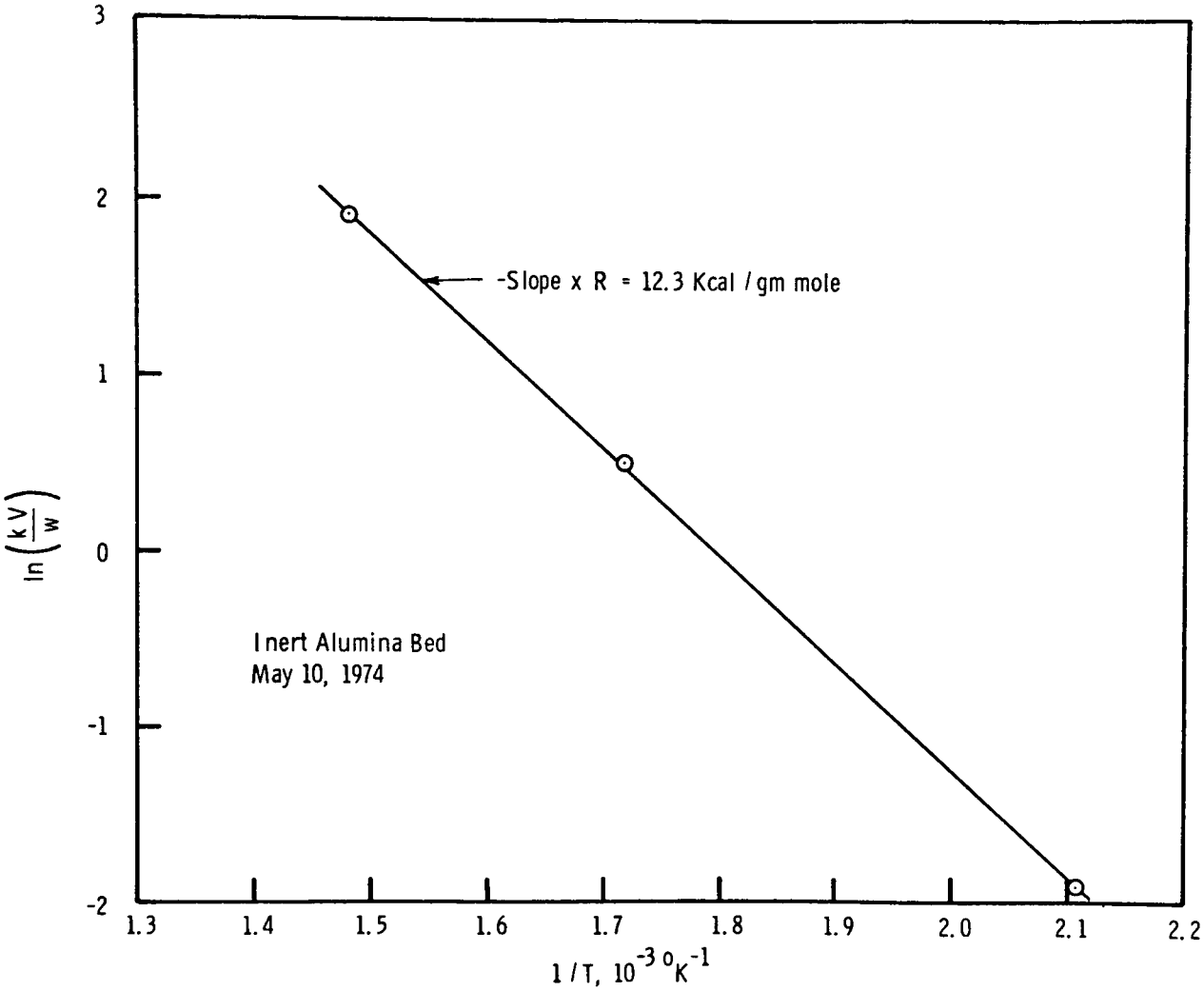

Figure 31. Arrhenius Plot for Inert Alumina Bed.

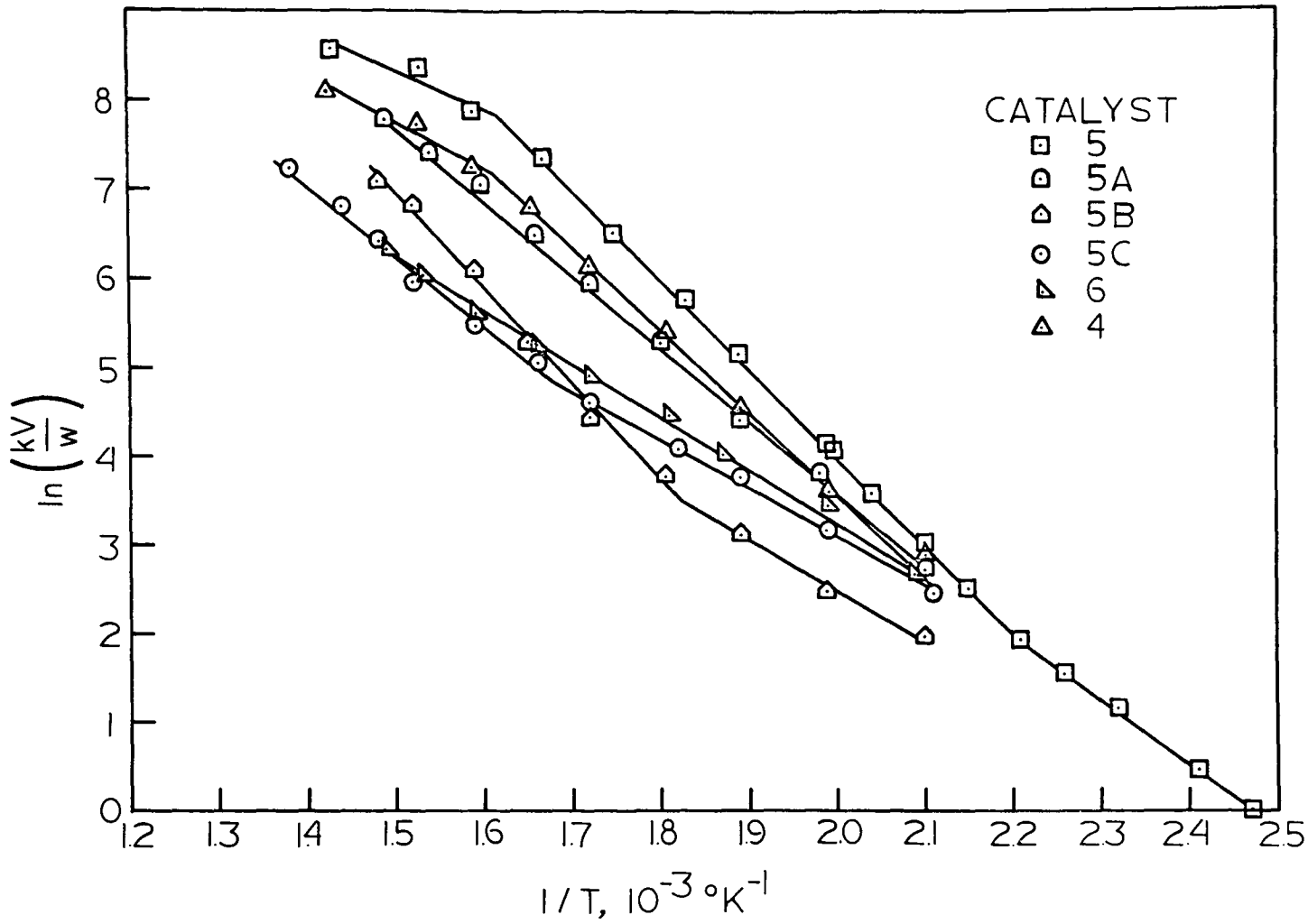

Figure 32. Arrhenius Plot for Catalysts 4, 5, 5A, 5B, 5C, and 6.

Table V

ARRHENIUS DATA FOR CATALYST NO. 1[a], MARCH 19, 1974

T, °C	Slope, kV cm^3/min.	Normalized slope, $\frac{kV}{W}$[b] cm^3/gm catalyst-min.	Plotted Data	
			ln kV/W	1/T, 10^{-3} $°K^{-1}$
295	30.8	393	5.96	1.76
323	57.2	748	6.61	1.68
353	98.5	1290	7.15	1.60
373	149.2	1960	7.58	1.55
394	200.0	2620	7.86	1.50

[a] Catalyst No. 1 contains 1.048 grams of cesium acetate per cm^3 of unimpregnated catalyst pore volume.

[b] k = pseudo first order rate constant, min^{-1}
V = volume of catalyst bed not including inert solids, cm^3
W = weight of catalyst used less the cesium acetate weight, 0.0763 grams

Table VI

ARRHENIUS DATA FOR CATALYST NO. 4[a], May 6, 1974

T, °C	Slope, kV cm^3/min.	Normalized slope, kV/W[b] cm^3/gm catalyst-min.	Plotted Data	
			ln kV/W	1/T, 10^{-3} $°K^{-1}$
203	2.34	18.1	2.89	2.1
229	4.84	37.5	3.62	1.99
255	11.98	92.67	4.53	1.89
281	29.0	224.6	5.41	1.81
308	60.2	465.8	6.14	1.72
331	111.2	859.8	6.76	1.66
355	187.96	1453.9	7.28	1.59
382	299.9	2319.8	7.45	1.53
404	428.0	3310.7	8.10	1.43

(a) Catalyst No. 4 contains 0.42 grams of cesium acetate per cm^3 of unimpregnated catalyst pore volume.

(b) k = pseudo first order rate constant, min^{-1}
V = volume of catalyst bed not including inert solids, cm^3
W = weight of catalyst used less the cesium acetate weight, 0.029 grams

Table VII

ARRHENIUS DATA FOR CATALYST NO. 5[a] BETWEEN 132°C AND 228°C, MARCH 25, 1974

T, °C	Slope, kV cm^3/min	Normalized slope, kV/W[b] cm^3/gm catalyst-min.	Plotted Data	
			ln kV/W	1/T, 10^{-3} $°K^{-1}$
132	0.87	1.01	0.007	2.47
142	1.35	1.57	0.45	2.41
159	2.71	3.15	1.15	2.32
169	3.93	4.56	1.52	2.26
180	5.83	6.77	1.91	2.21
192	10.4	12.08	2.49	2.15
203	17.6	20.44	3.02	2.1
218	31.2	36.26	3.59	2.04
228	50.5	58.65	4.07	1.996

[a] Catalyst No. 5 contains 0.35 grams of cesium acetate per cm^3 of unimpregnated catalyst pore volume.

[b] k = pseudo first order rate constant, min^{-1}
V = volume of catalyst bed not including inert solids, cm^3
W = weight of catalyst used less the cesium acetate weight, 0.861 grams

Table VIII

ARRHENIUS DATA FOR CATALYST NO. 5[a] BETWEEN 202°C AND 402°C, MARCH 28, 1974

T, °C	Slope, kV cm^3/min	Normalized slope, kV/W[b] cm^3/gm catalyst-min.	Plotted Data	
			ln kV/W	1/T, 10^{-3} $°K^{-1}$
202	4.03	16.7	2.82	2.1
228	15.4	63.7	4.15	1.97
255	42.0	174.2	5.16	1.89
275	77.5	321.0	5.76	1.83
300	163.0	678.0	6.51	1.75
327	381.9	1584.0	7.36	1.67
353	651.1	2700.0	7.89	1.59
378	1052.9	4375.0	8.39	1.53
402	1293.1	5385.0	8.58	1.43

[a] Catalyst No. 5 contains 0.35 grams of cesium acetate per cm^3 of unimpregnated catalyst pore volume.

[b] k = pseudo first order rate constant, min^{-1}
V = volume of catalyst bed not including inert solids, cm^3
W = weight of catalyst used less the cesium acetate weight, 0.244 grams

Table IX

ARRHENIUS DATA FOR CATALYST NO. 5A[a], April 9, 1974

T, °C	Slope, kV cm^3/min	Normalized slope, kV/W[b] cm^3/gm catalyst-min.	Plotted Data	
			ln kV/W	1/T, 10^{-3} $°K^{-1}$
202	3.98	15.2	2.72	2.1
232	11.95	45.7	3.82	1.98
256	21.74	83.0	4.42	1.89
283	52.7	201.0	5.3	1.80
309	100.0	382.0	5.94	1.72
331	172.5	658	6.5	1.66
353	306.9	1170	7.07	1.60
375	450.0	1720	7.44	1.54
398	641.0	2450	7.8	1.49

[a] Catalyst No. 5A contains 0.240 grams of cesium acetate per cm^3 of unimpregnated catalyst pore volume.

[b] k = pseudo first order rate constant, min^{-1}
V = volume of catalyst bed not including inert solids, cm^3
W = weight of catalyst used less the cesium acetate weight, 0.262 grams

Table X

ARRHENIUS DATA FOR CATALYST NO. 5B[a], APRIL 11, 1974

T, °C	Slope, kV cm^3/min	Normalized slope, kV/W[b] cm^3/gm catalyst-min.	Plotted Data	
			ln kV/W	1/T, 10^{-3} $°K^{-1}$
202	1.99	7.2	1.97	2.1
227.5	3.22	11.6	2.48	1.99
257	6.37	23.0	3.13	1.89
281	12.2	44.2	3.78	1.8
307	24.0	86.8	4.45	1.72
332	55.8	205.0	5.31	1.65
357	122.7	444.5	6.1	1.59
383	254.0	920	6.83	1.52
405	332.5	1200	7.1	1.48

[a] Catalyst No. 5B contains 0.141 grams of cesium acetate per cm^3 of unimpregnated catalyst pore volume.

[b] k = pseudo first order rate constant, min^{-1}
V = volume of catalyst bed not including inert solids, cm^3
W = weight of catalyst used less the cesium acetate weight, 0.276 grams

Table XI

ARRHENIUS DATA FOR CATALYST NO. 5C[a], APRIL 16, 1974

T, °C	Slope, kV cm^3/min	Normalized slope, kV/W[b] cm^3/gm catalyst-min.	Plotted Data	
			ln kV/W	1/T, 10^{-3} $°K^{-1}$
200	3.78	11.4	2.44	2.11
229	8.0	24.2	3.19	1.99
257	14.3	43.35	3.78	1.89
277	19.9	60.3	4.1	1.82
308	33.1	100.0	4.6	1.72
331	50.6	153.0	5.05	1.66
355	79.0	239.0	5.48	1.59
383	131.5	396.0	5.98	1.52
402	203.6	614.8	6.44	1.48
424	301.8	911	6.84	1.44
449	470.4	1430	7.27	1.38

[a] Catalyst No. 5C contains 0.070 grams of cesium acetate per cm^3 of unimpregnated catalyst pore volume.

[b] k = pseudo first order rate constant, min^{-1}
V = volume of catalyst bed not including inert solids, cm^3
W = weight of catalyst used less the cesium acetate weight, 0.331 grams

Table XII

ARRHENIUS DATA FOR CATALYST NO. 6[a], APRIL 22, 1974

T, °C	Slope, kV cm^3/min	Normalized slope, kV/W[b] cm^3/gm catalyst-min	Plotted Data	
			ln kV/W	1/T, 10^{-3} $°K^{-1}$
205	7.35	14.6	2.68	2.09
230	15.8	31.5	3.45	1.99
257	27.9	55.6	4.02	1.87
279	44.2	88.1	4.48	1.81
307	68.6	136.6	4.92	1.72
330	97.6	194.4	5.27	1.66
357	137.9	274.8	5.62	1.59
382	210.9	420.3	6.0	1.53
399	287.0	554.0	6.32	1.49

[a] Catalyst No. 6 contains no cesium acetate

[b] k = pseudo first order rate constant, min^{-1}
V = volume of catalyst bed not including inert solids, cm^3
W = weight of catalyst used less the cesium acetate weight, 0.502 grams

Table XIII

LINEAR REGRESSION DATA FOR ARRHENIUS PLOTS

	Catalyst					
	1	4		5		
Assumed Catalyst Phase	Molten	Molten	Diffusion Control	Solid	Molten	Diffusion Control
Temperature Range	295°C to 394°C	203°C to 346°C	346°C to 404°C	132°C to 183°C	183°C to 342°C	342°C to 402°C
Slope, $- E_a/R \times 10^{-3}$	-7.36	-8.86	-4.86	-7.29	-10.2	-4.07
Intercept, ln $(k_o V/W)$	18.9	21.39	15.07	18.0	24.3	14.4
Correlation Coefficient	-0.999	-0.998	-0.981	-0.999	-0.999	-0.922
Minimum Slope x 10^{-3}, 10% confidence	-7.87	-9.417	-10.89	-7.6	-10.7	-14.8
Maximum Slope x 10^{-3}, 10% confidence	-6.85	-8.312	+1.17	-6.97	-9.62	+6.7

Statistical Data entries obtained with the use of a Hewlett-Packard 9810A calculator and ANOVA linear regression package.

Table XIII - LINEAR REGRESSION DATA FOR ARRHENIUS PLOTS - continued

	Catalyst					
	5A	5B		5C		6
Assumed Catalyst Phase	Molten	Solid	Molten	Solid	Molten	Solid
Temperature Range	202°C to 398°C	202°C to 268°C	268°C to 405°C	200°C to 326°C	326°C to 449°C	205°C to 399°C
Slope, $- E_a/R \times 10^{-3}$	-8.43	-5.51	-10.7	-5.53	-8.19	-5.86
Intercept, ln $(k_o V/W)$	20.4	13.5	23.1	14.2	18.6	15.0
Correlation Coefficient	-0.999	-0.995	-0.997	-0.998	-0.995	-0.999
Minimum Slope x 10^{-3}, 10% confidence	-8.66	-8.89	-11.7	-6.01	-9.04	-6.08
Maximum Slope x 10^{-3}, 10% confidence	-8.19	-2.12	-9.8	-5.05	-7.33	-5.64

Table XIV

RESULTS FROM ARRHENIUS PLOTS

	Catalyst					
	1	4		5		
Assumed Catalyst Phase	Molten	Molten	Diffusion Control	Solid	Molten	Diffusion Control
Temperature Range	295°C to 394°C	203°C to 346°C	346°C to 404°C	132°C to 183°C	183°C to 342°C	342°C to 402°C
Activation Energy, Kcal/gm mole	14.6	17.6	9.7	14.5	20.3	8.1
Frequency Factor, min^{-1}	1.05×10^{8}	1.27×10^{9}	2.28×10^{6}	4.27×10^{7}	2.32×10^{10}	1.17×10^{6}

Table XIV - RESULTS FROM ARRHENIUS PLOTS - continued

	Catalyst					
	5A	5B		5C		6
Assumed Catalyst Phase	Molten	Solid	Molten	Solid	Molten	Solid
Temperature Range	202°C to 398°C	202°C to 268°C	268°C to 405°C	200°C to 326°C	326°C to 449°C	205°C to 399°C
Activation Energy, Kcal/gm mole	16.8	11.0	21.3	11.0	16.3	11.6
Frequency Factor, min^{-1}	4.7×10^{8}	4.74×10^{5}	7.0×10^{9}	9.55×10^{5}	7.78×10^{7}	2.12×10^{6}

VI. DISCUSSION AND RECOMMENDATIONS

In this section, we shall discuss the results and their significance from our studies of the "Aldridge" catalyst. We also give recommendations for further studies and for additional steps towards automating the catalytic reactor.

Presumed Melting Point Determination

The activation energies for catalytic reactions that have employed a molten salt catalyst have been observed to change markedly at the melting point. For example,

> Boreshkov noted an abrupt change in activation energy at the presumed melting point of a supported vanadium catalyst for the oxidation of SO_2.[5]
>
> Ruthven and Kenny observed a similar change in activation energy at the presumed melting point of a supported $LaCl_3$ catalyst for the oxidation of HCl.[7]

The melting point is expected to be a function of reactant gas composition as well as catalyst composition and thus is dependent upon the conditions actually existing within the catalytic reactor.

In our experiments performed on the "Aldridge" catalyst,

we observed abrupt changes in activation energy for catalysts 5, 5B, and 5C at temperatures of 183°C, 268°C, and 326°C, respectively. These changes in activation energy may be seen in Figures 25, 28, and 29 as increases in the absolute slope.

Data for the presumed melting points of catalysts 5, 5B, and 5C as a function of the relative amount of cesium acetate are presented in Table XV and Figure 33. Figure 33 shows a definite relationship between the presumed melting point and the amount of cesium acetate.

This relationship reaffirms our suspicion of a composition dependant, eutectic melt.

We are not certain that a linear relationship, as shown in Figure 33, is really appropriate. However, it is clear that the presumed melting point is related to the relative amount of cesium acetate.

Effect of Cesium Acetate

From the large amounts of cesium acetate contained in the "Aldridge" catalysts and shown in Table IV, we can conclude that cesium acetate acts as something other than a promoter. However, the exact role of cesium acetate is unclear. If indeed it is a melt, it might serve one of two functions:

1. It could dissolve the cobalt oxide - molybdenum

Table XV

Melting Point Data as a Function of the Amount of Cesium Acetate

Catalyst	grams CsAc/cm^3 pore volume	Melting point, °C
5	0.350	183
5B	0.141	268
5C	0.070	326

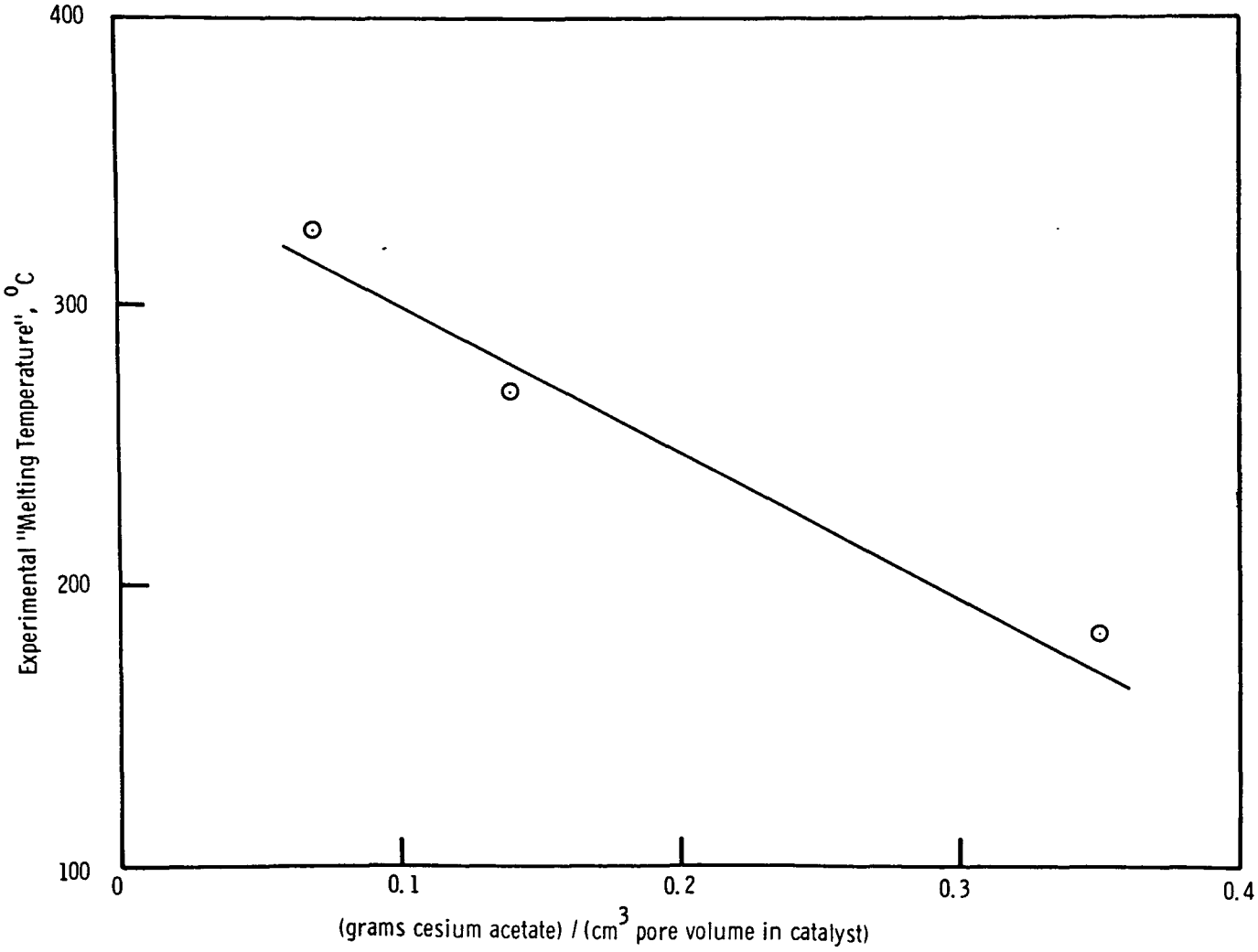

Figure 33. Melting Point Data as a Function of the Amount of Cesium Acetate.

oxide and absorb the reactant gases; thus, it would serve as a homogeneous reaction medium.

2. The reactants might adsorb directly on the melt surface; thus, reaction would occur in a typical heterogeneous fashion on the molten surface.

The integral plug-flow reactor plots serve mainly to enable us to obtain rate constants as a function of temperature, i.e. to determine the Arrhenius plots. We feel that the Arrhenius plots provide a readily observable indication of the "Aldridge" catalyst activity as a function of temperature.

We believe that Figure 32 is a good summary plot for the bulk of our data. If we look at this figure, we note that the various lines, indicative of catalyst activity, switch relative positions as a function of temperature. We believe that this relative change in catalyst activity may be explained in terms of the melting points of the various "Aldridge" catalysts and we will try to explain the relative activities of the "Aldridge catalysts at two different temperatures:

1. A temperature of 260^{o}C which is below the presumed melting points of catalysts 5B and 5C but above the presumed melting points of catalysts 4, 5, and 5A.
2. A temperature of 400^{o}C which is above the presumed

melting point of all the "Aldridge" catalysts that we studied.

Low Temperature Rate Constants. Figure 34 shows rate constants for catalysts 4, 5, 5A, 5B, 5C, and 6 plotted versus the relative amount of cesium acetate at a temperature of 260°C. From left to right along the abscissa, the data points represent catalysts 6, 5C, 5B, 5A, 5, and 4, respectively.

The first three data points, representing catalysts 6, 5C, and 5B, respectively, seem to move in the opposite direction from what we would guess. The more cesium acetate present, the lower the value of the rate constant. This can be explained if we note that 260°C is below the presumed melting points of catalysts 5C and 5B. The cesium acetate in these catalysts is present in its solid, ineffective form. We believe that the presumably non-molten cesium acetate covers the active cobalt-molybdenum catalytic sites and serves to inhibit catalytic activity. Thus, catalysts 5B and 5C have lower rate constants than catalyst No. 6, which has no cesium acetate.

The rate constant for catalyst No. 5A rapidly increases compared to catalyst No. 5B. This is expected since 260°C is above the presumed melting point of catalyst No. 5A, and the increased amount of cesium acetate should have an enhancing rather than an inhibiting effect. A similar trend

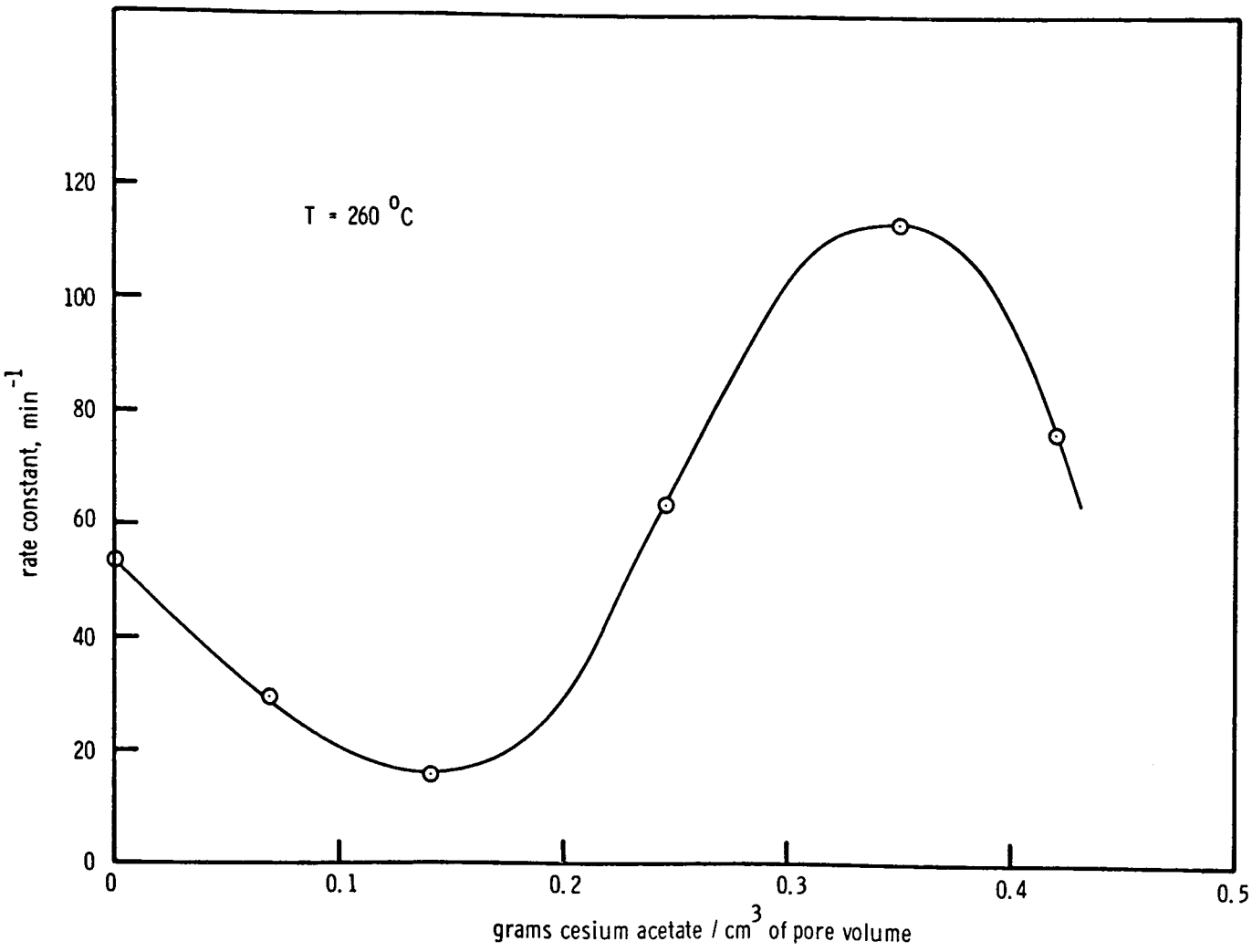

Figure 34. Effect of Cesium Acetate on Rate Constants at 260°C.

holds true for the rate constant of catalyst No. 5. We expect an increase in the rate constant since 260°C is above the presumed melting point of catalyst No. 5.

We observe that the rate constant for catalyst No. 4 at 260°C is lower than that for catalyst No. 5 at 260°C. This is at first perplexing, since 260°C is certainly above the presumed melting point of catalyst No. 4. However, we believe that there exists an optimum amount of cesium acetate. If this optimum is exceeded, some of the pore volume becomes blocked by molten cesium acetate, which lowers accessability to the active catalytic sites. Thus it appears that we have an optimum level of cesium acetate close to the value for catalyst No. 5 of 0.35 grams of cesium acetate per cm^3 of unimpregnated catalyst pore volume. This phenomenon has been observed previously for the vanadium based catalyst for phthalic anhydride production[6] and for the $LaCl_3$ catalyst for the oxidation of HCl.

High Temperature Rate Constants. Figure 35 is completely analogous to Figure 34 except that it is at a temperature of 400°C, which is higher than any of the presumed melting points. Catalyst No. 6 has a slightly higher rate constant than catalyst No. 5C at 400°C. However, the two values are quite close and catalyst No. 5C has the higher rate constant at slightly greater

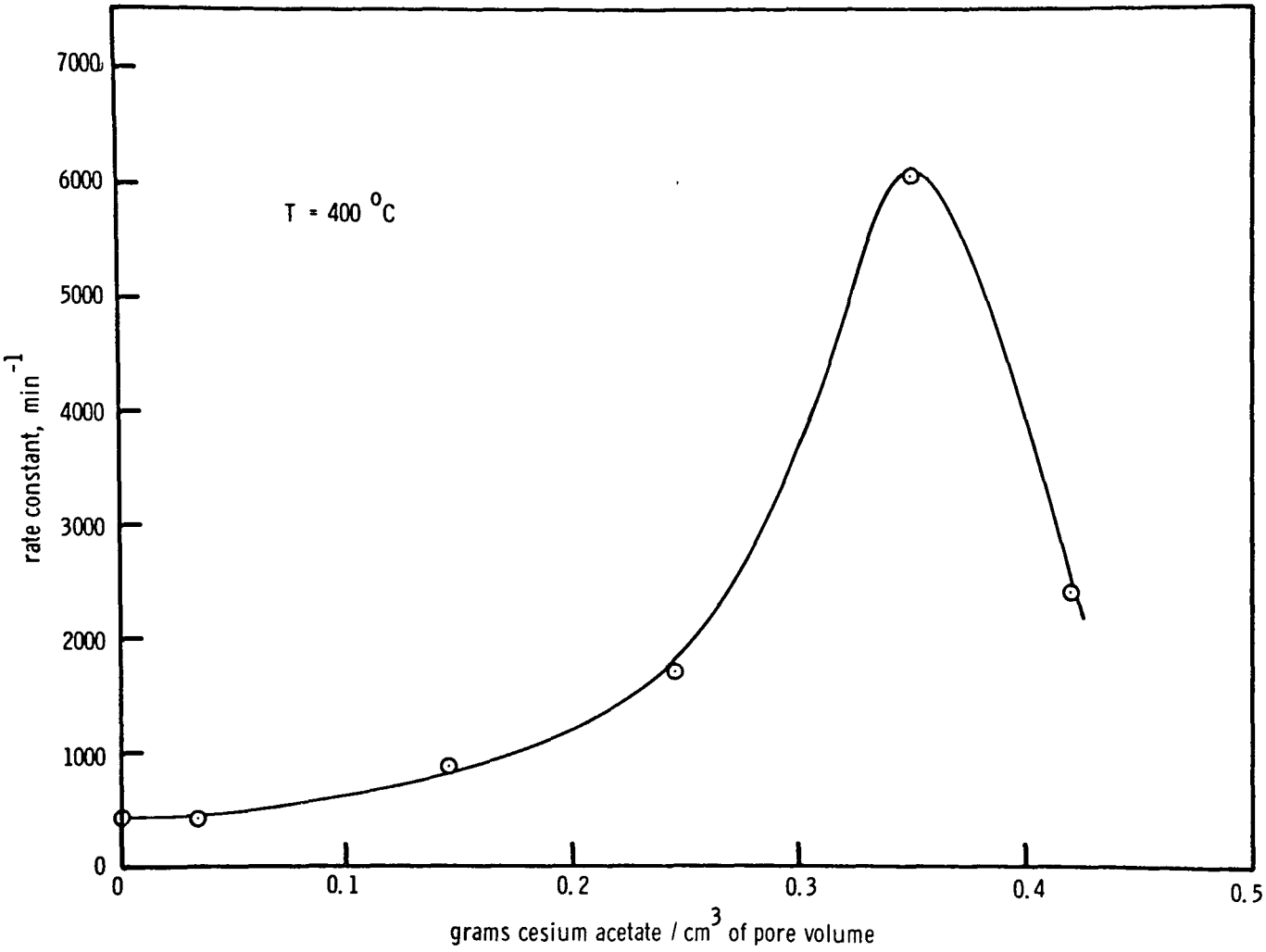

Figure 35. Effect of Cesium Acetate on Rate Constants at 400°C.

temperatures. Catalysts 5B, 5A, and 5 each have higher rate constants than their predecessors with respect to the amount of cesium acetate. Again, as expected, the rate constant for catalyst No. 4 falls off due to the blockage of pores. The data points for catalysts 4 and 5 were calculated from the rate controlled frequency factors and activation energies.

From Figures 34 and 35 we can observe that increasing the amount of cesium acetate can have a beneficial or deleterious effect depending on two factors:

1. Whether or not the temperature is above the catalysts' melting point.
2. Whether or not the amount of cesium acetate is below the optimum level.

Activation Energy and Frequency Factors. We have just shown how the relative values of the rate constants for the catalysts we studied may be qualitatively explained as a function of temperature. The frequency factors and activation energies which define the rate constants are given in Table XIV. The activation energies and frequency factors follow no progressive trends, either for the presumed solid phase or for the presumed molten phase. We are somewhat surprised by this result since we have just demonstrated that the combined effect of frequency factor

and activation energy in the form of a rate constant seems to follow, at least qualitatively, a logical progression.

Rate Advantage of Melt versus Non-Melt

In Table XVI, we present rate constants at 350°C for catalysts 5, 5B, and 5C obtained in two ways:

1. Rate constants obtained using the frequency factors and activation energies for the non-molten regions.
2. Rate constants obtained using the actual frequency factors and activation energies appropriate for 350°C.

By doing this we can clearly see the advantage of having the "Aldridge" catalyst in a molten state.

Effect of Diffusion

Weisz[34] was able to relate the Thiele modulus, Φ, to observable physical quantities such as the actual reaction rate:

$$\Phi = (dn/dt)\left(\frac{1}{[C-C^{eq}]}\right)(R^2/D)$$

where dn/dt is the actual, observed reaction rate per unit volume of the catalyst particles, $(C-C^{eq})$ is the externally applied reactant concentration driving force,

Table XVI

Rate Constants for Molten and Non-Molten Catalysts

At 350°C

Assumed Catalyst Phase	Catalyst		
	5	5B	5C
Non-Molten	353	68	133
Molten	1800	243	152

Entries are rate constants, min^{-1}

R is the size of an approximately equivalent particle radius, and D is the diffusivity of the reactant in the particle medium.

We can use Weisz's result to determine

a. whether or not the strong diffusion control that we observed for catalyst No. 5 at high temperatures is reasonable, and

b. the temperature at which we would expect diffusion control for larger size catalyst particles.

To do this, we note that the first temperature at which strong diffusion control appears for catalyst No. 5 is 353°C (Figure 26). We assume that a Thiele modulus of 1.0 corresponds to the onset of strong diffusion control. Using this result, we next calculate a diffusivity and decide if it is physically reasonable. A knowledge of the diffusivity allows us to then calculate the temperature at which diffusion control occurs for a larger catalyst pellet. Let us now proceed with the calculations.

At 353°C, the pseudo-first order rate constant is calculated from the frequency factor and activation energy given for catalyst No. 5 in Table XIV and found to equal 1740 min^{-1}. Recall from the theoretical section that the pseudo-first order rate constant also equals $\left(\frac{-r_{co}}{C_{co}-C_{co}^{eq}}\right)$ which in turn equals $(dn/dt)(1/[C-C^{eq}])$ in

equation 11. Therefore, substituting the value for the pseudo-first order rate constant into equation 11, we obtain $\Phi = (1740\ min^{-1})(R^2/D)$

If we rearrange this equation, using a Thiele modulus of 1.0 and an average particle radius of 300 microns, we have:

$$D = (1740\ min^{-1})([0.03cm]^2/1)$$

or, $$D = 1.57\ cm^2/min = 0.026\ cm^2/sec$$

The above value of the calculated diffusivity is intermediate between ordinary gas phase diffusivities and Knudson regime diffusivities[29]. This is quite reasonable in view of the high surface area of our catalyst, since the catalyst pores are undoubtedly quite small.

We now extrapolate the results of the determination of an effective diffusivity in order to calculate the temperature at which diffusion control would be expected for 1/8-inch (0.32 cm) catalyst extrudates. The calculated diffusivity, assumed Thiele modulus, and catalyst particle radius are substituted into equation 11, which yields after rearranging:

$$(dn/dt)(1/[C-C^{eq}]) = \Phi\ D/R^2 = (1)(1.57cm^2/min)/(0.16cm)^2$$

or, $(dn/dt)(1/[C-C^{eq}]) = 62.3\ min^{-1}$

Recall from our earlier discussion that this value also equals k, the pseudo-first order rate constant.

We now use the value calculated above for the pseudo-first order rate constant along with the frequency factor and activation energy for catalyst No. 5 (Table XIV, molten phase) to calculate the temperature at which diffusion control would be first expected. To do this, we solve the equation, $k = k_o \exp(E_a/RT)$, for temperature using a value of $k = 62.3\ min^{-1}$, $k_o = 2132 \times 10^{10}\ min^{-1}$, and $E_a = 20.3$ Kcal/gm mole. We find that $T = 245^oC$. Thus we predict diffusion control at temperatures above 245^oC using 1/8-inch extrudate catalyst pellets.

Significance of the Study

We believe that our work has substantially increased the amount of information available on the "Aldridge" catalyst. Our catalytic microreactor has given us very accurate data that has allowed us to obtain Arrhenius plots for seven different "Aldridge" catalysts. We have taken data over a sufficiently wide range of temperatures to observe a presumed melting point in three catalysts and diffusion control in two catalysts.

Typical data obtained by Aldridge (Appendix II) are conversions of carbon monoxide at several different temperatures and pressures with a fixed feed gas composition and a fixed space velocity. He makes no measurements that would allow the determination of a reaction rate.

We have strong reason to believe that Aldridge used 1/8-inch extrudates of Nalcomo 471 hydrotreating catalyst impregnated with cesium acetate to obtain most, if not all of his data. Our data were obtained using Nalcomo 474 hydrotreating catalyst impregnated with cesium acetate. Since Nalcomo 471 and Nalcomo 474 are both hydrotreating catalysts, we feel that we can critically look at much of Aldridge's data.

From our calculations involving catalyst No. 5, we predict diffusion control above 245°C for 1/8-inch catalyst pellets. Of course, this critical temperature is a function of the "hotness" of the catalyst, which is in turn a function of the relative amount of cesium acetate as we have shown. Aldridge's $CoO/MoO_3/CsOAc$ catalyst contains 1.7×10^{-3} moles of $CsOAc/cm^3$ of bed volume, whereas our catalyst No. 5 contains a comparable amount - 1.62×10^{-3} moles of $CsOAc/cm^3$ of bed volume. Virtually all of Aldridge's data were obtained at temperatures above 350°C. Thus, we believe Aldridge's data to have been taken in the diffusion controlled regime. We feel that our data gives a much better characterization of the "Aldridge" catalyst.

The pressures that Aldridge mentions in his German patents are given in terms of atmospheres, gauge. How-

ever, the high activity which we observed at one atmosphere lead us to believe that pounds per square inch, gauge was intended. Perhaps this is why the "Aldridge" catalyst has gone unnoticed. Some of his work was done at pressures as high as 550 psig which would tend to discourage potential researchers if they interpreted such a pressure as 550 atmospheres.

Recommendations

In this section, we discuss the steps that we feel should logically be taken next as a consequence of our work.

Kinetic Study

Our work was performed under the constraints of a fixed feed gas composition, a fixed catalyst particle size, and one atmosphere total pressure. We would like to make the following recommendations:

1. Partial pressures of reactants should be varied to determine a more complete rate expression.
2. An extended break-in period should be used to observe the "Aldridge" catalyst activity as a function of time. Our data were obtained immediately after catalyst pretreatment.

3. Catalyst particle size should be increased to test the validity of the temperatures at which we observed diffusion control.
4. Calculations should be made to see if it is reasonable to assume an isothermal reactor, as we did due to its small diameter and diluted catalyst bed.

Our presumed melting points were determined kinetically, not demonstrated unequivocally. We strongly recommend that an independant melting point test, especially an in situ melting point probe, be developed. Our resistance drop technique for melting point determination is a candidate for such a probe.

We also feel that the "Aldridge" catalyst should be used for other reactions. The obvious reaction to study next is catalytic methanation. We already have observed methane production at reactor pressures of 100 psig.

Another possibility for further study of the "Aldridge" catalyst, is to replace cesium by either sodium or potassium, which are less expensive. Aldridge gives some sketchy data for such systems in his German patents (Appendix II).

Digital Integrator - Minicomputer Interface

The Autolab 6300-02 digital integrator, which is used to integrate our chromatographic peaks, has been successfully interfaced to a PDP 8/E minicomputer. As mentioned earlier, this represents the first step towards an automated catalytic microreactor. We feel the next step should be an expansion of the interface so that complete data analysis can be made by the minicomputer.

The interface as it now stands is unable to perform complete data analysis because,

a. we are unable to transmit reactor temperatures and
b. we are unable to transmit reactant gas flow rates.

Our Kiethly 171 digital multimeter, used to measure reactor temperature with a thermocouple, has parallel BCD output available at the back of the instrument. Also, Dr. P. R. Rony, principal investigator of the molten electrolyte catalyst grant, has devised a flow measuring device that utilizes a pressure transducer to give an analog signal which may in turn be converted to BCD form. Thus, if we can somehow transmit the parallel BCD information for reactor temperature and flow rate as well as the currently transmitted digital integrator

data, we should be able to perform complete data analysis using the minicomputer.

We possess two devices from Analog Devices, an SMX 1004 Serial Multiplexer Module and an SMX 1007 Serial Multiplexer Control Module, which when used together, form an eight channel multiplexer. In other words, they allow information to be transmitted from eight separate devices using the interface we currently have. We feel that these two devices should be utilized to transmit reactor temperature and reactant gas flow rate information to allow complete data analysis by the PDP 8/E minicomputer.

VII. CONCLUSIONS

As a result of our investigation of the "Aldridge" water gas shift catalyst, we conclude the following:

1. The "Aldridge" catalyst is a highly active, sulfur tolerant, water gas shift catalyst.
2. The activity of the "Aldridge" catalyst is a strong function of the amount of the alkali metal component (CsOAc) present in the cobalt/molybdate catalyst particle. An optimum amount of this component exists.
3. A shift from a lower to a higher activation energy, as evidenced by a sudden change in slope of the Arrhenius plot, occurred in three "Aldridge" catalysts.
4. The above mentioned changes in activation energy occur at progressively higher temperatures as the ratio of cesium to cobalt/molybdate decreases.
5. A resistance drop technique is a viable method for measuring melting points of molten electrolytes.
6. A decrease in activation energy, indicative of diffusion control, occurred in two catalysts we studied.

7. Data listed by Clyde L. Aldridge in his German patents[2] for the water gas shift reaction, were most likely taken in the diffusion controlled regime if we assume 1/8 inch catalyst pellets were used.
8. Catalyst activity is quite reproducable for a catalyst containing a large amount of cesium acetate.

BIBLIOGRAPHY

1. Hottel, H. C. and J. B. Howard: "New Energy Technology, Some Facts and Assessments," The M.I.T. Press, Cambridge, Mass., 1971.

2. Aldridge, C. L. and T. Kalina, German Patents 1,928,389; 1,959,012; 2,054,869; and 2,054,946 (May 6, 1970 to May 19, 1971).

3. Thomas, Charles L.: "Catalytic Processes and Proven Catalysts," pp. 104-105, Academic Press, New York, 1970.

4. Shuit, G. and B. C. Gates: Chemistry and Engineering of Catalytic Hydrodesulfurization, AIChE Journal, 19, No. 3, 417 (1973).

5. Boreskov, G. K., L. P. Davydova, V. M. Mastikhin, and G. M. Polyakova: EPR Study of the Composition of Vanadium Catalysts, Doklady Akademii Nauk SSSR, 171, 648 (1966); 171, 760 (1966).

6. Nonnemacher, H., K. Andrussow, M. Appl, A. Feinaner, J. Haug, A. Helms, and K. Wiebusch, British Patent 941,293 (Nov. 6, 1963).

7. Ruthven, D. M. and C. N. Kenney: The Kinetics of the Oxidation of Hydrogen Chloride over Molten Salt Catalysts, Chem. Eng. Sci., 23, 981 (1968).

8. Rony, P. R.: Supported Liquid Phase Catalysts, Chem. Eng. Sci., 23, 1021 (1968).

9. _____: Diffusion Kinetics Within Supported Liquid Phase Catalysts, J. Cat., 14, 142 (1969).

10. Staff: Hydrogen, Likely Fuel of the Future, C & EN, June 26, 14-17 (1972).

11. _____: Hydrogen Fuel Use Calls for New Source, C & EN, July 3, 16-19 (1972).

12. _____: Hydrogen Fuel Economy; Wide Ranging Changes, C & EN, July 10, 27-29 (1972).

13. Shchibrya, G. G., N. M. Morozov, and M. I. Temkin: The Kinetics and Mechanism of the Catalytic Reaction between Carbon Monoxide and Steam: I. Reaction on Iron-Chromium Oxide Catalyst, Kinetika i Kataliz, 6, No. 6, 1057 (1965).

14. Bortolini, P.: Kinetics of Water-Gas Conversion Reaction, Chem. Eng. Sci., 9, 135-144 (1958).

15. Bohlbro, Hans: The Kinetics of the Water Gas Conversion at Atmospheric Pressure, Acta Chemica Scandinavica, 15, 502-520 (1961).

16. _____: The Kinetics of the Water Gas Conversion, II. Investigations at Elevated Pressures, Acta Chemica Scandinavica, 16, 431-438 (1962).

17. Hulburt, H. M. and C. D. Srini Vasan: Design of Experiments on the Kinetics of the Water-Gas Shift Reaction, AIChE Journal, 7, No. 1, 143 (1961).

18. Atwood, Kenton, M. P. Arnold, and E. G. Appel: Water Gas Shift Reaction--Effect of Pressure on Rate Over an Iron Oxide-Chromium Oxide Catalyst, Ind. Eng. Chem., 42, 1600-1602 (1950).

19. Tsuchimoto, Koji and Yoshiro Morita: Low Temperature Carbon Monoxide Conversion Reaction III - Rate of Carbon Monoxide Conversion on Copper-Zinc Catalyst, Kogyo Kagaku Zasshi, 73 (1), 137-42 (1970).

20. Catalysts and Chemicals, Inc.: Catalysts for Low Temperature Shift Reactions, British Patent 1,178,004 (Jan. 1970).

21. Shchibrya, G. G., N. M. Morozov, and M. I. Temkin: Kinetics and Mechanism of the Catalytic Reaction of Carbon Monoxide with Water Vapor II. Reaction of Zinc-Chromium-Copper Oxide Catalyst, Kinetika i Kataliz, 6, No. 6, 1115 (1965).

22. Field, P.E.: Personal Communication, June 13, 1973, Blacksburg, Va.

23. Levenspiel, O.: "Chemical Reaction Engineering," Chapter 5, John Wiley and Sons, New York (1962).

24. Smith, J. M.: "Chemical Engineering Kinetics," p. 274, McGraw Hill Book Company, New York (1970).

25. Tajbl, D. G.: The Mechamism of the Carbon Monoxide Oxidation Catalyzed by Transition Metals, p. 3, Unpublished Ph.D. thesis, Library, University of Notre Dame, South Bend, Indiana (1965).

26. Thiele, E. W., Ind. Eng. Chem., 31, 916-20 (1939).

27. Aris, R., Chem. Eng. Sci., 6, 262 (1957).

28. Peterson, Eugene, E.: "Chemical Reaction Analysis," Prentice Hall, Englewood Cliffs, N. J. (1965).

29. Satterfield, C. N.: "Mass Transfer in Heterogeneous Catalysis," M. I. T. Press, Cambridge, Mass. (1970).

30. Levenspiel, O., ibid, Chapter 14.

31. McNair, H. M. and E. J. Bonelli: "Basic Gas Chromatography," pp. 120-122, Varian Aerograph, Consolidated Printers, Oakland, California (1967).

32. Chemtron Corporation: "Physical and Thermodynamic Properties of Elements and Compounds," p. 30 (1969).

33. Shell Internationale Research Matschappij N.F., British Patent 908,022 (October 10, 1962).

34. Weisz, P. B., and C. D. Prater, Advan. Catal. and Related Subj., 6, 143 (1954).

35. Wold, I., M. Lindheimer, and M. Klapfish, Analog Dialogue, 7, 3 (1973).

36. Digital Equipment Corporation, PDP 8/E Field Service Manual.

APPENDIX I

Materials and Apparatus

This section contains a description of the various materials and apparatus used.

Materials Used for Catalytic Microreactor

Nitrogen

Obtained from Airco, New York, New York.

Used for detecting leaks in the reactor.

94% H_2/6% H_2S. Matheson Gas Products, Div. of Will Ross, Inc., East Ruterford, N. J. Used in pretreating catalysts.

49% H_2/49% CO/2% COS. 1000 psig delivery pressure. Obtained from Matheson Gas Products, Div. of Will Ross, Inc., East Rutherford, N. J. Used as feed for study of water gas shift reaction.

CoO-MoO_3 Catalyst. 12.5% CoO_3/3.5% MoO_3 Nalcomo 474 hydrotreating catalyst supported on Al_2O_3. Surface Area = 270 m^2/gm. Nalco Chemical Company, Houston, Texas. Used as hydration/dehydration component of "Aldridge" catalysts.

Al_2O_3. Hard Alumina Catalyst 200S, code #520-CP-45, Air Products and Chemicals, Inc., Paulsboro, N. J. Used for diluting catalyst beds.

Cesium Acetate. CsOAc, Research Organic/Inorganic Chemical Corporation, Belleville, N. J. Used as the alkali metal component of the "Aldridge" catalyst.

Apparatus Used for Overall Reactor System.

Regulator. Matheson Model 8-H two stage regulator, delivery pressure from 0 to 650 psig, Matheson Gas Products, Div. of Will Ross, Inc., East Rutherford, N. J. Used to regulate tank pressure.

Regulator. Airco, 2 stage, delivery pressure 0 to 50 psig, Airco, New York, New York. Used for regulation of gas pressure before precision value.

4-way, 5-port Ball Valve. Whitey Company, Oakland, Calif. Used for selection of feed gas.

Safety Valve. Hoke Model 6564L4Y Stainless Steel adjustable Safety Valve, Hoke Inc., Cresskill, N. J. Used to prevent excess pressure inside the reactor.

On/off Valves. Whitey Company, Oakland, Calif. Used for connecting reactant line to exhaust system when

flushing system.

Fittings. Fittings are either brass or stainless steel, several types, exclusively Swagelock, Crawford Fitting Company, Solon, Ohio. Used for connecting tubing throughout entire reactor system.

Pressure Gauge. Matheson 0 to 1000 psig, 6-inch dial, Div. of Will Ross, Inc., East Rutherford, N. J. Used to monitor reactant gas pressure before entering precision metering valve.

Water Saturator. Obtained locally [of unspecified origin]. An appropriate substitute would be the 100- to 500-ml stubby stainless steel bombs sold by Whitey, with one end welded closed and the other end welded to a stainless steel Swagelock tee. Used for saturating dry gas feed with water vapor.

Temperature Controller. Love Model 72-1, 0 to 800°C with type J thermocouples. Love Controls Corp., Wheeling, Ill. Used to control temperature of central portion of catalytic microreactor.

Temperature Controllers. Love Model 72-1, 0 to 200°C, with type J thermocouples, Love Controls Corporation, Wheeling, Ill. Used for controlling temperatures of water saturator, sampling valve, and exit tube.

Temperature Controller. Southland Chemitronics Model A solid state temperature controller, 0 to 800°C, Southland Chemitronics, Newport, Va. Used for controlling temperature of reactor ends.

Heating Tapes. Arthur H. Thomas 5954-H50 heating tapes of various dimensions, Hotwatt, Inc., Danvers, Mass. Used for heating reactor and for heat-tapping lines.

Glassrope Heaters. Hotwatt, Inc., Danvers, Mass. Used for heat tapping various lines.

Insulation. Johns-Manville 4-lb density cerafelt. Used to insulate reactor tube and various lines. Johns-Manville Co., New York.

Insulation. Cerakote 5" by 1-1/2" thermo 12 pipe covering. Used to enclose reactor insulated with Cerafelt. Porter Hayden Co., Baltimore, Md.

Sampling Valve. Valco Model ACMV5V-10-HPx C-20 valve, 10 port, multifunctional with 1.16" zero volume fittings, carpenter 20 steel, with UA-1 air operator and 0.7 ml loop. Used for obtaining gas samples from reactor exit. Valco Instruments Co., Houston, Texas.

Gas Sampling Region. Made by VPI&SU Chemical Engineering Shop. Box made of pressed asbestos, insulated with cerafelt, heated with 150 watt light bulb. Contains

a fan to circulate air. Used to maintain the sampling valve at a constant temperature and to minimize water condensation.

Chromatograph. Perkin-Elmer model 900 with thermal conductivity detector, Perkin Elmer Corporation, Norwalk, Conn. Used for analysis of exit gas stream.

Chromatographic Columns. 1/8" stainless steel columns, 6' long, packed with 80/100 mesh chromosorb 102.

Digital Integrator. Autolab Model 6300-02 with parallel BCD output available at back, area and retention time output, Autolab Company, Mountain View, Calif. Used to analyze chromatographic areas.

Recorder. Beckman 10-inch recorder equipped with linear-log button, Beckman Instruments, Fullerton, Calif. Used for obtaining analog representation of chromatograph output.

Sifter. Allen-Bradley #3 Sonic Sifter, with No. 20 and 60 sieves, Fisher Scientific Company, Pittsburgh, Pa. Used to obtain 20/60 mesh catalyst for use in reactor.

Apparatus Used for Melting Point Determination

Alumina Tubing. 1/8" O.D. alumina tubing with four holes, No. 24 gauge, obtained from VPI&SU Ceramic Engineering Department. Used for holding the $LiNO_3$-KNO_3 eutectic.

Aluminum Block. 2" x 2" x 5/8" aluminum block with holes drilled in it for the nitrogen sweep gas, the alumina tubing containing four holes for thermocouple and platinum wires, and a 50-watt cartridge heater. Made by VPI&SU Chemical Engineering Shop.

No. 24 Gauge Platinum Wires. Obtained from VPI&SU Chemistry Glass Shop. Used for measuring resistance of melt.

No. 24 Gauge Iron Constantan Thermocouple Wires. Obtained from VPI&SU Chemical Engineering Shop. Used for measuring temperature of melt.

Decade Resistance Box. Heathkit Model IN-37 Resistance Substitution Box. Heathkit Company, Benton Harbor, Mich. Used for balancing bridge circuit.

Audio Frequency Sine Wave Generator. Hewlett Packard Model 202A low frequency function generator, Palo Alto, Calif. Used as 1000 hertz source for Wheatstone bridge.

Hotwatt Cartridge Heater. 50 watt cartridge heater, Hotwatt, Inc., Danvers, Mass. Used to heat aluminum block which contained melt.

Potentiometers. Two Beckman Helipot 2000 ohm potentiometers, Helipot Corp., South Pasadena, Calif. Used for two resistances of the Wheatstone bridge.

Digital Voltmeter. Keithley 171 Digital Multimeter, Cleveland, Ohio. Used as null indicator for Wheetstone bridge.

Digital Voltmeter. Hewlett Packard #3043A digital voltmeter, Palo Alto, Calif. Used for measuring temperature of melt.

Cement. Ultrabond 552 Ceramic Adhesive. Aremco Products, Briarcliff Manor, N. Y. Used in forming well at the top of the alumina tubing to hold melt.

Materials Used for Melting Pt. Determination

KNO_3-$LiNO_3$ Eutectic. 57.5 mole % KNO_3, 42.5 mole % $LiNO_3$ eutectic, M.P. = 124°C, obtained from P. R. Rony. Used as sample to demonstrate the feasibility of the resistance drop technique for melting point determination.

Apparatus Used for the Digital Integrator-Minicomputer Interface

8 Bit Switch Registers. Four SN74165 8 bit switch registers. Obtained from Poly Paks, Inc., 16-18 Carmine Street, Wakefield, Mass. 01880. Used for transmitting the last three magnitudes of retention time.

Nand Gate. One SN7420 Dual 4-input positive nand gate. Obtained from Poly Paks, Inc., 16-18 Carmine Street, Wakefield, Mass. 01880. Used in logic circuitry to transmit a carriage return.

Digital Integrator. 6300-02 Digital Integrator with built in printer and 20620-011 RT/TA board. Obtained from Autolab, Inc., 1390 Valley Road, Suite 2-B, Stirling, N. J. 07980. Used for obtaining retention time and area information for eluted chromatographic samples.

STX 1003 Serial Transmitter Module. Obtained from Analog Devices, Rtel Industrial Park, Norwood, Mass. 02062. Used for converting parallel BCD data to serial ASCII form and transmitting the ASCII data.

SCL 1006 Clock Module. Obtained from Analog Devices, Rtel Industrial Park, Norwood, Mass. 02062. Used to supply -15 volts and a clocking frequency to the transmitter module.

Printed Circuit Board. One 19F3219 Kepro P2-1212G printed circuit board. Obtained from Newark Electronics, 3865 Wilson Blvd., Arlington, Va. 22203. This board was photo-etched to form the Larsen printed circuit board.

Breadboard. One 10-DE-77 breadboard. Obtained from Douglas Electronics, 718 Marina Blvd., San Leandro, Calif. 95577. Used for receiving BCD data from the digital integrator and for mounting shift registers and nand gate.

Teletype. One ASR #33 teletype. Obtained from Teletype Corporation, 5555 Touhy Ave., Skokie, Illinois. Used for receiving two wires from the transmitter module and for printing out results.

The following materials were all obtained from: Digital Equipment Corporation, Executive Park, 3700 Chapel Hill Blvd., Durham, N. C. 27707.

Conductor Flat Cable. Ten feet of 91-07722 conducter flat cable. Used for transmitting parallel BCD data from the digital integrator to the breadboard.

Connector Block. One H 803 Connector Block and Pins. Used in establishing parallel connections between the Larsen board and the breadboard.

Bus Strips. Ten units 933 bus strips. Used for wrapping the connector block.

Minicomputer. One PDP lab 8/E minicomputer. Used for receiving the processing data.

APPENDIX II

Appendix II contains the data obtained by Clyde L. Aldridge in his study of the water gas shift reaction. We believe that this information is very valuable in view of the fact that no English translation of this information is available elsewhere.

In the original German patents, reactor gauge pressure was written in terms of atmospheres. In view of the large catalytic activity that we have observed at zero gauge pressure, *we believe that pounds per square inch was actually intended*. We have referred to pressure in such units in the following pages.

Table XVII

Aldridge Water Gas Shift Data for the $CoO-MoO_3$-CsOAc Catalyst

Experiment		1	2	3
Metal		Co,Mo	Co,Mo	None
Alkali metal compound		CsOAc	CsOAc	CsOAc
γ-Aluminum oxide support		Type A	Type B	Type B
		% CO in Product		
Temperature, °C	Pressure, psig			
625	550	1.16	1.17	48.61
525	550	0.53	0.54	---
475	550	0.43	---	---
425	550	0.32	0.40	---
425	200	0.31	0.23	---
350	200	20.57	---	---
350	0	45.54	41.35	---

Gas Mixture: $46\%H_2/53\%CO/1\%H_2S$ (dry gas)
Steam/Dry gas ratio: 1 to 1
Space velocity: 27 hr^{-1} @ 25°C, 1 atm
Catalyst: 3.5 wt % CoO/13 wt % MoO_3 on γ-Alumina support with a surface area between 200 and 400 m^2/gm and a pore volume between 0.6 and 0.7 cm^3/gm; Impregnated with 1.7×10^{-3} moles CsOAc/cm^3 of bed volume;
Catalyst Pretreatment: Pretreated with dry reactant gas mixture for 1 hour at 330°C.

Aldridge, C. L. and T. Kalina, German Patent 1,928,389, Table I (Sept. 1970).

Table XVIII

Aldridge Water Gas Shift Rate for CoO-CsOAc and MoO_3-CsOAc Catalyst

Experiment		4	5
Metal		CoO (4.4 wt %)	MoO_3 (11 wt %)
Alkali metal		CsOAc	CsOAc
		% CO in Product	
Temperature, °C	Pressure, psig		
625	550	4.1	1.53
525	550	28.3	11.56

Conditions of the Experiment not shown above are the same as given in Table XVII.

Aldridge, C. L. and T. Kalina, German Patent 1,928,389, Table II (Sept. 1970).

Table XIX

Aldridge Water Gas Shift Data for $CoO-MoO_3$-KOAc and $CoO_3-MoO_3-Cs_2CO_3$ Catalysts

Experiment	6	7
Metal	Co,Mo	Co,Mo
Alkali metal	KOAc (1.7×10^{-3} moles/ml catalyst)	Cs_2CO_3 (8.7×10^{-4} moles/ml catalyst)
	% CO in Product	
Temperature, °C	Pressure, psig	
625	550	1.19	1.28
525	550	---	0.59
475	550	---	---
425	550	0.39	0.37
425	200	0.77	0.35
350	200	---	---
350		---	43.67

Conditions of the Experiment not shown above are the same as given in Table XVII.

Aldridge, C. L. and T. Kalina, German Patent 1,928,389, Table III (Sept. 1970).

Table XX

Aldridge Water Gas Shift Data for Fe-Mo-CsOAc and Ni-Mo-CsOAc Catalysts

Experiment		9	10
Metal		Fe,Mo	Ni,Mo
Alkali metal		CsOAc	CsOAc
		% CO in Product	
Temperature, °C	Pressure, psig		
625	550	1.15	1.26
525	550	11.32	0.87
475	550	---	---
425	550	---	35.07

Conditions of the Experiment not shown above are the same as given in Table XVII.

Aldridge, C. L. and T. Kalina, German Patent 1,928,389, Table IV (Sept. 1970).

Table XXI

Aldridge Water Gas Shift Data for Co-V-CsOAc, Co-Cr-CsOAc, and Co-W-CsOAc Catalysts

Experiment		12	13	14
Metal		Co,V	Co,Cr	Co, W
Alkali metal		CsOAc	CsOAc	CsOAc
		% CO in Product		
Temperature, °C	Pressure, psig			
625	550	7.18	17.24	22.93
525	550	46.08	---	42.41

Conditions of the Experiment not shown above are the same as given in Table XVII.

Aldridge, C. L. and T. Kalina, German Patent 1,928,389, Table V (Sept. 1970).

Table XXII

Aldridge Water Gas Shift Data for a CoO-MoO_3-CsOAc Catalyst with varying Amounts of Sulfur

Experiment	16	17	18
Pretreatment	No sulfur	Catalyst treated in situ	Catalyst pretreated
Entering Gas (mole %)			
H_2	45.9	46.44	45.9
CO	54.1	52.51	54.1
H_2S	0.0	1.4	0.0
Product Gas (mole % CO)	17.32	1.19	1.18
Conversion of CO	57.9%	96.5%	96.7%

Conditions of the Experiment not shown above are the same as given in Table XVII.

Aldridge, C. L. and T. Kalina, German Patent 1,928,389, Table VI (Sept. 1970).

Table XXIII

Aldridge Water Gas Shift Data for CoO-MoO_3-CsOAc and MoO_3-CsOAc Catalysts with Various Supports

Experiment		2	19	20	21
Support		α-Al_2O_3	zeolite material	α-Al_2O_3	activated charcoal
Metal		Co, Mo (3.5% CoO 13% MoO_3)	Co, Mo (3.7% CoO 13.8% MoO_3)	Co, Mo (1.6% CoO 6.0% MoO_3)	Mo (12% MoO_3)
Alkali Metal		CsOAc	CsOAc	CsOAc	CsOAc
		% CO in Product			
Temperature, °C	Pressure, psig				
625	550	1.17	1.15	1.18	1.42
525	550	0.54	0.62	0.51	34.00
475	550	---	---	(<1.03)	---
425	550	0.40	---	---	---
425	200	0.23	32.3	---	---
350	200	---	---	---	---
350	0	41.35	---	---	---

Conditions of the Experiment not given above are the same as given in Table XVII.

Aldridge, C. L. and T. Kalina, German Patent 1,928,389, Table VII (Sept. 1970).

Table XXIV

Aldridge Water Gas Shift Data for a $CoO-MoO_3-Na_2CO_3$ Catalyst

Reaction Temperature, °C	Pressure, psig	% CO in Product	
		Measured	at thermodynamic equilibrium
288	38.7	0.64	0.63
318	14.1	0.20	0.22

Na_2CO_3 added to yield 8.7×10^{-4} moles/ml catalyst.

Conditions of the Experiment not shown above are the same as in Table XVII.

Aldridge, C. L. and T. Kalina, German Patent 1,928,389, Table VIII (Sept. 1970).

APPENDIX III

COMPUTER PROGRAM

Explanations for each section of the computer program used to analyze data for this study are given in this appendix. Instructions on how to use the program as well as an actual listing of the program are included.

Main Program. The main program has several important functions:

1. It receives data for chromatographic sensitivity factors, reaction equilibrium constants, component peak areas, reactor temperatures and reactant gas flow rates.
2. It calls various subprograms and performs minor calculations.
3. It prints out the data analysis results.

Subroutine BACK. Given the final chromatographic areas for CO, CO_2, H_2S, H_2O, and COS, subroutine BACK calculates initial and final mole fractions for H_2, CO, CO_2, H_2S, H_2O, and COS. The following assumptions are used in making the calculations:

1. Initial mole fractions of CO_2 and H_2S are zero.
2. The initial mole fractions of CO and H_2 are equal.

The rest of the assumptions used in subroutine BACK involve straightforward mass balances.

Function TERPOL. Function TERPOL interpolates logarithmically to find the equilibrium constant from the array of equilibrium constants for either of the following two reactions:

$$H_2O + CO \rightleftharpoons CO_2 + H_2 \qquad (1)$$

$$H_2S + CO \rightleftharpoons COS + H_2 \qquad (2)$$

The equilibrium constants for the two reactions were found in:

Chemtron Corporation, "Physical and Thermodynamic Properties of Elements and Compounds," p. 30 (1969).

The interpolation procedure may be found in:

Carnahan, B. and J. Wilkes, "Introduction to Alogorithms and Numerical Methods," pp. 3-12, Univ. of Michigan (1969).

Subroutine NONLIN. If we know the initial mole fractions of all components and equilibrium constants for reactions (1) and (2), the task is to calculate final mole fractions of all components. Subroutine NONLIN solves for X, the moles of CO consumed in reaction (1), and Y, the moles of CO consumed in reaction (2). The main program then makes the final computation of

equilibrium mole fractions. A two dimensional Newton-Rapheson technique is used to solve the two, non-linear equations for X and Y. The procedure is outlined in:

Haggerty, G. B., "Elementary Numerical Analysis with Programming," pp. 255-6, Allyn & Bacon, Boston, Mass. (1972).

Subroutine ONELIN. Subroutine ONELIN performs a function similar to subroutine NONLIN except that the procedure is done for reaction (1) only. This subroutine is only used if reaction (2) does not occur.

Subroutine LSR. Subroutine LSR does a least squares analysis on the arrays of conversion parameters, $- \ln \left\{ \frac{X_{co} - X_{co}^{eq}}{X_{co}^{o} - X_{co}^{eq}} \right\}$, versus 1/flow rate for a set of flow rates at a single temperature. Slopes, intercepts, and correlation coefficients are found both with and without the assumption that (0,0) is a valid data point. A general reference is:

Miller, Irwin, et. al., "Probability and Statistics for Engineers," Prentice-Hall, Englewood Cliffs, N. J. (1965).

Listing of the Program. The following is a listing of the computer program used for data analysis.

```
      LOGICAL FLAG
      REAL KP1(25),KP2(25),T1(25),T2(25),K1,K2,CPP(25),FLOWIV(25)
      COMMON A,B,C,D,R,S
      IU=25
      EPS=0.0005
      READ (5,101) N,J
      DO 3 I=1,N
      READ (5,103) T1(I),KP1(I)
    3 CONTINUE
      DO 5 I=1,J
      READ (5,105) T2(I),KP2(I)
    5 CONTINUE
      READ(5,104) SFCO,SFCO2,SFH2O,SFCOS,SFH2S
    6 WRITE(6,121)
  121 FORMAT(1H1)
      IP=0
    7 READ,T,X,Y,FLOD
      IF (T.EQ.0.0) GO TO 23
      IF (T.LT.0.0) STOP
      T=1.8*T+32.
      READ,AF,DF,SF,BF,RF
      AF=AF*SFCO
      BF=BF*SFH2O
      DF=DF*SFCO2
      RF=RF*SFCOS
      SF=SF*SFH2S
      CALL BACK(AF,BF,CF,DF,RF,SF)
      FLOW=FLOD/(1.-B)
      IP=IP+1
      FLOWIV(IP)=1./FLOW
      K1=TERPOL(T1,KP1,T,N)
      K2=TERPOL(T2,KP2,T,J)
```

```
      IF (Y.EQ.0.0) GO TO 9
      CALL NONLIN(K1,K2,X,Y,EPS,IU,FLAG)
      GO TO 19
    9 CALL ONELIN(K1,X)
      FLAG=.FALSE.
   19 T=(T-32.)/1.8
      WRITE (6,111) T,X,Y,K1,K2,FLOD,FLOW,FLOWIV(IP)
      WRITE (6,113) A,B,C,D,R,S
      IF (FLAG) GO TO 21
      FCO=(A-X-Y)
      FH2O=(B-X)
      FH2=(C+X+Y)
      FCO2=(D+X)
      FCOS=R+Y
      FH2S=S-Y
      WRITE (6,115) FCO,FH2O,FH2,FCO2,FCOS,FH2S
      WRITE(6,116) AF,BF,CF,DF,RF,SF
      CP=(AF-FCO)/(A-FCO)
      IF (CP.LE.0.0)  GO TO 21
      CPP(IP)=-ALOG(CP)
      WRITE(6,118) CPP(IP)
      GO TO 7
   21 WRITE (6,117)
      FLAG=.FALSE.
      IP=IP-1
      GO TO 7
   23 CALL LSR(CPP,FLOWIV,SLOPE,XCEPT,IP,SLOPEP,XCEPTP,CORCO,CORCOP)
      WRITE (6,119) SLOPE,XCEPT,SLOPEP,XCEPTP
      WRITE (6,120) CORCO,CORCOP
      GO TO 6
  101 FORMAT (I2,3X,I2)
  103 FORMAT (F10.2,5X,F15.5)
```

```
104 FORMAT (5(F10.5,5X))
105 FORMAT (F10.2,5X,F15.7)
111 FORMAT (1H ,///, 5X,'TEMPERATURE=',F7.2,1X,'DEG C',11X,'X=',F10.5,
   25X,'Y=',F10.5,/,10X,'K1=',F15.5,5X,'K2=',F15.7,5X,'DRY FLOW=',F10
   3.5,/,2X,'FLOW =',F10.5,5X,'1/FLOW =',F10.7)
113 FORMAT (1HO,24X,'CARBON MONOXIDE',5X,'WATER',8X,'HYDROGEN',3X,'CAR
   3BON DIOXIDE',7X,'COS',7X,'H. SULFIDE',/,2X,'INITIAL CONCENTRATION:
   4',2X,6(F10.5,5X))
115 FORMAT (1H ,1X,'FINAL EQUIL. CONC.    :',2X,6(F10.5,5X))
116 FORMAT (1H ,1X,'FINAL CONCENTRATION   :',2X,6(F10.5,5X))
117 FORMAT (1H ,5X,'NO CONVERGENCE')
118 FORMAT (1H ,5X,'CONVERSION PARAMETER=',F10.5)
119 FORMAT (1HO,10(/),5X,'SLOPE =',F10.5,5X,'INTERCEPT =',F10.5,
   15X,'SLOPE WITH 0,0=',F10.5,5X,'INTERCEPT WITH 0,0=',F10.5)
120 FORMAT (1HO,5X,'CORRELATION COEFFICIENT =',F10.5,5X,'CORRELATION C
   5OEFFICIENT WITH 0,0 =', F10.5)
    END
    SUBROUTINE NONLIN(K1,K2,X,Y,EPS,IU,FLAG)
    LOGICAL FLAG
    COMMON A,B,C,D,R,S
    REAL K1,K2
    FLAG = .FALSE.
    JOB=1
  3 F=K1*(A-X-Y)*(B-X)-(C+X+Y)*(D+X)
    FPX=K1*(2.*X+Y-(A+B))-(2.*X+Y+C+D)
    FPY=-K1*(B-X)-(D+X)
    G=K2*(A-X-Y)*(S-Y)-(C+X+Y)*(R+Y)
    GPX=K2*(Y-S)-(R+Y)
    GPY=K2*(X+2.*Y-(A+S))-(X+2.*Y+C+R)
    DENOM=(FPX)*(GPY)-(FPY)*(GPX)
    TOPX=(F)*(GPY)-(G)*(FPY)
    TOPY=(G)*(FPX)-(F)*(GPX)
```

```
      XONE=X-TOPX/DENOM
      YONE=Y-TOPY/DENOM
      IF ((ABS(XONE-X)).GT.EPS) GO TO 5
      IF ((ABS(YONE-Y)).GT.EPS) GO TO 5
      X=XONE
      Y=YONE
      RETURN
    5 IF (JOB.LT.IU) GO TO 7
      FLAG = .TRUE.
      RETURN
    7 X=XONE
      Y=YONE
      JOB=JOB+1
      GO TO 3
      END
      SUBROUTINE ONELIN(K1,X)
      REAL K1
      COMMON A,B,C,D,R,S
      Z=(K1*(A+B)+(C+D))/(1.-K1)
      W=(K1*A*B-C*D)/(K1-1.)
      RAD=SQRT(Z**2-4.*W)
      XL=-Z/2.-RAD/2.
      XH=-Z/2.+RAD/2.
      IF (XL.LE.0.0) GO TO 3
      X=XL
      RETURN
    3 X=XH
      RETURN
      END
      FUNCTION TERPOL(T,K,TIQ,N)
      REAL  K(25),T(25)
      NM1=N-1
```

```
      DO 3 I=1,NM1
      IF ( TIQ.LT. T(I+1) .OR. I.EQ. NM1  ) GO TO 5
    3 CONTINUE
    5 TERPOL=EXP((((ALOG(K(I)))*(T(I)+460.))+((TIQ-T(I))/(T(I+1)-T(I)))*
     1((ALOG(K(I+1)))*(T(I+1)+460.)-(ALOG(K(I)))*(T(I)+460.)))/(TIQ+460.
     2))
      RETURN
      END
      SUBROUTINE BACK(AF,BF,CF,DF,RF,SF)
      COMMON AI,BI,CI,DI,RI,SI
      DI=0.
      SI=0.
      AI=AF+DF-SF
      BI=BF+DF
      RI=RF+SF
      CI=AI
      CF=CI+DF-SF
      Q1=AI+BI+CI+DI+RI+SI
      Q2=AF+BF+CF+DF+RF+SF
      AI=AI/Q1
      BI=BI/Q1
      CI=CI/Q1
      DI=DI/Q1
      RI=RI/Q1
      SI=SI/Q1
      AF=AF/Q2
      BF=BF/Q2
      CF=CF/Q2
      DF=DF/Q2
      RF=RF/Q2
      SF=SF/Q2
      RETURN
```

```
      END
      SUBROUTINE LSR(CPP,FLOWIV,SLOPE,XCEPT,IP,SLOPEP,XCEPTP,CORCO,CORCO
     1P)
      REAL CPP(25),FLOWIV(25)
      IPP=IP+1
      X2=0.
      X=0.
      Y=0.
      Y1=0.
      Y2=0.
      DO 3 I=1,IP
      X2=X2+(FLOWIV(I))**2
      X=X+FLOWIV(I)
      Y=Y+CPP(I)
      Y1=Y1+(CPP(I))*(FLOWIV(I))
      Y2=Y2+(CPP(I))**2
    3 CONTINUE
      D=X2*FLOAT(IP)-X**2
      A=Y1*FLOAT(IP)-Y*X
      B=X2*Y-X*Y1
      SXY=Y1*FLOAT(IP)-X*Y
      SYY=Y2*FLOAT(IP)-Y**2
      SXX=X2*FLOAT(IP)-X**2
      SLOPE=A/D
      XCEPT=B/D
      CORCO=SXY/SQRT(SXX*SYY)
      AP=Y1*FLOAT(IPP)-Y*X
      DP =X2*FLOAT(IPP)-X**2
      SXYP=Y1*FLOAT(IPP)-X*Y
      SYYP=Y2*FLOAT(IPP)-Y**2
      SXXP=X2*FLOAT(IPP)-X**2
      SLOPEP=AP/DP
```

```
XCEPTP=B/DP
CORCOP=SXYP/SQRT(SXXP*SYYP)
RETURN
END
```

Instructions of Using Data Analysis Program

1. Follow the given deck with two data cards for each flow rate:

   a. card 1: T, X, Y, FLOW

   b. card 2: CO, CO_2, H_2S, H_2O, COS

   where, T = temperature of reaction, °C

   X = guess for the fraction of CO converted by reaction 1. X = 0.3 is a good guess.

   Y = guess for the fraction of CO converted by reactor 2. Y = -0.01 is a good guess. (If reaction 2 is ignored, let Y = 0.0).

   Flow = flow rate of inlet reactant gases on a dry basis at reactor conditions, ml/min.

   CO, CO_2, H_2S, H_2O, COS = areas of their respective components.

   Non-formatted data input is acceptable.

2. Follow each set of data at a given temperature by a card with 0,0,0,0 as input.

3. The last data card should have the entries -50,0,0,0.

APPENDIX IV

Calculation of Pseudo First Order Rate Constant for an Iron Oxide-Chromium Oxide Catalyst and a Zinc-Chromium-Copper Oxide Catalyst

Iron-Oxide-Chromium Oxide Catalyst

Data for a water gas shift reaction are analyzed at one atmosphere, and 760°F (404°C). The data were presented by Atwood.[18] An unspecified industrial catalyst of 16/20 mesh size was used.

For the one atmosphere run under consideration, 23.1% of the dry inlet synthesis gas is carbon monoxide and the inlet steam to dry gas ratio is 0.9. Thus, from a mass balance, we have three equations and three unknowns:

$$\frac{P^o_{H_2O}}{P^o_{co} + P^o_{H_2}} = 0.9$$

$$\frac{P^o_{co}}{P^o_{co} + P^o_{H_2}} = 0.23$$

$$P^o_{co} + P^o_{H_2} + P^o_{H_2O} = 1$$

Solving these equations we find that $P^o_{H_2O} = 0.474$, $P^o_{H_2} = 0.404$, and $P^o_{co} = 0.122$.

We are also given that the fraction of CO converted is 0.645 and the equilibrium conversion of CO is 0.889. Thus,

$$\frac{P^{o}_{co} - P_{co}}{P^{o}_{co}} = 0.645$$

$$\frac{P^{o}_{co} - P^{eq}_{co}}{P^{o}_{co}} = 0.889$$

Solving these equations, we find that $P_{co} = 0.434$ and $P^{eq}_{co} = 0.0135$.

Substituting the results for the initial, final, and equilibrium partial pressures of carbon monoxide into the integrated plug flow reactor design expression, we obtain:

$$- \ln \left\{ \frac{P_{co} - P^{eq}_{co}}{P^{o}_{co} - P^{eq}_{co}} \right\} = - \ln \left\{ \frac{0.0434 - 0.0135}{0.122 - 0.0135} \right\}$$

$$= 1.29$$

or, $1.29 = \frac{kV}{F}$, where k is the pseudo first order rate constant. The space velocity for the experiment is F/V = 3780 hr^{-1}. Thus k = 4870 hr^{-1} = 81.2 min^{-1}.

For the "Aldridge" catalyst No. 5 at the same temperature, the psuedo first order rate constant is 6481 min^{-1} as determined from the frequency factor and activation energy extrapolated from the molten region.

Zinc-Chromium-Copper Oxide Catalyst

A water gas shift study was made using a catalyst of $7ZnO \cdot Cr_2O_3 . 0.5\ CuO$ and a grain size of 0.1-1.0 mm. The data were claimed to be in the kinetic regime and were presented by Shchibrya.[21]

Shchibrya, in his one atmosphere run at 300°C, had an initial partial pressure of CO equal to 0.097 with a fractional conversion of 0.305. From a mass balance,

$$0.305 = \frac{P^o_{co} - P_{co}}{P^o_{co}} = \frac{0.097 - P_{co}}{0.097}$$

Solving the equation, we obtain $P_{co} = 0.0675$. Also, $P^{eq}_{co} = 0.00066$.

Proceeding similarly as with the iron catalyst, partial pressures of carbon monoxide are inserted into the plug flow reactor design expression:

$$- \ln \frac{P_{co} - P^{eq}_{co}}{P^o_{co} - P^{eq}_{co}} = - \ln \frac{0.0675 - 0.00066}{0.097 - 0.00066} = 0.372$$

or, $0.372 = \frac{kV}{F}$. Space time, or V/F, is 0.279 sec. Thus, $k = 1.34\ sec^{-1} = 80\ min^{-1}$.

For the "Aldridge" catalyst No. 5 at 300°C, the pseudo first order rate constant is $418.9\ min^{-1}$.

APPENDIX V

DIGITAL INTEGRATOR-MINICOMPUTER INTERFACE

In this section, we are concerned with the description of an interface between our digital integrator and a PDP 8/E minicomputer.

We may define interfacing as the joining of members of a group in such a way that they are able to function in a compatible and coordinated fashion. At the United Nations, the many skilled translators interface the representatives of the member nations through the rapid translation of the language of one country into that of another. In the electronics world, we have the problem of translating one digital language or digital code, into another.

The simplest digital code is a two state, or binary, code which consists of two logic states, either 0 or 1. Numbers larger than one are generated by a binary number system based upon powers of two. As an example, the number 11101_2, where the subscript "2" represents the binary system, is equivalent to, reading from left to right, $(1 \times 2^4) + (1 \times 2^3) = (1 \times 2^2) + (0 \times 2^1) + (1 \times 2^0)$, or 29 in decimal notation. Since almost all electronic circuits operate with two states, they generally perform operations with binary arithmetic. However

humans prefer to work with decimal arithmetic, in which the integers 0,1,2,3,4,5,6,7,8, and 9 are used with powers of 10 to represent any desired number. In view of this fact, it is useful to encode a decimal number into binary form, have the electronic circuitry operate upon the resulting binary number, and finally, when output is desired, decode the binary numbers back into decimal form. While a computer both encodes decimal numbers and decodes binary numbers stored in core, a laboratory instrument only needs to decode binary information generated during the course of an analysis.

The above encoding and decoding process can be applied to the alphabet as well as to decimal numbers. It is always the case that spare positions in so-called alphanumeric digital codes exist. These are used to encode letters, symbols, and certain keyboard operations such as back space, shift, and carriage return. Therefore, we may state that the object of a digital code is to encode numbers, alphabets, control functions, keyboard operations, or symbols in binary form.

In laboratory instrumentation, such as our digital integrator, the most popular digital code for encoding decimal numbers is the 8 4 2 1 code, more commonly known as binary coded decimal (BCD), which is, in effect, a

simple four-bit binary code that starts at 0000_2 and terminates at 1001_2, the binary equivalent to the decimal integer nine.

The most popular alphanumeric code for the transmission of the 26 letters of the alphabet, the ten decimal numbers, 28 symbols, and a variety of keyboard control functions is known as the ASCII code, otherwise called the American Standard Code for Information Interchange. The ASCII code is a seven-bit binary code that has the potential of encoding $2^7 = 128$ different pieces of information. In addition to 26 letters, ten numerals, and 28 symbols, roughly 35 keyboard control functions have also been encoded. At present there are 29 unassigned seven-bit words in the code which are immediately available to the user for any purpose that he desires. A partial listing of the ASCII code is shown in Table XXV.

Our digital integrator utilizes the BCD code whereas the teletype associated with our minicomputer utilizes the ASCII code. Thus, our interface must convert from the BCD code to the ASCII code, as well as transmit the converted data.

The BCD data from our digital integrator is available in a parallel fashion, i.e., the bits representing the various numerals are all available simultaneously. Once the data are converted to the ASCII code, they are most easily transmitted in a serial fashion; that is, the bits

Table XXV

A PARTIAL LISTING OF THE ASCII CODE

ASCII Code	Represented Character or Function
0110000	0
0110001	1
0110010	2
0110011	3
0110100	4
0110101	5
0110110	6
0110111	7
0111000	8
0111001	9
1000001	A
1000010	B
0100001	!
0001101	carriage return

composing a digital numeral and the numerals themselves are sent sequentially. This is the method generally used to transmit information over a distance since it requires only a single pair of twisted wires.

An overall schematic of our interface is shown in Figure 36.

Note that 44 lines of parallel BCD data are shown entering the interface, whereas only one pair of wires is used to transmit the serial ASCII data to the computer. This demonstrates the advantage of serial over parallel transmission.

Digital Integrator Data

The Autolab 6300-02 Digital Integrator has two major circuit boards which give access to two sets of data:

1. The Digital Board J1 gives access to parallel BCD area data.
2. The Retention Time/Totalize Board J2 gives access to parallel BCD retention time data.

We have seven orders of magnitude of area available from board J1 and four orders of magnitude of retention time available from board J2. The data are accessable from edge connectors on each board at the back of the integrator.

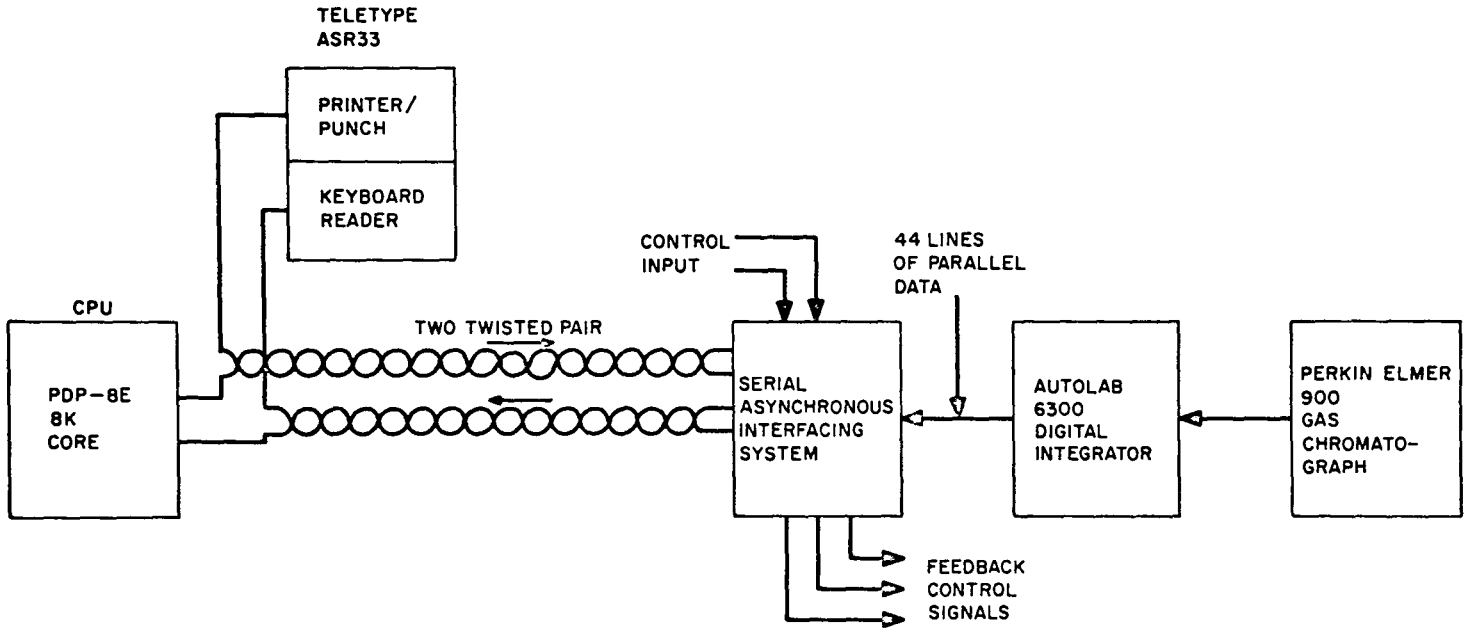

Figure 36. Overall Interfaced Gas Chromatograph System.

Table XXVI shows the data we used from boards J1 and J2 of the digital integrator. From the digital board J1, we use pins 23 through 50, representing the four bits of each of seven orders of area magnitude (10^0 through 10^6). The only other pin of interest from board J1 is pin 13, the integrate gate. This pin is ordinarily at +5 volts. At the start of integration, when the chromatographic base line slope changes from zero to positive, pin 13 changes to 0 volts. At the end of integration, when the slope changes from negative to zero, pin 13 changes from 0 volts back to +5 volts. As we will show later, this transition from 0 volts to +5 volts is used to initiate the transmission of serial ASCII data to the minicomputer.

From the Retention Time/Totalize board J2, we are interested in pins 19 through 34. These pins represent the four bits of each of the four orders of magnitude of retention time (10^0 through 10^3). At the middle of the integration, when the chromatographic peak slope changes from positive to zero, the retention time data is latched onto pins 19 through 34. No other pins are used from board J2.

As evidenced by Table XXVI, a total of 44 bits are required to represent the seven orders of magnitude of area and four orders of magnitude of retention time. All of these 44 bits are available in a parallel BCD form from the digital integrator and must be converted to a serial ASCII form for transmission to the minicomputer.

Table XXVI

DIGITAL INTERGRATOR REAR PANEL PIN CONNECTORS, J1 AND J2

Digital Board Connector J1		Retention Time/Totalize Board Connector J2	
Pin No.	Function	Pin No.	Function
13	Integrate gate	19	10^2 - 2 bit
23	10^6 - 4 bit	20	10^3 - 1 bit
24	10^6 - 8 bit	21	10^2 - 1 bit
25	10^6 - 2 bit	22	10^3 - 2 bit
26	10^6 - 1 bit	23	10^2 - 8 bit
27	10^5 - 4 bit	24	10^3 - 4 bit
28	10^5 - 8 bit	25	10^2 - 4 bit
29	10^5 - 2 bit	26	10^3 - 8 bit
30	10^5 - 1 bit	27	10^1 - 1 bit
31	10^4 - 4 bit	28	10^0 - 8 bit
32	10^4 - 8 bit	29	10^1 - 2 bit
33	10^4 - 2 bit	30	10^0 - 4 bit
34	10^4 - 1 bit	31	10^1 - 8 bit
35	10^3 - 4 bit	32	10^0 - 2 bit
36	10^3 - 8 bit	33	10^1 - 4 bit
37	10^3 - 2 bit	34	10^0 - 1 bit
38	10^3 - 1 bit		
39	10^2 - 4 bit		
40	10^2 - 8 bit		
41	10^2 - 2 bit		
42	10^2 - 1 bit		
43	10^1 - 4 bit		
44	10^1 - 8 bit		
45	10^1 - 2 bit		
46	10^1 - 1 bit		
47	10^0 - 4 bit		
48	10^0 - 8 bit		
49	10^0 - 2 bit		
50	10^0 - 1 bit		

Module Description

A Serdex STX 1003 Serial Transmitter Module and a Serdex SCL 1006 Clock Module form the electronic heart of our digital integrator-minicomputer interface. The transmitter module is designed to accept parallel BCD data and, upon receipt of an appropriate signal, transmit this data in serial ASCII fashion over a single pair of twisted wires. This is precisely what we need to do to interface our digital integrator to the minicomputer.

The SCL 1006 Clock Module serves as a source of precisely spaced timing pulses for transmission of serial ASCII data as well as a source of -15 volts for the transmitter module. A +5 volt power supply is necessary for operation of the clock module.

The two modules are basically "black boxes" with all circuitry being self-contained (Figure 37). They take advantage of modern serial data communication techniques and have only recently been made available commercially[35].

The simplicity of our interface lies in the fact that only a single pair of twisted wires connects the transmitter module to the minicomputer teletype. The interface between the teletype and the computer is already available; hence, there is no need to tie directly into the minicomputer.

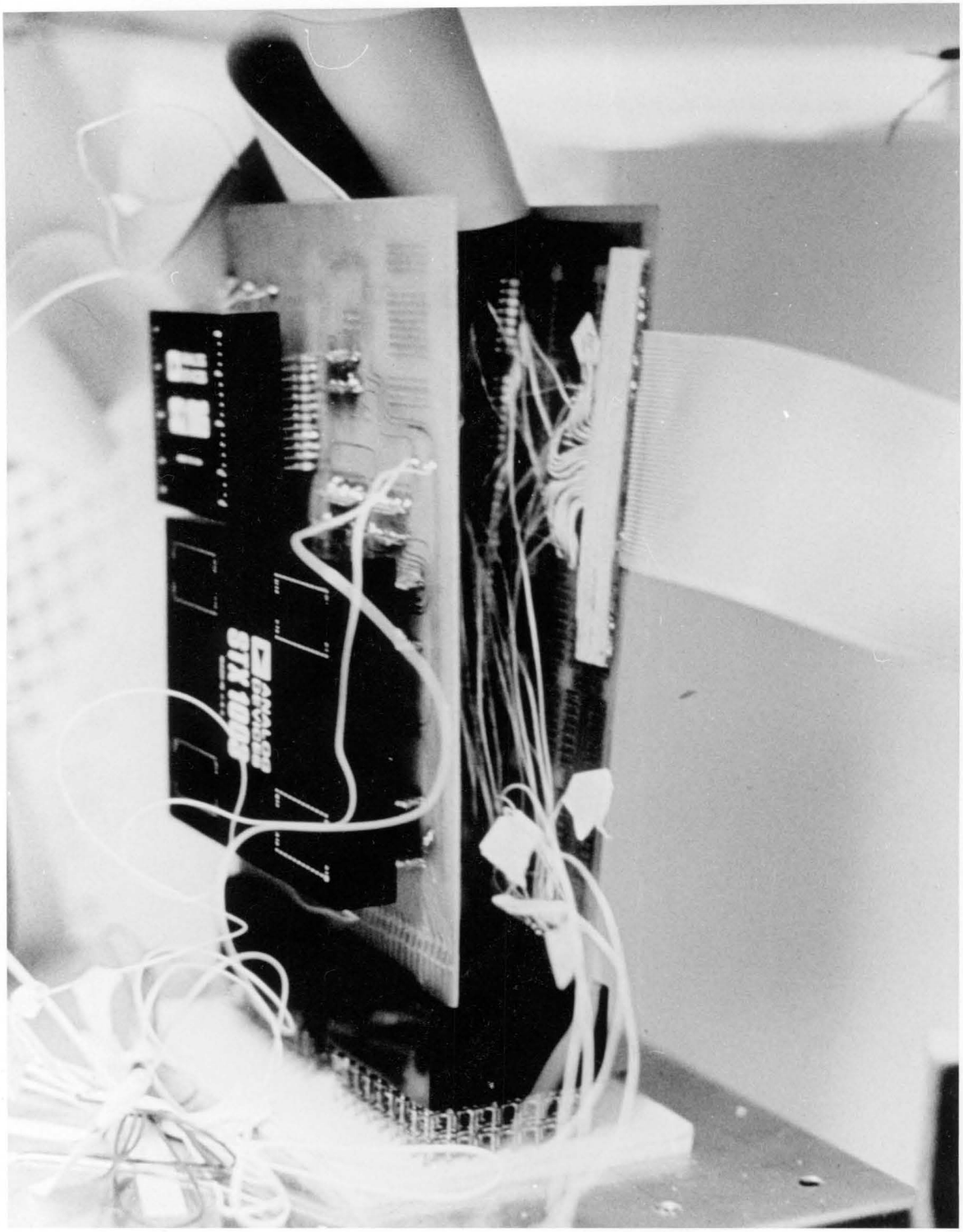

Figure 37. Photograph of Interface.

Transmitter Module Inputs. Figure 38 is a logic diagram of the STX 1003 Serial Transmitter Module. The connections to the module are available as ninety-six pins extending from the module casing. A number of the connections shown have functions other than conversion of parallel BCD data to serial ASCII form and were not used in this work.

As shown in Figure 38, eight words (digital numerals) are allowable as parallel data input. Four bits are required to represent each word. In our system, we transmit seven orders of magnitude of area plus four orders of magnitude of retention time as a single 11-word digital number. The first word shown in Figure 38, is the most significant numeral transmitted, which is the 10^6 area digit for our problem. Words two through seven are used to transmit the remaining six orders of magnitude of area, leaving only the eighth word available as direct parallel data input for retention time. Word eight is used for transmission of the most significant retention time character--the 10^3 retention time numeral. Table XXVII shows the pin connections for each of the eight words allowable as direct parallel data input to the transmitter module.

Obviously, we have three orders of magnitude of retention time information which cannot be fed directly

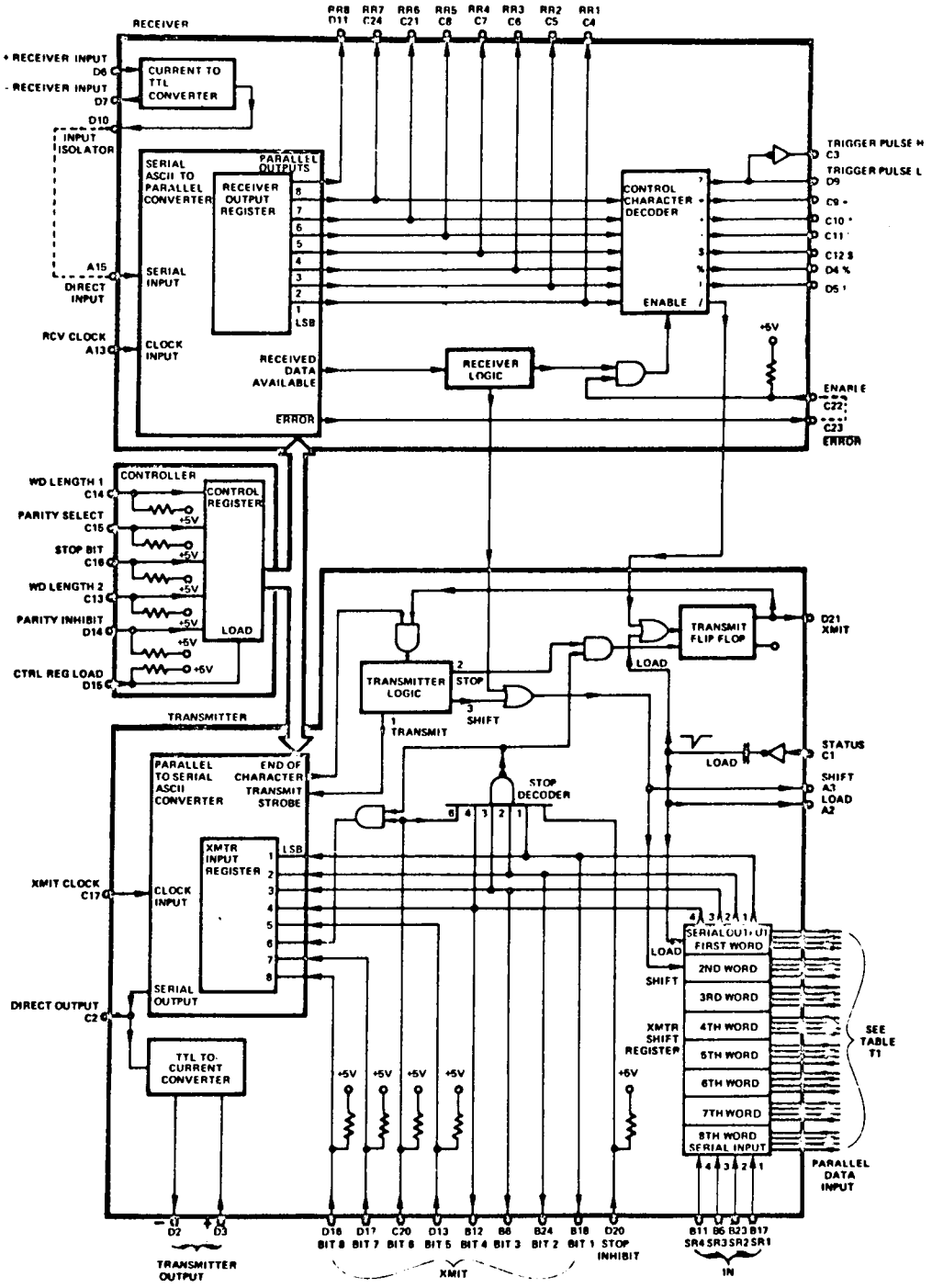

Figure 38. Analog Devices STX 1003 Transmitter Module Logic Diagram.

From Analog Devices, SERDEX USER'S GUIDE, p. 4 (1973).

Table XXVII

PARALLEL INPUTS OF THE TRANSMITTER SHIFT REGISTER

Characters to be Transmitted are Parallel-Loaded and Shifted Upward

Serial Output	Representation	Pin Number			
		Bit 4(23)	Bit 3(22)	Bit 2(21)	Bit 1 (20)
1st word	10^6 area	A12	A7	A23	A18
2nd word	10^5 area	A11	A6	A22	A19
3rd word	10^4 area	A10	A5	A21	A17
4th word	10^3 area	A9	A4	A20	A16
5th word	10^2 area	B10	B1	B19	B13
6th word	10^1 area	B9	B2	B20	B14
7th word	10^0 area	B8	B3	B21	B15
8th word	10^3 Retention Time	B7	B4	B22	B16

Similar to Table T1, Analog Devices, SERDEX User's Guide, p. 8, (1973).

into the transmitter module. We remedy this problem using four external shift registers, which have their inputs at pins B11, B6, B23, and B17, as shown in Figure 38. We will explain in detail how the shift registers are used in a later section.

ASCII Data Format. Eight bits, including the parity bit, are necessary for ASCII representation of a digital numeral, or word. However, we only have four bits available per word as parallel data input to the transmitter module. We use the values of bits 1, 2, 3, and 4 to determine the values of the remaining four bits.

Note two facts from Figure 38:

1. When the four bits representing a word are transmitted, their values are available simultaneously at pins B12, B6, B24, and B18.
2. The inputs for the values of bits 8, 7, 6 and 5 are given at pins D16, D17, C20, and D13.

Thus, we employ a digital logic connection so that the values of bits 1, 2, 3, and 4 available at pins B12, B6, B24, and B18 of the transmitter module determine the values of bits 5, 6, 7 and 8 available at D16, D17, C20, and D13 of the transmitter module. The four bits per word available from the digital integrator are therefore adequate for defining a complete ASCII word of eight bits.

Initiation of Data Transmission. Upon receipt of a 0 to +5 volt transition at the status pin C1 of the transmitter module, the parallel BCD data inputs from the digital integrator are sequentially shifted upward, converted to serial ASCII form, and transmitted to the teletype via a pair of wires connected to pins D2 and D3. The 0 to +5 volt transition required at pin C1 to initiate transmission is obtained from J1-13 of the digital integrator. Pin J1-13 changes from 0 to +5 volts at the end of integration of a particular peak, as explained earlier.

Additional Transmitter Module Connections. Besides the pins that we have already mentioned and appropriate ground and +5 volt connections, four other pins are necessary for operation of the transmitter module in the mode being described:

1. Pin C17 is the transmitter module clock input. This pin is connected to the output frequency pin B6 of the clock module and determines at what rate serial ASCII data are transmitted.
2. Pin A1 is the -15 volt DC supply. The source of the supply is pin A12 from the clock module.

3. Pin A2 is used to load external shift registers; it is connected to the shift/load input of the four SN74165 external shift registers.
4. Pin A3 is used to shift characters out of the external shift registers. It is connected to the clock input of the four SN74165 external shift registers.

Clock Module. Figure 39 shows a diagram of the SCL 1006 Clock Module. A +5 volt power supply is necessary at pins A15 and B4. Pin A12 serves as a source of -15 volts for the transmitter module. If pin B12 is left open, then pin A10 will supply a clocking frequency of 110 bits per second, or 110 baud. This frequency is compatible with most teletypes. Pin A10 is connected to pin B7 and the final output clocking frequency is available in a buffered form from pin B6. Pin B6 is connected to the transmitter module clock input. Appropriate grounds must also be made to the clock module.

Expansion of the System

The capabilities of the transmitter module in its purchased condition must be expanded to meet our requirements:

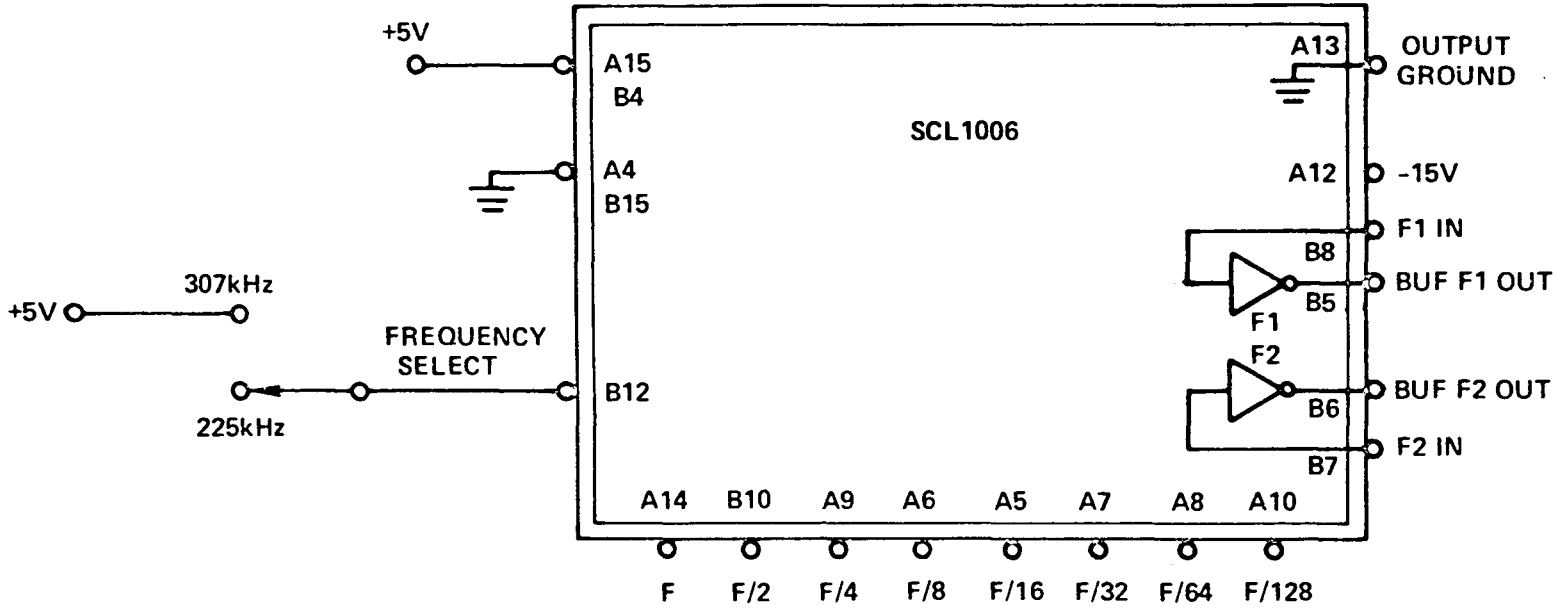

Figure 39. Analog Devices SCL 1006 Clock Module Connection Diagram.

From Analog Devices, SERDEX USER'S GUIDE, p. 18 (1973).

1. As explained previously, only eight words are allowable as direct parallel BCD input to the module. Thus, we must provide a means whereby our last three orders of magnitude of retention time can be transmitted.
2. We must provide a logic connection so that the values of bits 1, 2, 3, and 4 of the word being transmitted control the value of bits 5, 6, 7, and 8. This is due to the fact that eight bits are necessary to define an ASCII word but only four are available per word from the digital integrator.
3. We need to be able to signal to the minicomputer that a given chromatographic sample has been completely eluted. This will allow the minicomputer to process data.

Figure 40 shows the transmitter module in its expanded state. Four external 8-bit shift registers are used to transmit the last three orders of magnitude of retention time and a dual-quad input nand gate provides the logic to determine the transmitted values of bits 5, 6, 7, and 8.

External Shift Registers. We used four SN 74165 external shift registers to transmit the last three orders of magnitude of retention time. Figure 41 shows how the four external shift registers were added to pins B11, B5,

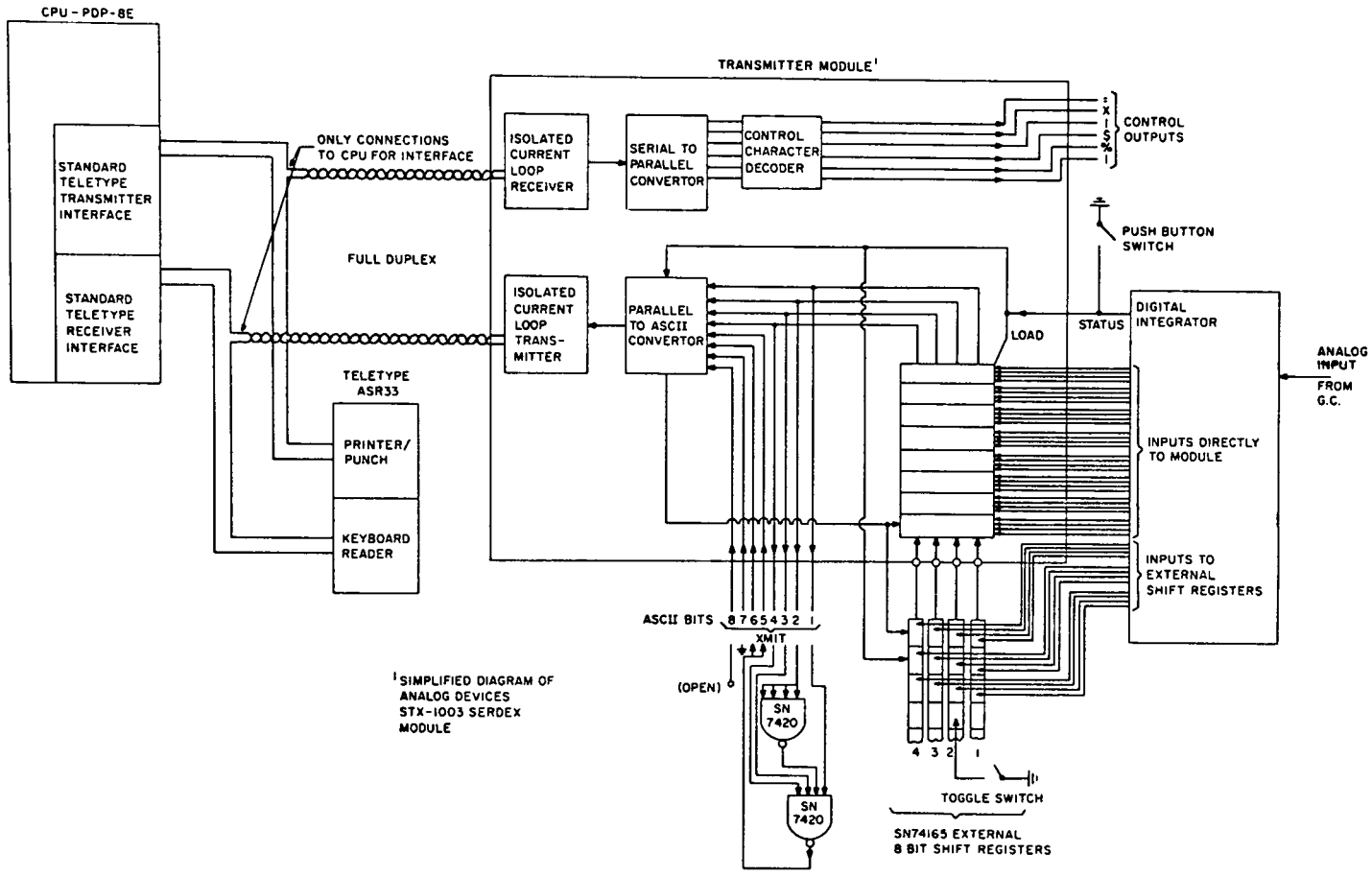

Figure 40. Transmitter Module with Input Data and C.P.U. Connections.

B23, and B17 of the transmitter module. Figure 42 gives a detailed schematic of a single external shift register. The clock inhibit is grounded on each shift register. The load pin A2 from the transmitter module is connected to the shift/load input of each shift register and the shift pin A3 from the transmitter module is connected to the clock input of each shift register.

The remaining three orders of magnitude of area--10^2, 10^1, and 10^0--are each represented by four bits. One switch register is alloted to each of the four bits for the three orders of magnitude of retention time. From Figure 41, we note that switch register 4, connected to bit 4 of the 10^2, 10^1, and 10^0 magnitudes of retention time, is connected to pin B11 of the transmitter module. Similarly, switch register 3, switch register 2, and switch register 1 are connected to pins B5, B23, and B17 of the transmitter module, respectively.

From Figure 42, we see that the output from a shift register proceeds in the order H, G, F, E, D and so on. We desire to transmit our most significant retention time first. Thus, the four bits representing the 10^2 magnitude of retention time are connected to the respective H pins on the four external shift registers. Similarly, pins G and F of each shift register are connected to the respective bits representing the 10^1 and 10^0 orders of magnitude of retention time.

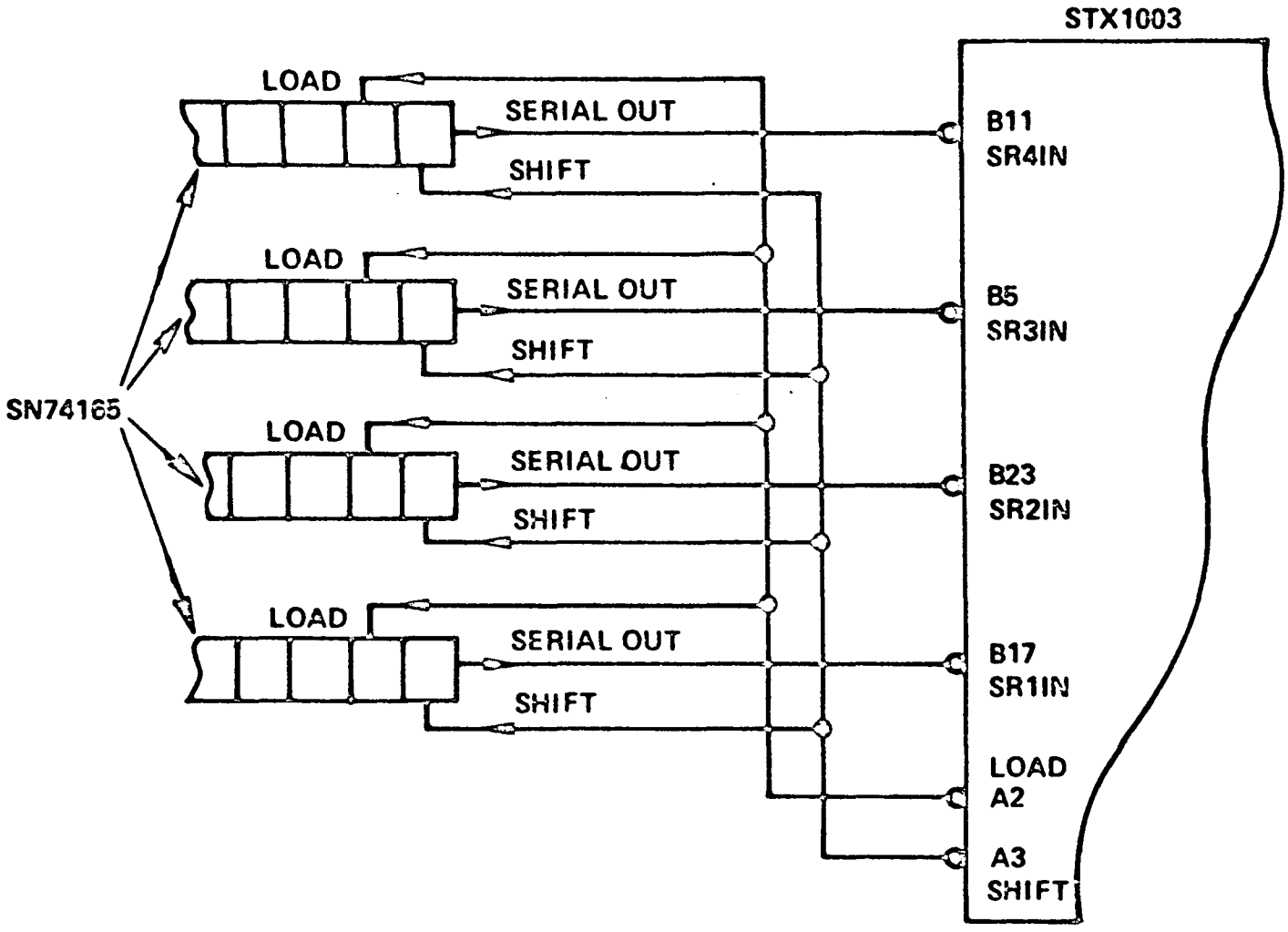

Figure 41. Wiring Diagram of External Shift Registers.

From Analog Devices, SERDEX USER'S GUIDE, p. 11 (1973).

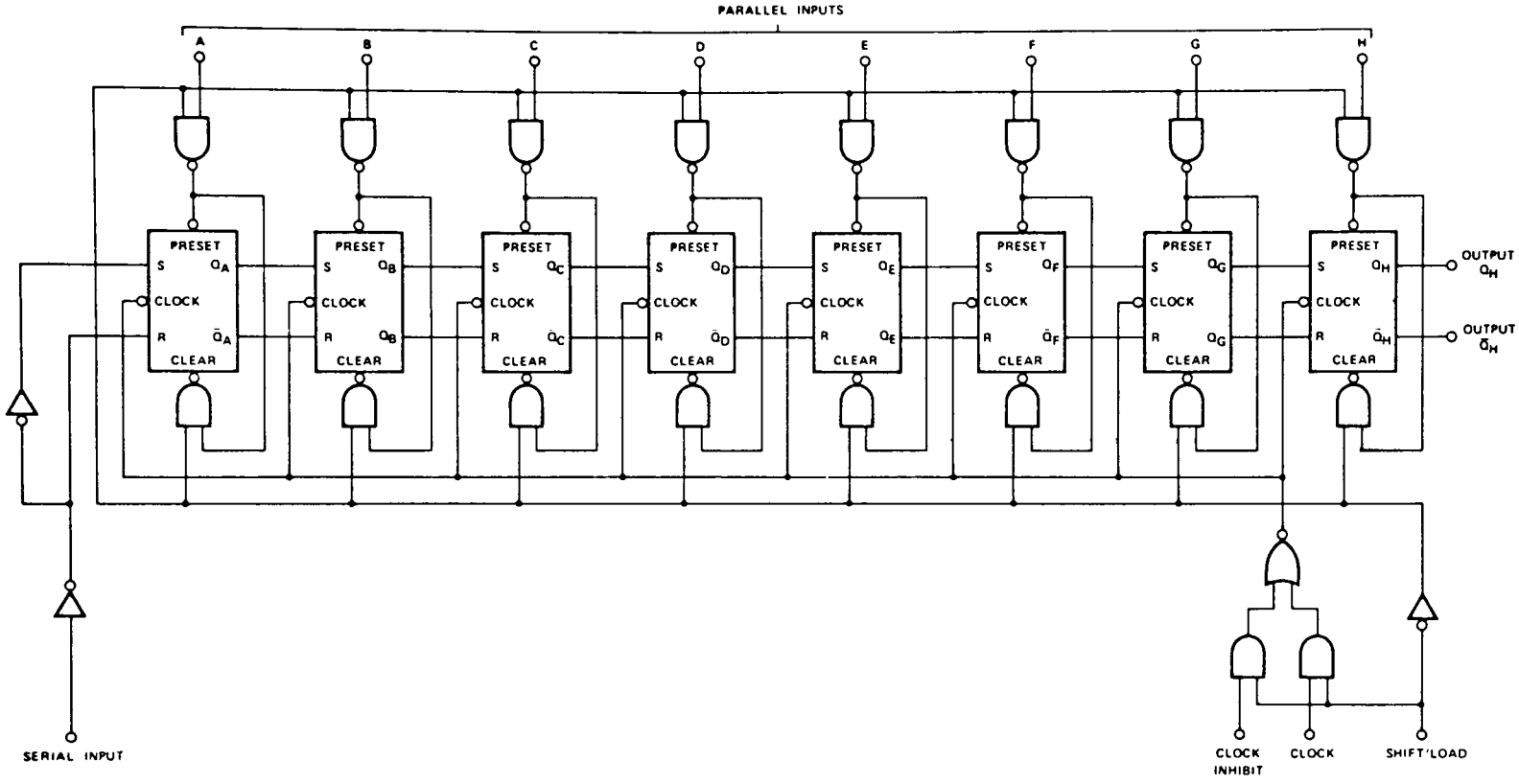

Figure 42. SN74165 Parallel-Load 8-bit Shift Register.

Logic Connection. As shown in Figure 40, the values from bits 1, 2, 3, and 4 being transmitted determine the values of bits 5, 6, 7, and 8 that are transmitted via an SN 7420 dual-quad input nand gate. The digital logic is such that if an ordinary digital number (between 0 and 9) is being transmitted via bits 1, 2, 3, and 4, then bits 5, 6, 7, and 8 will be 1, 1, 0, and 1 respectively. Thus, as shown in Table XXV, a number is represented in ASCII form.

Signal to Process Data. We need to be able to signal the minicomputer that a particular chromatographic run has been completed and that the data are ready to be analyzed. This represents an entirely new use for the transmitter module, since it basically was not designed for this type of purpose.

Note from Figure 42, that the connections following pin F on the shift registers are ordinarily open, or 1, since only three connections are required for the three orders of magnitude of retention time. The open connections on pin E of the four external shift registers are transmitted as 1, 1, 1, and 1 immediately following the last order of magnitude of retention time data. The transmitter module interprets the 1, 1, 1, and 1 values for bits 4, 3, 2, and 1 being transmitted as an ASCII non-printing stop character. Thus it stops transmitting data after it receives the values from the E pins of the external shift

registers.

Our software employs a FOCAL ASK statement to receive the eleven digits for area and retention time. Upon receipt of the non-printing transmitter module stop character, a new ASK statement is employed in expectation of more data.

We placed a toggle switch on pin E of shift register 2. As shown in Figure 43, if a 1, 1, 0, 1 is transmitted for bits 4, 3, 2, and 1 respectively then the logic connection will cause a carriage return (see Table XXV) to be transmitted. By switching the toggle to ground, a carriage return is transmitted from the E pins of the four external shift registers immediately following the last order of magnitude of retention time data. Following the carriage return are the open D pins of the shift registers, interpreted by the transmitter module as the non-printing stop character.

When pin E of shift register 2 is grounded, a carriage return is transmitted following the data. The software receives the carriage return and readies itself to accept more data. However, following the carriage return is the non-printing stop character. The software interprets the stop character as a zero, since it was already expecting more data. The zero, is the flag our software uses to initiate processing of data.

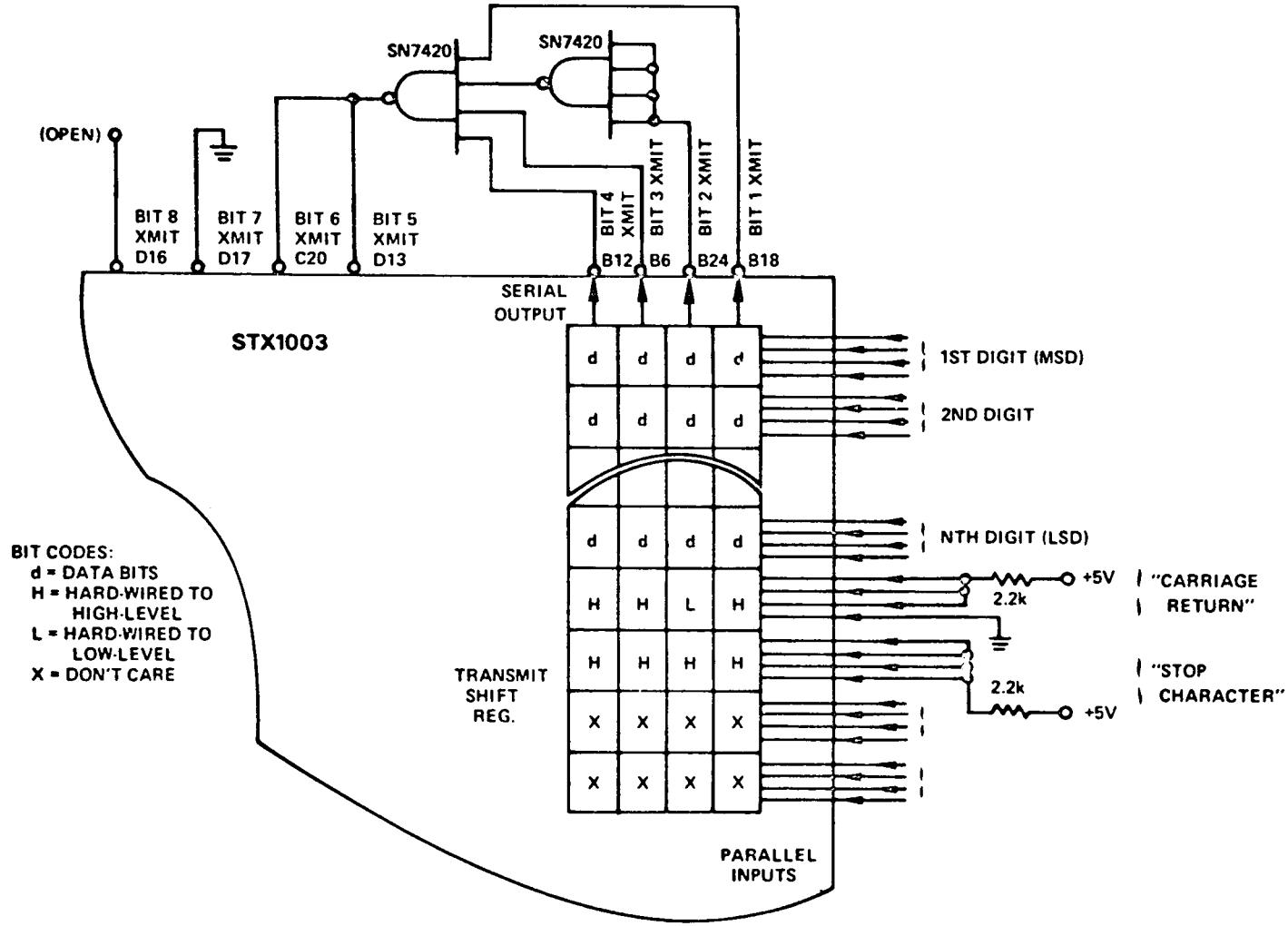

Figure 45. Hard-Wired Carriage Return.

From Analog Devices, SERDEX USER'S GUIDE, p. 9 (1975).

We placed a push button switch connected to ground on the line connecting the integrate gate (pin J1-13) of the digital integrator to the status input (pin C1) of the transmitter module (Figure 40). The integrate gate is ordinarily +5 volts. Thus, by pressing and releasing the switch, a 0 to +5 volt transition occurs at the status input of the transmitter module, which initiates transmission of data.

Thus our procedure to initiate processing of data becomes clear:

1. Initially, keep the toggle switch connected to pin E of switch register 2 in the open position.
2. At the end of a chromatographic run, place the toggle to the ground position to set up the carriage return.
3. Press and release the push-button switch to artificially transmit the carriage return and stop character, which will initiate data processing.

Physical System

In this section, we describe the way in which the digital integrator-minicomputer interface is actually constructed.

Module Connections. Many connections must be made to the transmitter module and clock module, including the individual bits from the digital integrator and the external shift registers. Hardwiring directly to the module pins presents two major problems:

1. Many wires would be required and would be difficult to work with.
2. The modules would be committed to one function only.

David G. Larsen of the Virginia Polytechnic Institute and State University's Department of Chemistry has designed a printed circuit board, hereafter called the Larsen board, to hold the two modules. The Larsen board, shown schematically in Figures 44 and 45, basically pulls out the module pin connections to the fingers of the board as well as making some internal connections. Molex pins are soldered to the Larsen board allowing the two modules to be inserted rather than hardwired (Figure 37). Thus, the modules may be easily removed for use elsewhere.

With the transmitter module and clock module mounted on the Larsen board, we must make connections to the pins, via the fingers of the board. To do this effectively, we use a breadboard and a bus block made from a standard Digital Equipment wire wrap block with like pins wired in parallel. Connections to the fingers of the Larsen board

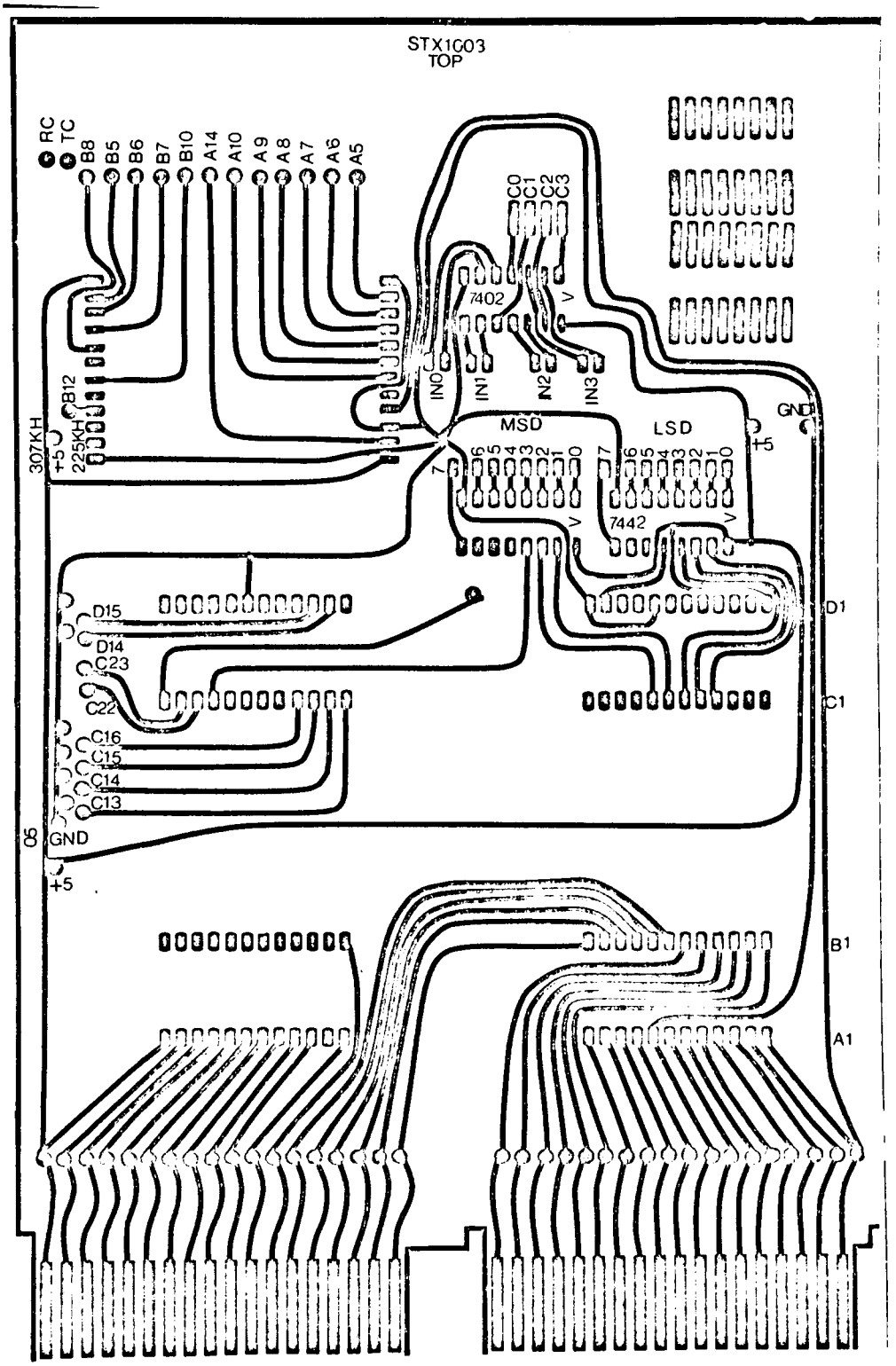

Figure 44. Front Side of Larsen Board.

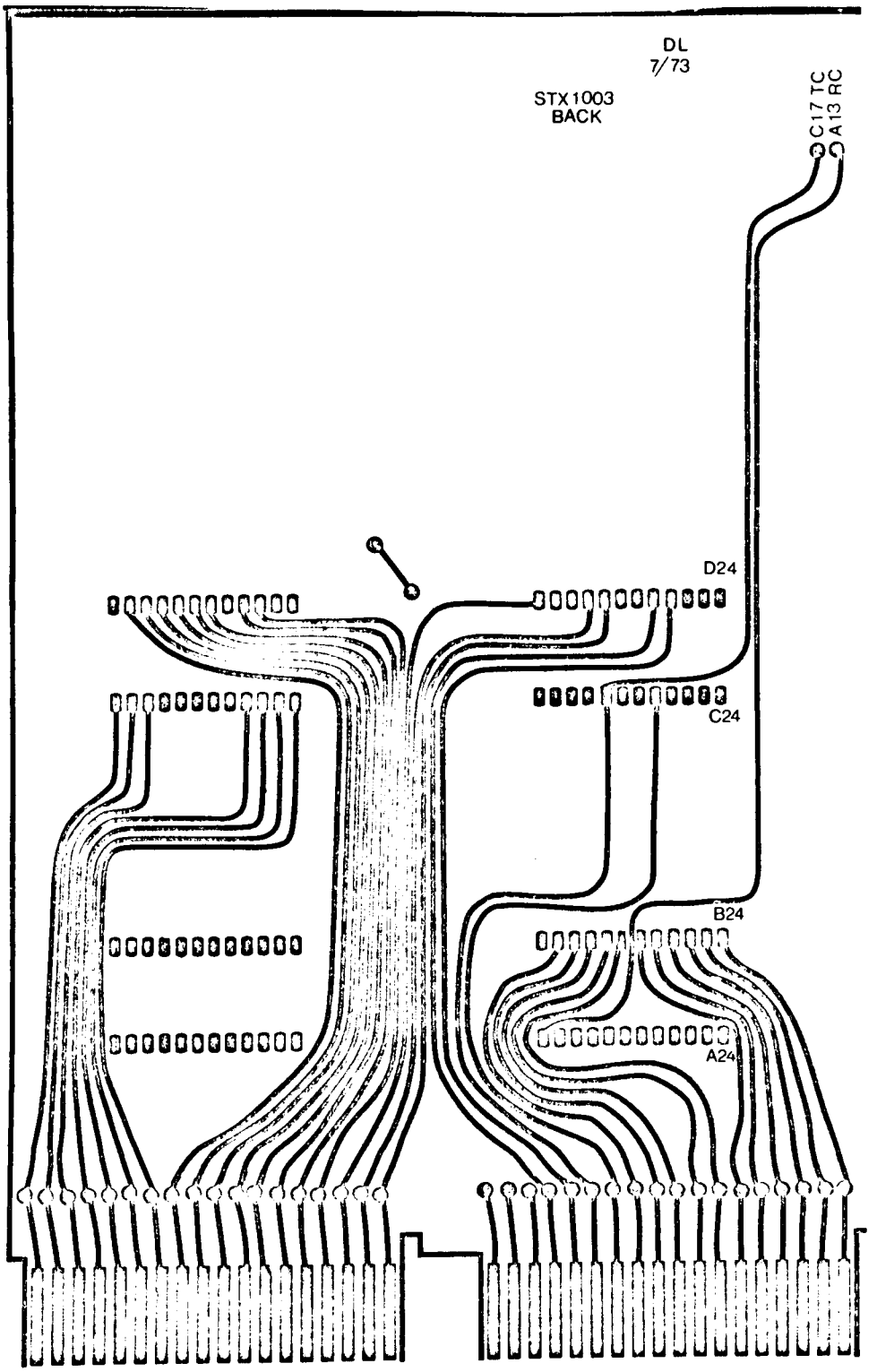

Figure 45. Back Side of Larsen Board.

are made through the breadboard. Parallel connections between the fronts and backs of the two boards are made via the bus block (Figure 37). The four external shift registers and dual-quad input nand gate are also located on the breadboard.

Digital Integrator Data Connections. We connect the 44 bits of data from the digital integrator, representing 11 digital numerals, to the breadboard where they are either connected to the external shift registers located on the breadboard or connected to the transmitter module via the bus block. The bits of data are available from two 3M connectors which are associated with the area board and the retention time board of the digital integrator. Two flat cables are used to take data from the 3M connectors to the breadboard.

The flat cable is attached to the breadboard as follows:

1. Slice the cable into individual wires (after peeling back the shielding) approximately 2.5 inches long.
2. Slice off any unused wire.
3. Epoxy the cable to the breadboard immediately beyond the individual wires.
4. Epoxy a small piece of wood over the cable for increased stability (Figure 37).

5. Solder the individual wires of the cables to pads on the breadboards.
6. Make appropriate connections between the pads and the shift registers, nand gates, or fingers at the end of the breadboard.

Detailed Wiring Diagram. The fingers of the Larsen board each represent a specified pin of the transmitter module. Thus, we know what input should be made to each finger of the Larsen board. Since connections to the Larsen board are made from parallel fingers on the breadboard, we must match the appropriate breadboard finger with a particular bit from the digital integrator, an output from a shift register, or some others required connection. The end result of this matching process is the detailed wiring diagram shown in Figure 46.

The front and back pin specifications for the Larsen board (STX 1003 board) and the breadboard are shown as well as the required connections to and from the external shift registers and dual-quad input nand gate. Obviously, some of the connections to the transmitter module are not used. Pin numbers from the digital integrator are specified on the breadboard and pin numbers from the STX 1003 transmitter module are specified on the Larsen board.

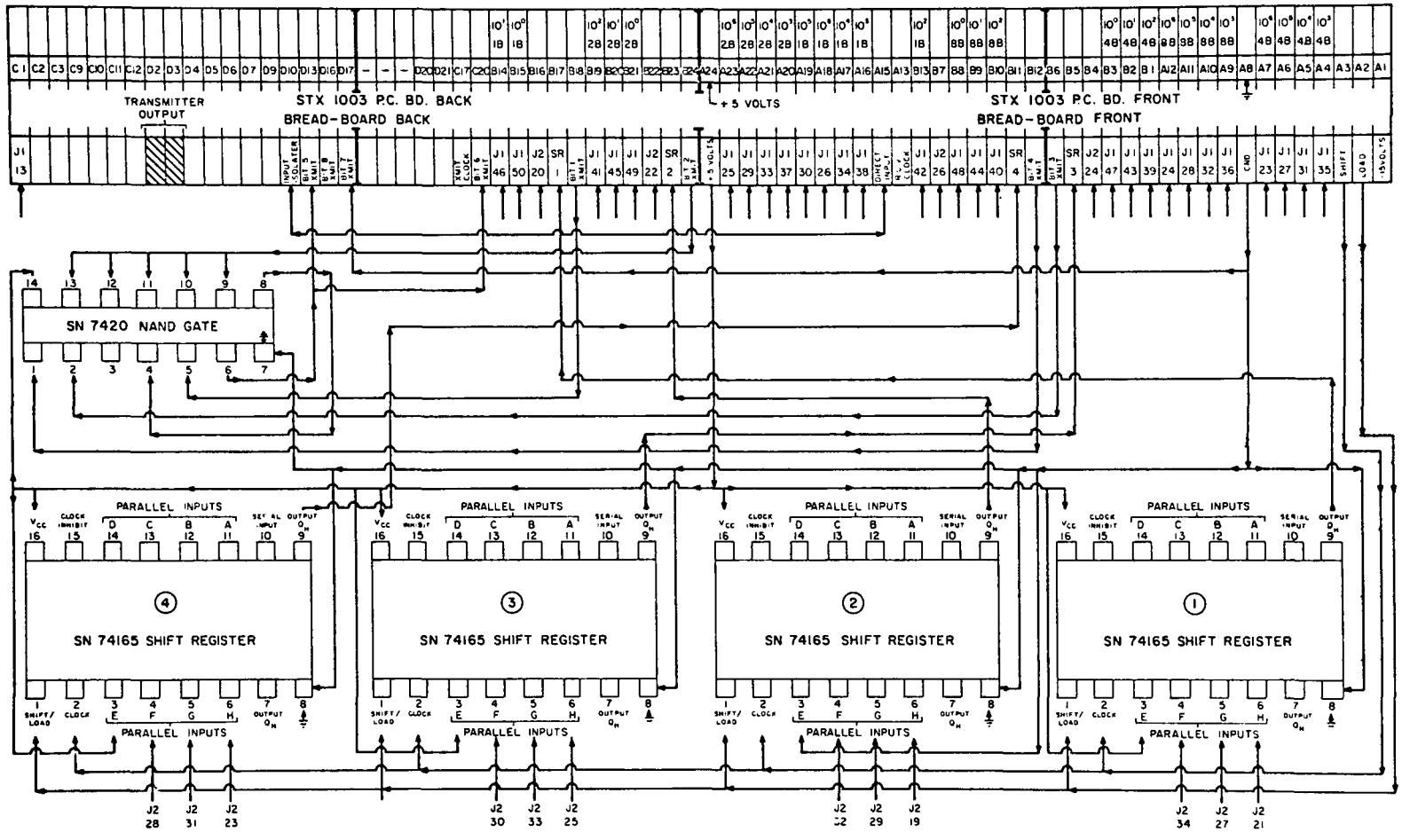

Figure 46. Detailed Interface Wiring Diagram.

Additional Connections. Pin B6 from the clock module, the frequency output, is wired to pad TC on the Larsen board. The +5 volt input to the Larsen board (pin A24) and the ground input to the Larsen board (pin A8) are obtained from a power supply designed by S. C. Reid.

Pins D2 and D3, shown in Figure 46, are the two connections required for the transmission of serial ASCII data. They are connected by two wires of unknown type to the teletype. The connection at the teletype is made via a single pole, triple throw switch to internal connection three of the teletype.[36]

Software

A FOCAL program is used to receive area and retention time data as well as to reduce the data. The program receives the eleven digits for each eluted component and separates them into seven area digits and four retention time digits. The areas from the eluted components are used with appropriate sensitivity factors to calculate initial and final mole fractions of all components.

A listing of the program and some typical output are listed in Figures 47 and 48, respectively.

Discussion

In the following section, we discuss certain aspects of the digital integrator-minicomputer interface including

```
:  00046110030⎫
:  00699000048⎬    3 components eluted; Toggle switch
:  00238260150⎭                        open;

:  00000000150}    Artificially induced transmission
                   caused by pushing button; Toggle
                   switch grounded; data ignored;

:            }     stop character; stored as zero
```

	Area	Retention Time
=	4611	= 30
=	69900	= 48
=	23820	= 150

	CO	H20	H2	CO2	COS	H2S
XI	=0.2946	=0.4109	=0.2946	=0.0000	=0.0000	=0.0000
XF	=0.0208	=0.1371	=0.5683	=0.2738	=0.0000	=0.0000

Figure 47. Data Received and Processed by Minicomputer for One Sample.

```
01.06 A !"NUMBER OF COMPONENTS"N;
01.11 T !!" COMPONENT NO.   SENSITIVITY  FACTOR    LOW TIME    "
01.13 T "HIGH TIME"
01.16 F I=1,N;T %3 !"      "I;A "          "SF(I);D 01.18
01.17 G 01.21
01.18 A "            "LT(I);A "      "HT(I)
01.21 S J=0;S L=0
01.26 S J=J+1;A !D(J);I (D(J))01.31,01.31;G 01.26
01.31 S J=J-2;I (J)01.21,01.21;G 01.36
01.36 T !!"    AREA            RETENTION TIME"
01.41 F I=1,J;D 3
02.06 I (L-N)02.11,02.16,02.11
02.11 T !" INCORRECT NO. OF COMPONENTS";G 01.21
02.16 I (N-3)02.21,02.21;S AS=1;S BS=4;S DS=2;S RS=5;S SS=3;G 02.26
02.21 S A(10)=0;S AS=1;S BS=3;S DS=2;S RS=10;S SS=10
02.26 S AF=A(AS);S BF=A(BS);S DF=A(DS);S RF=A(RS);S SF=A(SS)
02.31 S DI=0;S SI=0;S AI=AF+DF-SF;S BI=BF+DF;S RI=RF+SF;S CI=AI
02.36 S CF=CI+DF-SF;S Q1=AI+BI+CI+DI+RI+SI;S Q2=AF+BF+CF+DF+RF+SF
02.41 S AI=AI/Q1;S BI=BI/Q1;S CI=CI/Q1;S DI=DI/Q1;S RI=RI/Q1
02.43 S SI=SI/Q1;S AF=AF/Q2
02.46 S BF=BF/Q2;S CF=CF/Q2;S DF=DF/Q2;S RF=RF/Q2;S SF=SF/Q2
02.51 T !!"           CO       H2O       H2       CO2        COS"
02.53 T "       H2S"
02.56 T %5.2,!"  XI  ";T AI," "BI," "CI," "DI," "RI," "SI
02.61 T !"  XF  ";T AF," "BF," "CF," "DF," "RF," "SF;T !!!
02.71 G 01.21
03.06 S A(I)=FITR(D(I)/1E4);S RT(I)=D(I)-A(I)*1E4
03.11 T %7,!," ",A(I),"             ",RT(I);S L=L+1
03.16 I (RT(I)-LT(L))03.21;I (HT(L)-RT(I))03.21
03.18 S A(L)=A(I)*SF(L);G 03.23
03.21 S L=L-1
03.23 C
```

Figure 48. FOCAL Data Analysis Program.

reliability, expansion of the interface, and advantages of this type of interface.

Reliability. The interface system is capable of transmitting ten characters per second. Therefore, slightly over one second is required for transmission of the seven area and four retention time digits of a given eluted component. It is necessary that a delay of slightly greater than one second be present between the end of one integration and the start of another.

Data transmitted to the computer is completely consistent with the data printed out locally by the digital integrator itself. This shows the great accuracy of digital data transmission.

Debugging. Debugging a complex electronic system can be a very frustrating experience. A detailed wiring diagram, such as Figure 46, is quite helpful--in fact, virtually a necessity.

Two errors were made in the initial system. The SN 7420 integrated circuit was plugged into its molex pins backwards and two molex pins holding the transmitter module were touching, and consequently shorting each other. Errors such as these are painstakingly tracked down.

Expansion of Interface. Another pair of twisted wires from the teletype to the transmitter module allows the module to receive as well as transmit. The module recognizes certain control characters transmitted by the computer such as the dollar sign or apostrophe. When receiving one of these control characters, a pulse is generated at a particular module pin. By using the computer's real time clock to initiate a print out of a control character at specified times, pulses from the appropriate module pins can be used to activate a sampling value, start a programmed temperature run, etc.

Advantages of this type of Interface. Eight advantages of this type of interface can be listed:

1. No additional interface is required at the computer. Two pairs of twisted wires connected to the existing teletype part are the only interface connections to the computer.
2. Problems associated with digital data transmission are eliminated--no noise problems exist, therefore shielded cable is not necessary.
3. A high level programming language such as BASIC or FOCAL is appropriate for both data acquisition and control.

4. The system is easily expandable to perform more functions than just one on line data acquisition and control system.
5. Little knowledge of digital electronics is required for this type of interfacing.
6. The cost is very low (about $400 for this system) because the existing teletype port at the computer is being used.
7. The time of implementation is short.
8. Any instrument with BCD output can be put on line in a closed loop system.

It is easy to see that this approach to interfacing will solve many of the interfacing needs in the laboratory for any instrument with BCD output with real cost-time economics.

The vita has been removed from the scanned document

A SCREENING STUDY OF A NEW WATER GAS SHIFT CATALYST

by

Andrew D. Overstreet

(ABSTRACT)

Hardware and software techniques have been developed to study water gas shift catalysts over a temperature range of 150°C to 400°C, a pressure range of 0 atmospheres gauge to 30 atmospheres gauge, and a space velocity range of 600 hr^{-1} to 60,000 hr^{-1}. The hardware consists of a 5-foot long 3/16 inch-I.D. stainless steel temperature-controlled jacketed reactor over which temperatures can be maintained to within $\pm$ 2°C at 250°C and to within $\pm$ 4 °C at 500°C. The effluent from the reactor is sampled at 150°C and analyzed by gas chromatography for carbon monoxide, carbon dioxide, water, and other low molecular weight gaseous components. A computer program converts the conversion data to plots of $- \ln \left\{ \frac{X_{co} - X_{co}^{eq}}{X_{co}^{o} - X_{co}^{eq}} \right\}$ versus the reciprocal flow rate. The slopes at low values of 1/F are then divided by the weight of catalyst, and the quantity $\ln (\frac{kV}{W})$ plotted against the reciprocal temperature

to determine activation energies. Particle sizes studied were 20/60 mesh.

Using the above reactor system, a sulfur-tolerant water gas shift catalyst was studied using a feed gas composition of 49% CO/49% H_2/2% COS. The composition of the catalyst was varied and an attempt was made to determine whether there were any "breaks" in the activation energy plots.

Two types of breaks were observed which we tentatively ascribe to (a) a phase change, perhaps a melting point, at low temperatures ranging between 175°C and 350°C, and (b) a change to diffusion controlled reaction at higher temperatures in the region of 350°C to 400°C.

We also report preliminary studies on a resistance drop technique for measuring melting points of molten electrolytes as well as a digital electronic interface between an Autolab 6300-02 digital integrator and a PDP 8/E minicomputer.